MANUAL FOR INVESTIGATION OF HYDROLOGICAL PROCESSES IN MANGROVE ECOSYSTEMS

Björn Kjerfve
Baruch Institute for Marine Biology and Coastal Research
Department of Geological Sciences
and Marine Science Program
University of South Carolina
Columbia, SC 29208, U.S.A.

April 1990

Supported by the UNESCO/UNDP Regional Project
"Mangrove Ecosystems in Asia and the Pacific"
RAS/79/002 and RAS/86/120

TABLE OF CONTENTS

ps-8
missing

2.4. Rainfall and Evapotranspiration

The second critical factor is the ratio of rainfall to evapotranspiration. Although mangroves are found in both humid and arid climates, mangrove growth and species diversity is generally greatest in humid equatorial areas where rainfall is plentiful and evenly distributed throughout the year. Such conditions exist in the humid equatorial regions, e.g the Sunderbans of Bangladesh and India, Malaysia, Indonesia, Papua New Guinea (Blasco, 1984), and the Pacific coast of Colombia (Snedaker, 1984), where some of the largest single areas of mangroves stands are found.

According to Walter (1977), mangrove ecosystems exist mainly in four of nine main climate types, as determined from over 8,000 climate diagrams collected in the Klimadiagramm-Weltatlas (Walter and Lieth, 1960-1967). Of these four types, the greatest abundance of species is in the equatorial zone of Asia between 10°N and 10°S, where annual precipitation is high and the annual temperature range is small. The second most prevalent region is the tropical summer rainfall zone (to 25-30°N and S), where seasonal gradients in both rainfall and temperature are well defined. A smaller number of species exist in parts of the subtropical dry zone, where daily temperature ranges are large and annual precipitation is less than 200 mm. Several species are also found on the eastern border of continents in the warm temperate zone, where winters are mild and humidity is high. Walter (1977) suggested that these climatic restrictions are due to the sensitivity of mangroves to frost, but more likely, they are due to warm ocean boundary currents.

Rainfall does not appear to limit the global distribution of mangroves because they grow in arid desert climates as well as wet (Galloway, 1982). Rainfall does, however, have a significant influence on the distribution and zonation of species. Rainfall serves as a primary control of salinity in mangrove environments. Several species of mangrove are facultative, i.e. they appear to survive and even flower and fruit, but do not establish permanent groves in freshwater. *Avicennia marina* and *Aegialitis angulata* appear to be the most salt resistant species, with the upper limit being 90 ppt in interstitial water (Macnae, 1968; UNESCO, 1987a), but lower salinities in tidal waters. Rainfall and accompanying surface and through-flow of freshwater to tidal swamps leaches the soil of excess salts and thereby helps to keep soil salinity within a tolerable range (Oliver, 1982).

Rainfall leaching can also cause substantial nutrient loss from mangroves (Boto, 1982). The degree of nutrient loss from mangrove plants appears to vary with plant type as well as season. Tukey (1971) provides a good overview on qualitative and quantitative aspects of macrophyte leachates, and a study on the leaching effects of rain on a mangrove canopy in Southern Florida has been done by Lugo and Snedaker (1973).

Rainfall periodicity is yet another critical factor. In climates that are humid throughout the year, soils are continuously leached of salts by heavy but evenly distributed rainfall. Salinity levels are generally constant and stable throughout the year. The greatest diversity of species exists in these regions, which are mainly found in Malaysia, Indonesia, and Papua New Guinea (Macnae, 1968; UNESCO, 1987a). But in arid climates or monsoonal areas with strongly seasonal rainfall distribution, the low rainfall or drought periods lead to high evaporation rates, and consequently, increased soil salinities. During the rainy season, this situation reverses, and soil salinity drops considerably. Mangrove species diversity in arid and monsoonal regions is thus low because of the requirements for tolerance of high salinities and large salinity fluctuations. Dying mangroves are commonly observed around bare areas in the tropics that experience high evaporation (Galloway, 1982) because of increased interstitial salinities (Macnae, 1966; Spenceley, 1976).

2.5. Climate Types

Species zonation differs between mangrove ecosystems in humid climates as opposed to arid climates

(Blasco, 1984). In humid climates, rainfall leaches the soil more effectively in the landward zone, whereas on the outer fringe, salinities are elevated by frequent periods of tidal inundation. The less salt-resistant species thus exist in the landward zone, occasionally in association with freshwater marsh vegetation, such as *Pandanus*. But in arid climates subject to dry seasons or long periods of drought and little river flow, high evaporation rates increase salinities on the landward margin, while salinity concentrations along the outer edge are moderated by tidal inundation. The most salt-resistant species are thus found in the landward zone, often alongside extensive areas of bare sand with hypersaline soil conditions (Blasco, 1984). Bare salt flats exist, for example, in northeastern Queensland, Australia (Oliver, 1982) and Tanga in East Africa, where soil salinity can range from 25 ppt at the seaward edge to 41 ppt at the landward zone (Walter, 1973).

Because mangrove zonation and distribution is greatly influenced by rainfall and evaporation rates, UNESCO (1979) developed the Map of the World Distribution of Arid Climates, which classifies climates according to degree of aridity. The common climatological method for expressing aridity is to compute the difference between mean annual rainfall in a region, expressed as P, and the mean annual potential evapotranspiration, PET. When PET is greater than P, i.e., when water loss is greater than water received, a water deficit results. UNESCO (1979) selected Penman's (1956) procedure for computing potential evapotranspiration, although there are several alternative methods available (Thornthwaite and Mather, 1957; Papadakis, 1965; Turc, 1954). Blasco (1984) provides a comparison of Penman's technique to several other methods of computation.

According to the UNESCO (1979) classification map, four degrees of aridity were established based on (1) the ratio P/PET; (2) temperature regimes; (3) drought periods; and (4) temperature of the coldest month. In comparing the UNESCO (1979) aridity map to that of the world distribution of mangrove ecosystems, Blasco (1984) concluded that (1) 90% of the world's mangroves are found in humid regions where $P/PET > 0.75$; (2) mangroves are occasionally found in sub-humid climates where $0.50 < P/PET < 0.75$, such as Kenya, Tanzania, Venezuela, Australia, and Mexico; (3) very few mangroves are found in semi-arid conditions where $0.20 < P/PET < 0.50$, mainly only in Ecuador, the Indus delta in Pakistan, Gujarat in India, and parts of Australia; and (4) mangroves are almost non-existent in arid climates where $0.03 < P/PET < 0.20$, except around the Red Sea, the Persian Gulf, and Gulf of California. Blasco (1984) does point out several weaknesses in this provisional methodology for classifying mangrove ecosystems, principally among them the lack of systematically collected climatological data and refined techniques for data synthesis. All climate classification schemes thus far developed are based on data largely obtained from meteorological stations and averaged over some twenty years or more. These data suppress yearly climatic variability and stability measures, which are essential to mangrove distribution and zonation. More emphasis needs to be placed on the systematic collection of climatological data, particularly temperature and rainfall measurements from localized areas, to develop an improved scheme for classifying mangrove ecosystems as a means of understanding and managing mangrove wetlands.

2.6. Substrates

Heavy rains and subsequent high river flow carry alluvial sands and muds to tidal flats, thus forming a substrate for mangrove colonization and succession. Specimens of some species of mangroves do grow on sand, gravel, or rock shores, but these substrates are generally abrasive and cause considerable damage to most seedlings (Bird and Rosengren, 1986). Mangroves typically colonize on fine-grained alluvial muds and sands deposited from river and surface runoff onto deltas, inlets, estuaries, lagoons, and other protected regions of the coastal plain (Thom, 1984). Classic examples of mangrove colonization and succession can be seen along the west coast of Malaysia, where extensive mudflats are accreting seaward (Coleman et al., 1970; Diemont and van Wijngaarden, 1975); in the Sunderbans of Bangladesh (Vannucci, 1989); in Borneo (Anderson and Muller, 1973); and along several lagoon shores of Tabasco, Mexico (Thom, 1967).

The accretion of alluvial muds by rainfall can be a slow, long-term process, as would occur in a humid environment with evenly distributed rainfall and continuous deposition of muds. But it can also be caused by short-term (1-2 days) catastrophic events such as flash flooding. In this case, huge quantities of alluvium can be deposited over a brief period, often causing initial destruction to mangrove stands before rebuilding would take place.

2.7. Winds and Weather

Wind affects mangrove establishment in many ways. Local winds increase evaporation rates, aid in the dispersal of seedlings, and modify the strength of tidal currents and longshore drift, which can increase deposition of sands, silts, and clays along coastlines. Heavy sand deposition can bury pneumatophores and existing stands of mangroves. This has been observed on the southwest coast of Madagascar (Blasco, 1984). More often, however, deposition of muds and silts by strong wave action and longshore currents provides a substrate for more mangrove colonization, as can be observed in Cairns Bay during high spring tides (Bird, 1972).

Stocker (1976) defined four types of physical damage to mangroves caused by wind and waves: (1) windthrow; (2) crown damage; (3) bole damage; and (4) death. The susceptibility or resistance to each type of wind damage is species specific (Stocker, 1976). Because of the damaging effects of high winds and wave action, mangrove stands are generally located along low energy coastlines, for example, the leeward side of islands or in sheltered areas such as lagoons, estuaries, inlets, river deltas, and coastlines protected by barrier reefs.

Few studies exist on the effects of wind on mangrove physiology, mainly because of the lack of systematic climatological data from localized mangrove communities. Prevailing wind speeds and directions are frequently available from meteorological stations, but these data are not necessarily representative of conditions within specific mangrove canopies, which have highly localized microclimates. Emphasis should thus be placed on collection of climatological data directly from within mangrove canopies for more accurate studies on mangrove physiology and response to wind and other climatic factors.

The effects of natural weather disturbances (tropical storms, hurricanes/cyclones, lightning, etc.) on mangroves is another area lacking in available data and references. According to Johns (1986), the majority of case studies dealing with hurricane or cyclone effects on mangrove stands are focused on Central America. But results from these studies are probably not representative of mangrove stands in general. The ability of certain species to withstand hurricane, typhoon, or cyclone damage is regionally highly variable. For example, Jennings and Coventry (1973) and Chapman (1976) both found *Rhizophora* to be highly resistant to hurricane damage, but Spenceley (1976) observed that *Rhizophora* suffered the most damage from a tropical storm in Townsville, Australia (cf. Oliver, 1982).

Stoddart (1962) studied the effects of Hurricane Hattie in October, 1961, on mangrove stands in British Honduras. He reported that defoliation of *Rhizophora, Avicennia, Laguncularia,* and *Conocarpus* occurred over a 20-25 mile zone north and south of the storm track. Those mangroves exposed to flooding and high wave action as well as wind gusts suffered more defoliation than those exposed to high winds alone (Stoddart, 1971). A survey four years after the hurricane showed that most of the defoliation resulted in mangrove death, with no evidence of recolonization (Stoddart, 1965). In most cases, recolonization does not occur on dead mangrove stands (Stoddart, 1971).

The influence of lightning strikes on mangrove communities has also received little attention (cf. Johns, 1986), although lightning strikes are common in the tropics and have caused considerable damage to mangrove stands in Ponape (Sturges, 1865) and potentially long-term community restructure to

mangrove stands in Papua New Guinea (White, 1975; Johns, 1981).

Solar radiation influences the growth of mangroves as well. Requirements for light and shade vary among mangrove species, and frequently change during a plant's life cycle (Saenger, 1982). Seasonal fluctuations in mangrove productivity appear to be influenced by seasonal variations in solar radiation (cf. Clough et. al, 1982), although little research has actually been done to this effect. But solar radiation, wind, temperature, and rainfall act together to influence humidity and evaporation rates in mangrove communities.

Periodicity and duration of data collection are critical factors. Most existing data sets in mangrove environments are based on weekly, or more usually, monthly mean values. The frequency of climatic measurements needs to be increased to at least twice daily sampling, with measurements collected during both day and night. Also, the raw daily measurements should be analyzed as well as the monthly or annual mean data. The daily measurements provide excellent information on stability of mangrove environments, while the mean monthly data can be used to analyze long-term overall climatic effects.

3. GEOMORPHOLOGICAL SETTING OF MANGROVE ECOSYSTEMS

3.1. Deltas

Mangroves exist under a wide range of climatological settings, but their geomorphological setting is far more restrictive. It is largely controlled by substrate type, degree of shelter from wind and wave action, amount of river runoff or surface through-flow, tidal inundation, interstitial salinity, and soil type.

Deltas are by far the most common geomorphological setting for mangrove colonization. There are several reasons for this. Because mangroves typically colonize from the mid to high tide zone, low-lying, broad deltaic plains subject to extensive tidal inundation provide the largest reaches for mangrove colonization. Although tidal range has often been cited as a major control over mangrove distribution and spread (Macnae, 1966; Galloway, 1982), some of the most extensive mangrove stands in the world are located in deltaic regions that exhibit a low to moderate tidal range of 2–4 m, e.g., the upper Gulf of Thailand. Mangroves also exist along coasts that have insignificant tides (cf. Lugo and Snedaker, 1974). According to UNESCO (1987a), freshwater discharge is probably a more critical factor in controlling mangrove productivity than is tidal range.

Although mangrove species vary in their salinity tolerance, salinity is not necessarily a major influence over mangrove zonation. Most mangrove species are facultative halophytes and thus do not require saline conditions for survival. Rather, they prefer brackish to saline waters at least part of the year, maybe because salinity eliminates competition from glycophytes (Thom, 1967). Freshwater discharge or terrestrial runoff, on the other hand, greatly favors mangrove colonization; it supplies nutrients and leaches the soil, thus keeping soil salinity within a tolerable range.

Frequency and range of tidal inundation are critical factors in arid regions with low annual or only seasonal freshwater flow and high rates of evapotranspiration. Under these climatic conditions, bare hypersaline flats are frequently found just landward of the high tide level. These flats rarely support vegetation and are only inundated by an occasional extreme spring tide, which decreases evaporation and temporarily alleviates hypersaline soil conditions.

Deltas are typically prograding because of the continuous supply of alluvial deposits from river discharge. This also favors the colonization of mangroves. Mangroves contribute to land building because they colonize a suitable substrate first and add to progradation once they have been established. Examples of mangrove succession along actively prograding shores can be seen along the coastlines of west Malaysia (Coleman et al., 1970), the Sunderbans, and lagoon shores of Tabasco, Mexico (Thom, 1967). Fine-grained alluvial silts and sands deposited into deltas are also ideal substrates for mangrove colonization. Soil substrate acts as a major geomorphological constraint in mangrove development and zonation (Thom, 1967). Although some mangrove species do colonize on gravel or rocky substrates, their growth is stunted to varying degrees because of the sheer lack of soil, as well as the abrasiveness of the substrates to the roots of mangroves. Exposed beaches are also ill-suited for mangrove growth because marine sands deposited by wind and wave action cover and drown mangrove pneumatophores. Mangrove establishment is optimal in muddy sediments with a high silt content, such as the alluvial muds carried down by river or freshwater surface runoff.

Deltas are typically low-wave energy environments, and thus provide mangroves with protection against harsh winds and waves. Wave action can be highly destructive to mangrove roots that run in the surface layer of the substrate, and can cause erosion where mangroves are growing.

Whereas all deltas are associated with a river system actively depositing sediment to the deltaic plain,

their geomorphological setting varies greatly, depending on the physical process dominating the system. Deltas can be located along low wave energy coastlines with negligible tides and high river discharge, or high wave energy coastlines, or coastlines with extreme tidal ranges. Because each physical process gives rise to different landform types, soils, and biological and ecological characteristics (cf. Coleman, 1976), Coleman and Wright (1975) classified deltas according to their dominating physical process: (1) wave dominated, (2) tidally dominated, or (3) river dominated.

3.2. Mangrove Settings

Thom (1982) modified Coleman and Wright's (1975) classification of deltas by describing five general environmental settings in which mangrove colonization often occurs (c.f. Thom, 1984). However, this classification may not be well suited in all cases and should be used cautiously.

The first setting consists of river dominated deltas along coastlines of low tidal range. Rapid deposition of sands, silts, and clays causes progradation over a flat, gently sloping continental shelf. Wave energy along the shoreline is low. Because of high freshwater discharge, the active distributaries may not themselves be inhabited by mangroves; however, chenier plains, which form in the margins of these distributaries due to mud deposition from longshore drift, are ideal sites for mangrove colonization. River dominated deltas are also characterized by rapid habitat change and morphologically diverse flora and fauna (Thom, 1982). The Mississippi, the Ganges-Brahmaputra, and the Orinoco deltas are examples of this form of deltaic plain.

The second setting is tidally dominated. The main distributaries are fed by numerous tidal creeks and are usually funnel-shaped with broad intertidal shoals throughout the mouth. Mangroves colonize along the shoals and the shores of the main distributaries and tidal creeks. Examples of this setting are the Klang delta in Malaysia and Ord River delta in Australia (Thom, 1982).

The third setting is wave dominated with relatively low river discharge. High wave energy results in a more steeply sloped inner continental shelf than in the other settings. The wave dominated setting is characterized by bay barriers or barrier islands that enclose either drowned river valleys or lagoons, and

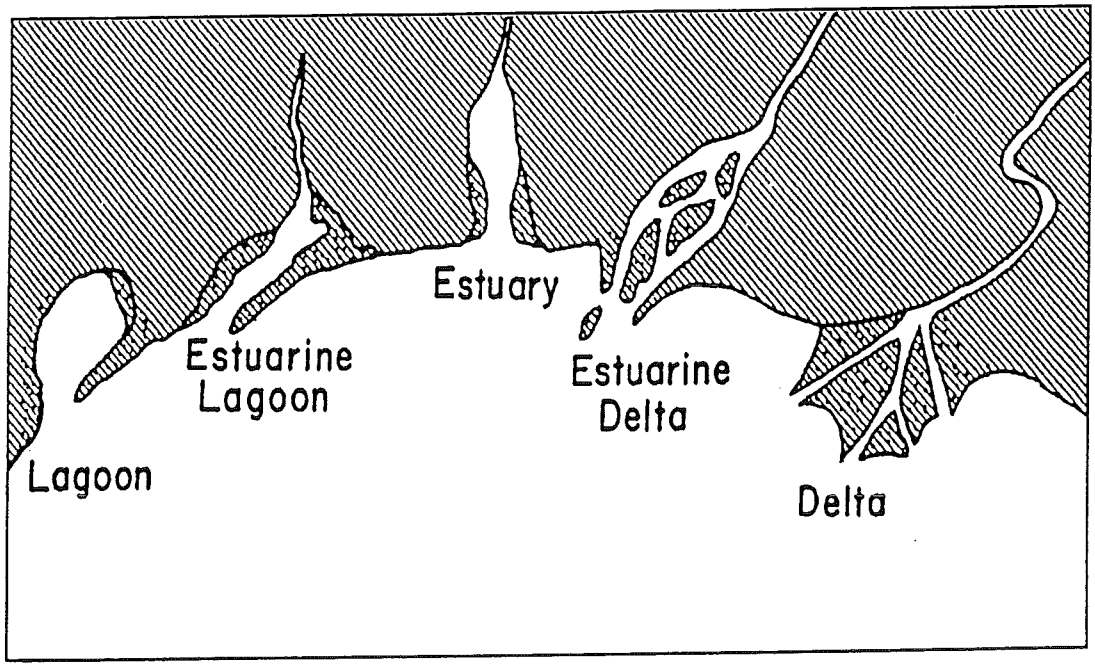

Fig. 1. Spectrum of coastal systems (after Davies, 1973; Kjerfve, 1989).

act to dissipate wave energy. Mangroves are found on the protected leeward side of the barriers and along the shores of the lagoon or drowned river valley. Examples are Laguna de Términos in Mexico and the barrier coastline of El Salvador (Thom, 1982).

The fourth setting is a combination of wave and river dominated processes, with a coastal plain characterized by sand beach ridges and narrow coastal lagoons. Mangroves colonize along abandoned distributaries, near river mouths, and along lagoon shores. A good example of this setting is the Grijalva delta in Mexico and the Purari delta in Papua New Guinea.

The fifth setting is a drowned river valley system with low river discharge, low wave action, and low tidal range. Sediment deposition is minimal, creating an open estuarine system. Mangroves colonize the heads of drowned tributary valleys and along the shores of lagoons behind bay barriers near the estuary mouth. An example of this setting is Broken Bay, Australia (Thom, 1982).

In South Florida, Lugo and Snedaker (1974) recognized five basic mangrove community types distinguished by their hydrological and tidal characteristics. These are: (1) the fringe forest, (2) riverine forest, (3) overwash forest, (4) basin forest, and (5) dwarf forest. This classification scheme has also been applied to mangroves in Puerto Rico, Mexico, and Central America. Its limitation is that mangrove community structure in South Florida differs from that in other parts of the world, for example, Malaysia or Papua New Guinea. This classification may not be well-suited for all regions.

Davies (1973) viewed coastal environments as part of a continuum of geomorphic types from deltas via estuaries to lagoons (Fig. 1). At one end of the spectrum exist coastal lagoons, which are located behind wave-built barrier systems and are characterized by sand sediments. Good examples of this type of environment are the lagoons of the Mexico Gulf Coast (Lankford, 1976). At the opposite end of the spectrum lie deltas, which are river dominated, protrude into a receiving basin, and are characterized by fine-grained sediments derived from terrestrial run-off. Between lagoons and deltas are estuarine lagoons, estuaries, and estuarine deltas, representing a mixture and gradation of the two extreme coastal

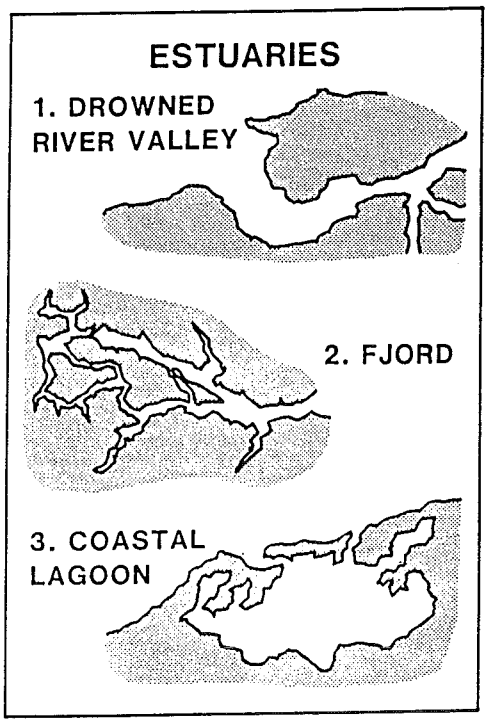

Fig. 2. Schematic diagram of major estuarine types (cf. Kjerfve and Magill, 1989).

environments. Presumably, a decrease of wave energy coupled with an increase of river sediments shifts a system from the lagoon extreme toward the delta extreme.

3.3. Estuaries

Mangrove wetlands are often associated with estuaries and deltas. Kjerfve (1989) developed a functional definition for estuaries which includes the main geomorphic types: (1) drowned river valley or coastal plain estuary, (2) fjord, and (3) bar-built estuary or coastal lagoon (Fig. 2). Although mangroves do not exist adjacent to fjord systems, they are often associated with estuaries and lagoon systems. Kjerfve (1989) defined an estuarine system functionally as a partial coastal indentation with a restricted ocean connection that remains open at least intermittently (Fig. 3). The estuary can be divided into three regions: (1) tidal river zone, a fluvial zone characterized by lack of ocean salinity but subject to tidal rise and fall of water level; (2) mixing zone, or estuary proper, characterized by water mass mixing and existence of strong property gradients reaching from the tidal river zone to the seaward mouth of the system, which is best defined by the location of a river-mouth-bar or ebb-tidal-delta; and (3) nearshore zone, a turbid region, usually in the open ocean seaward of the mixing zone but landward of the main tidal front defined by the extent of the ebb tidal plume.

The boundaries of the three zones are dynamic and change positions continuously, on time scales ranging from geologic to less than a tidal cycle. The landward extent of the tidal river zone can be expected to move downriver with increasing fresh water discharge and change in tidal range from spring to neap. The interface between the tidal river and mixing zones will oscillate over a tidal cycle and move seaward with increasing river runoff. The interface between the mixing and nearshore zones will change much more slowly, usually on time scales longer than the seasonal cycle, but more dramatically, over thousands of years. A severe storm could, however, breach a barrier island or reef (see Hayes, 1978) and drastically relocate this interface overnight. The seaward boundary of the nearshore zone will change

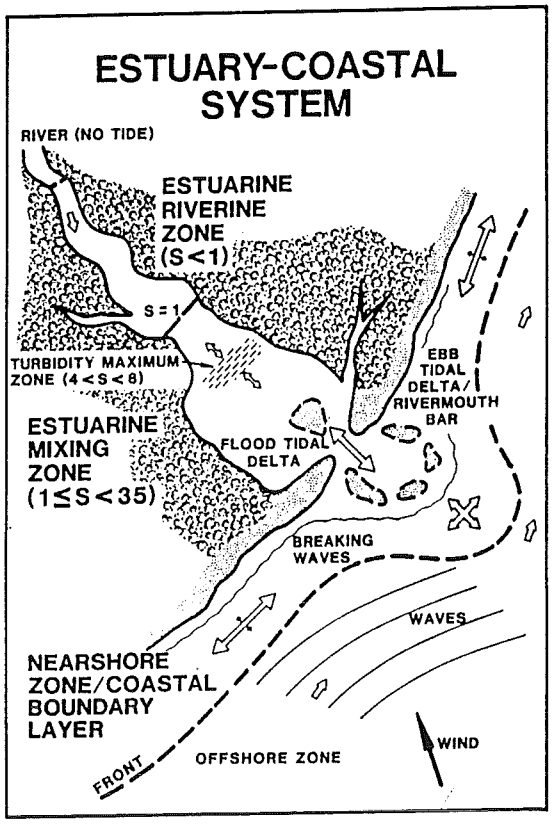

Fig. 3. Functional regions in a hypothetical estuary (Kjerfve, 1986).

positions depending on the stage of the tide, river discharge, and prevailing oceanographic and meteorologic conditions.

In a given system, all zones may not be present. For example, lagoons in arid or semi-arid coastal regions with a small tidal range may not exhibit a tidal river zone, such as in the case of several "hors" along the Makran coast of Pakistan. Similarly, an estuarine/lagoon system may not exhibit a mixing zone if a major river debouching into the estuary happens to be in flood. In such a case, the tidal river could border directly on the nearshore zone, and the estuarine mixing processes would then take place within the nearshore zone. This situation occurs in the Amazon River (Gibbs, 1970). Finally, the nearshore zone may not exist in lagoons where the tidal range and river discharge are small, such as in Cancun Bay.

Mangroves are generally most common in the highly protected intertidal regions of deltas, estuaries, and coastal lagoons, corresponding to Kjerfve's (1989) zones 1 and 2 (Fig. 3). To a lesser extent, they colonize shorelines associated with carbonate reef; however, in such locations mangrove stands are found in protected areas behind a fringing reef, which dissipates strong wave action.

3.4. Coastal Lagoons

Coastal lagoons cover 13% of coastal environments on a global basis (Barnes, 1980) and represent a type of coastal system different from coastal plain estuaries, although both can conveniently be classified as estuaries. They are particularly common in tropical settings and are often associated with fringing mangrove systems, e.g. Laguna Joyuda, Puerto Rico. Kjerfve (1986a) sub-divided lagoons into three major types according to their degree of water exchange with the coastal ocean (Fig. 4). The rate of oceanic exchange reflects the dominant forcing function(s) and the time scale of hydrologic variability.

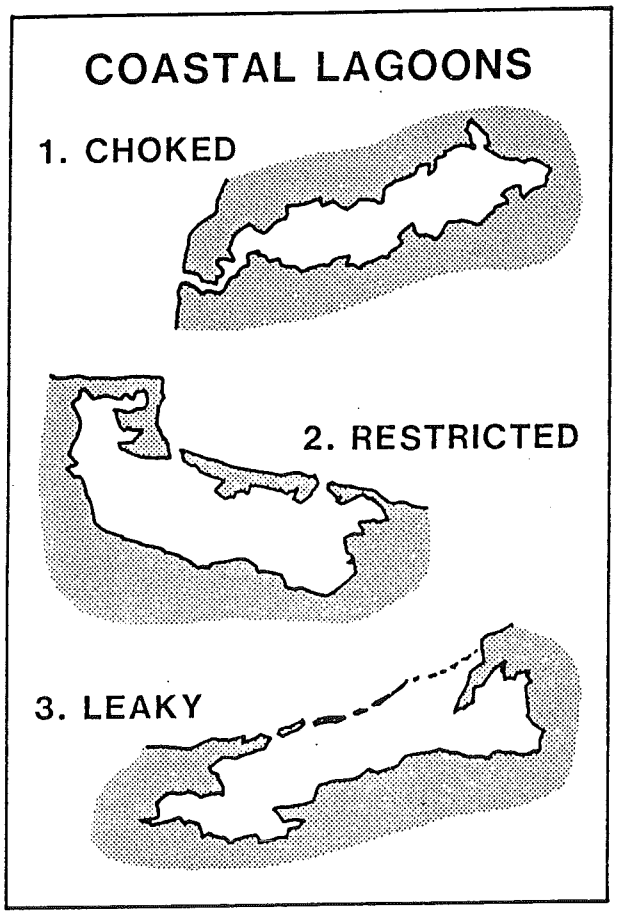

Fig. 4. Main types of coastal lagoons (after Kjerfve, 1986; Kjerfve and Magill, 1989).

Type 1, examplified by Lake Songhkla in Thailand, are choked lagoons, characterized by a single narrow entrance channel, long residence times, and dominant wind forcing. Type 2, examplified by Laguna de Términos in Mexico, are restricted lagoons with two or more entrance channels, a well-defined tidal circulation, strong wind influence, and usually vertically mixed waters. Type 3, examplified by the Belize barrier reef lagoon, are leaky lagoons, characterized by wide tidal passes, unimpaired water exchange with the ocean, strong tidal currents, and the existence of sharp salinity and turbidity fronts. Mangroves flourish particularly in restricted lagoon environments.

3.5. Coastal Waters

Mangrove distribution along coastlines is influenced by oceanic forcing in the form of tides, waves, sea level fluctuations, ocean temperatures, and structure and bathymetry of the continental shelf and slope. The portion of the ocean that comes into direct contact with mangrove wetlands is the coastal boundary layer, a nearshore open coast turbid water mass with estuarine characteristics, separated from adjacent continental shelf waters by a distinct front. An example of the coastal boundary layer (CBL) along the coast of South Carolina, USA, has been redrawn (Fig. 5) from a Landsat 5 thematic mapper (TM) image. The coastal boundary layer usually exhibits high concentrations of sediment, nutrients, and dissolved and particulate organic matter, and is the area for spawning of several species of *Penaeus* shrimp and fish.

The dynamic behavior and physical characteristics of coastal waters induce far-field forcing of circulation in adjacent deltas, estuaries, lagoons, and other sheltered coastal features that are colonized by mangroves. For example, estuarine tides are largely forced by ocean tides at the mouth. Similarly, surface water accelerations in the estuary are forced more by the synoptic wind stress on the coastal ocean surface than by local wind stress in the estuary. This is especially true in the case of narrow, branching, and winding coastal inlets.

Meteorological forcing of coastal and shelf waters by propagating atmospheric pressure systems and wind stress generates continental shelf waves (Mysak and Hamon, 1969; LeBlond and Mysak, 1978). These are trapped, long waves with periods from 2 to 15 days and wavelengths on the order of 1,000 km. They travel parallel to the coast on the continental shelf at phase speeds from 0.1 to 1.0 m s-1 (Brooks and

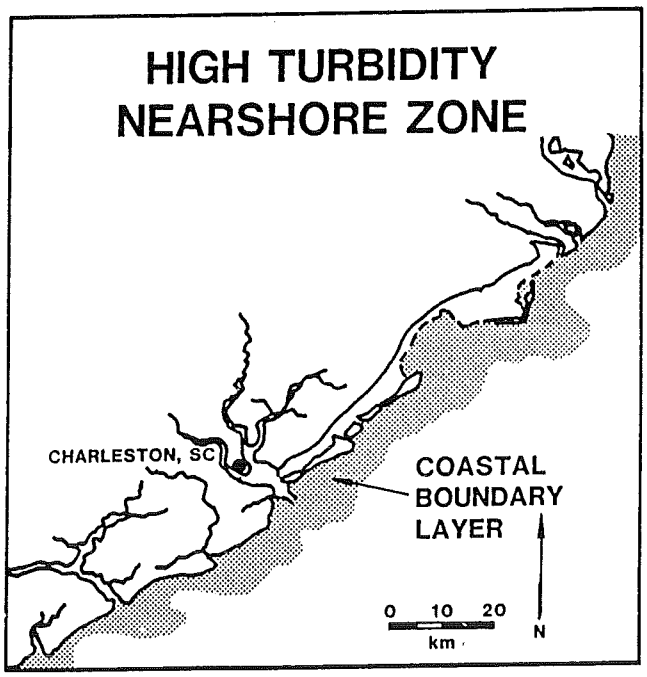

Fig. 5. The coastal boundary layer off the coast of South Carolina, USA, from Landsat 5 Thematic Mapper image.

Mooers, 1977). At the coastline and in estuaries, their associated wave height may be as great as 0.8 m (Kjerfve et al., 1982), but heights decrease exponentially away from the coast.

Continental shelf waves are either forced by local meteorological conditions, i.e., wind and pressure fields, or are free-propagating long waves as a result of distant weather systems. Continental shelf waves represent a commonly occurring form of far-field forcing in estuaries and lagoons; however, the estuarine sea level is also often influenced by nonlinear processes associated with wind-induced surface gravity waves entering the mouth of estuaries and bays.

When high ocean waves of long period either break or impinge on an estuarine entrance, wave momentum is radiated or transferred into the estuary. The result is a raised estuarine water level associated with large and long-period waves as compared to times of little or no oceanic wave action (Thompson and Hamon, 1980).

There are several ecological implications of these long-period estuarine events of non-local origin. Although they are most readily detected by analysis of tidal records, they also have associated low-frequency water flows and material transports, which have bearing on the dispersal of mangrove seeds and propagules. Tidal inundation of mangrove wetlands and adjacent salt flats is considerably more extensive during the passage of a continental shelf wave crest as compared to the passage of a trough for the same tidal conditions. When making measurements of tidal transports or budgets, it is imperative to account for the non-local events with periods of a few days. Otherwise, the material transport and mass budget estimates run the risk of being severely biased. Also, continental shelf waves force up-and down-estuary oscillations of the turbidity maximum zone and the longitudinal position of the salinity field in estuaries.

Dynamic coupling exists between ocean temperatures in the coastal boundary layer, estuarine temperatures, and mangrove distribution. Major eastern boundary currents, such as the California current and the Benguela current, supply cold waters to the adjacent coastal ocean. Mangrove proliferation tends to decline in colder water temperatures, which is one explanation for the low species diversity and growth in mangroves on the western side of continents as compared to mangroves at the same latitude on the eastern side of continents.

4. PHYSICAL PROCESSES

4.1. Sea Level Variations

Coastal mangrove-covered landscapes and landforms exist at their present location as a result of eustatic changes in sea level and global and local land adjustments. During glaciation periods, a considerable fraction of the world oceans have been frozen into continental glaciers. At such times, global sea level reached low stands, with coastlines located near the outer edges of the continental shelves. Deltas and estuaries were then probably both small and rare coastal features because of the short time during which sea level remained at any one elevation. Since the onset of the most recent interglacial stage at the beginning of the Holocene period 16,000 years ago, eustatic sea level has risen 130 m at a rapid but variable pace (Nichols and Biggs, 1985) (Fig. 6). In the process, river valleys and low-lying coastal plain depressions were flooded, river channels were invaded by sea water, and the presently existing coastal plain estuaries and coastal lagoons were formed. Eustatic sea level reached its present elevation approximately 5,000 years ago (Fairbridge, 1980). Since then, small fluctuations in global sea level on the order of a few meters have allowed for the formation of coastal barrier systems due to wave, tide, river, and wind processes. With the flooding of shallow depressions behind the coastal barriers and the continued accumulation of sediment, coastal lagoons were formed (Lankford, 1976), along with protected salt marsh and mangrove wetlands.

Measurements during this century indicate that sea level along tectonically stable coastlines, away from geosynclines, has been rising at a global mean rate of 0.10-0.15 cm/century at the same time that the global temperature has increased 0.4°C (Hoffman et al., 1983) as a consequence of a warming climate and the greenhouse effect.

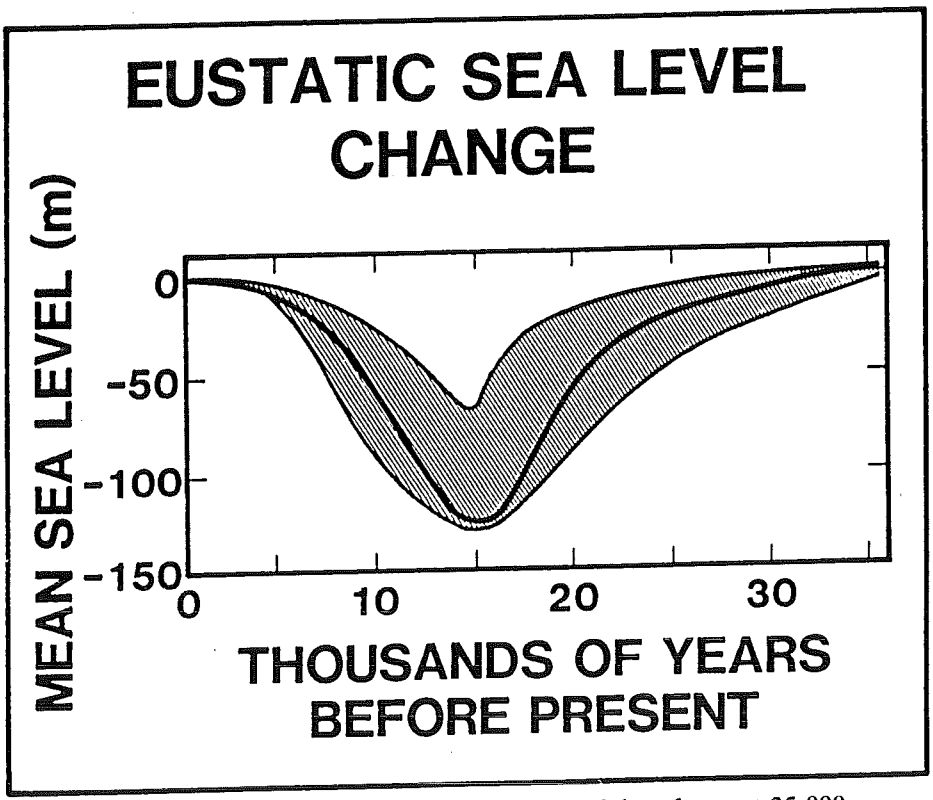

Fig. 6. Eustatic sea level change and uncertainty of data for past 35,000 years.

The relative change in sea level along a particular coast depends on many factors, however. Global sea level rise, due to melting of snow and ice, and volume expansion, due to warming of the oceans, are only two factors. Equally important are (1) changes in the geoid, (2) regional and local tectonic adjustments of the land level, (3) changes in the ocean-atmosphere dynamics (currents, winds, pressure, runoff, wave, and tides), and (4) sedimentation changes (erosion, sedimentation, compaction, land-use, dams, and pumping of ground fluids). Relative sea level rise is often accelerated by human activities such as pumping of groundwater, oil, and gas; construction of dams on rivers; and cutting of forests in river drainage basins. The rapid relative sea level rise of 0.30-0.50 m/century in Bangkok since 1960 represents an extreme case of local delta subsidence, in part the result of pumping of groundwater (Milliman, 1988). In comparison, most of the east coast of North America experiences a more modest relative sea level rise of 0.10-0.40 m/century (Hicks and Crosby, 1974). Palynology, in general, and the distribution of *Nypa* pollen, in particular, have been useful for the dating and marking of mangrove shorelines (Thanikaimoni, 1987; Vannucci, 1989).

Sea level rise is currently receiving much attention, although equal weight ought to be focused on regional and local land level change. The present rate of eustatic sea level rise, 0.10-0.15 m/century, is small compared to the 1.4 m/century rise during the early Holocene. Various scenarios have been modeled to predict sea level rise during the next century as a function of greenhouse warming. Doomsday predictions (Hoffman et al., 1983) go as far as to suggest a possible global sea level rise of 4.5 m during the next century. Although most scientists seem to favor an estimate of sea level rise of 0.5-1.0 m during the next century, there continues to be much disagreement.

In comparison, eustatic sea level has remained at an approximate stand-still for the past 5,000 years (Fig. 6), enabling marine and fluvial processes to fill estuaries with sediment and build deltas and in the process reshape seaward boundaries of continents (Meade, 1969). The time-scale of this sediment infilling is extremely short from a geologic perspective. In fact, it is so short that estuarine deposits laid down more than a million years ago are indistinguishable from other shallow-water marine deposits (Schubel and Hirschberg, 1978). Emery and Uchupi (1972) estimated that if sea level remained constant and all

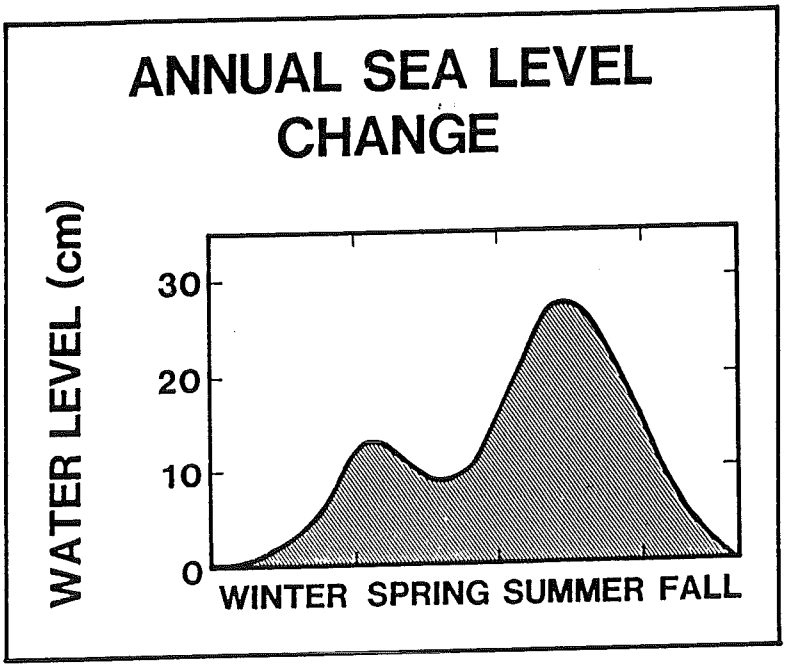

Fig. 7. Typical seasonal mean sea level variation (northern hemisphere).

sediments with the exception of the Mississippi River load were deposited into the estuaries that presently border the United States of America, these estuaries would be completely filled in 9,500 years. Because all deltas do not build at the same rate, various stages of estuarine and deltaic geological development exist along different coastlines (Schubel and Hirschberg, 1978).

The deltas, estuaries, and coastal lagoons formed during the Holocene eustatic sea level standstill (cf. Fig. 6) are the environments that provide the setting for mangroves and salt marshes. Because deltas, estuaries, and lagoons are more common along coasts with broad and flat, rather than narrow and steep continental margins (Schubel and Hirschberg, 1978), mangrove wetlands are more common there as well. Mangroves are best established along actively prograding coastlines (Thom, 1984), a direct consequence of a broad and flat continental shelf margin.

Local relative change in sea level occurs as a result of eustatic sea level change, local subsidence, and tectonic activity. The build-up of mangrove systems, formation of deltas, and shoaling of coastal embayments, estuaries, and lagoons also depend on (1) transport of terrestrial materials from eroding continents by rivers and (2) net up-estuary transport of sand-sized materials from nearshore waters (Meade, 1969), and are enhanced by deposition of mud around mangrove roots. As infilling and progradation continue and coastal landforms progress through different stages of geological development, mangrove succession occurs with one community preparing the ground for another until a climax community is reached. This is often considered to be a tropical rain forest devoid of mangroves (Thom, 1984).

Not only does mean sea level change on the time scale of glaciation and interglaciation stages, but it also changes significantly over a year (Fig. 7). The annual cycle in mean sea level at coastal and estuarine stations is largely explained by changes in specific volume (steric changes) as a result of summer heating and winter cooling of shallow waters with depths less than 100 m (Pattullo et al., 1955). This effect is significant even along tropical coasts where the seasonal variations measure 10-30 cm. At tropical locations, however, the temperature effect is less pronounced and seasonal sea level variability is more a function of changes in synoptic wind and atmospheric pressure patterns, changes in the coastal ocean circulation, long-term astronomical tides, and seasonal pulses in freshwater runoff, including monsoon effects (Pattullo et al., 1955). For example, extreme seasonal mean sea level changes of 1.65 m occur in the upper Gulf of Bengal due to monsoon runoffs (Pattullo et al., 1955). Semiannual changes in mean sea level (cf. Fig. 7) also occur as a result of runoff events, as in the case of the Mississippi River, USA, which produces a springtime high mean sea level. At other stations the semiannual oscillation in mean sea level is associated with variability in the large scale ocean basin circulation (Pattullo et al., 1955). It is clear that seasonal sea level variability can have a dramatic effect on the flooding of coastal wetlands. In the case of North Inlet, SC, tidal inundation of the entire salt marsh is more likely to occur in September than in February, bearing associated ecological impacts (Kjerfve and McKellar, 1980).

4.2. Circulation

Water circulation in coastal waters and wetlands controls turn-over times and plays an important role in the transport of nutrients, sediment, salt, and other dissolved and suspended materials. Thus, water quality is directly related to water circulation. Also, larval recruitment of many species into estuaries and mangrove or salt marsh wetlands depends on local circulation patterns. In calculating mass budgets for coastal ecosystems, it is essential to be able to estimate the import and export of water-borne materials. This requires a good understanding of the circulation and local mixing processes. But care must be exercised in interpreting estuarine processes. Just because the circulation causes water transport does not necessarily mean that dissolved and particulate constituents will be transported in the same direction as the water flow, because material transport also depends on local mixing.

In designing studies of mangrove ecosystem processes, it is essential to have a good understanding of the dominant hydrodynamic time scales. For example, the hydrodynamic residence time of an estuary is the water volume of the system divided by the rate of change of volume due to freshwater discharge, tidal exchange, or water circulation. Comparison of hydrodynamic turnover time to a biogeochemical turnover time indicates whether or not the biogeochemical processes are dependent on the hydrological characteristics of the system. For example, if a coastal water body has a hydrodynamic turnover time of several days, but a phytoplankton population has a turnover time on the order of hours, the two processes are not linked and can be treated separately. Similarly, when considering the sedimentation rate in the same water body with a time scale of centuries, the coupling between the circulation and sedimentation can be treated separately. However, when the hydrodynamic and biogeochemical turnover times are similar, the two processes are coupled and it becomes necessary to study the hydrology in analyzing the biogeochemical process.

Circulation refers to residual or time-averaged water movement. Because water movement occurs on a continuum of time scales, it is critical to choose an averaging time corresponding to the periodic motion with the greatest variability in calculating residual currents. Because coastal and estuarine currents are largely tidal, one or more complete semidiurnal tidal cycles is the appropriate averaging time. Circulation can never be determined from a single instantaneous measurement; rather, it is a quantity that must be calculated based on systematic measurements over an extended time period (Kjerfve, 1979).

The time-averaged currents that constitute the circulation vary depending on location within an estuarine or coastal system and the depth at which the measurements are made. It is common practice to refer to these time-average currents as net currents, tidal residuals, or non-tidal flow.

Three forcing functions drive the circulation in estuarine and coastal waters: (1) freshwater discharge, (2) tidal currents, and (3) wind stress. Variability in oceanographic conditions on the continental shelf can also modify the circulation in many estuaries. This process is referred to as far-field forcing (Elliott, 1976). Wind waves can modify the circulation in wide or exposed coastal systems as well. In mangrove systems, however, the effect of wind waves is of minor importance because mangroves only grow well where wind waves are absent.

Geometry and bathymetry of coastal systems, bottom friction, and rotation of the earth (Coriolis acceleration) do not drive currents directly, but can significantly alter currents in enclosed water bodies. These effects become increasingly important in modifying the circulation as the magnitude of the instantaneous currents becomes greater. Only when currents already exist do these factors alter the flow. Man-made alterations such as dredging, channelization, damming, and channel diversion, can also alter circulation patterns in coastal water bodies.

Each one of the three forces drives a particular kind of water circulation: (1) freshwater discharge induces gravitational circulation, (2) tidal currents drive a residual non-tidal circulation, and (3) wind stress causes wind-driven circulation. Although an estuary or coastal water body is dominated by one of these circulation types, two or all three types could be operating simultaneously in the same estuary, resulting in a complex flow structure that is often difficult to interpret from measurements.

Gravitational circulation is caused by density differences between freshwater runoff and high salinity ocean water. Freshwater runoff, being less dense, has a tendency to remain mostly in the surface layer, although tidal and wind effects tend to mix the water column. This turbulent mixing causes a sustained vertical exchange with high salinity water from the bottom layer mixing into the surface layer, and low salinity water from the surface mixing into the bottom layer. As a result, longitudinal and vertical salinity and density gradients are formed in coastal water bodies. These density gradients correspond to

time-averaged pressure gradients, which drive the gravitational circulation.

The pressure surfaces along the main axis of an estuary tilt seaward in the surface layer, causing a net outflow, and up-estuary in the bottom layer, causing a net landward flow. At mid-depth, the pressure surfaces become horizontal or parallel to an equipotential surface, upon which the gravitational potential is constant. Where the pressure surfaces become horizontal, the net flow vanishes. This level of no motion usually slopes slightly across an estuarine channel as a result of earth rotation (Pritchard, 1952 and 1956) or channel curvature (Stewart, 1957).

The main circulation induced by the mixing of fresh and ocean waters in estuarine systems is the classical estuarine circulation, a form of gravitational circulation (Pritchard, 1956; Pritchard and Kent, 1956; Dyer, 1973). Analytical similarity solutions of the dynamic equations have been obtained for the two-dimensional case, ignoring changes occurring across the estuary (Rattray and Hansen, 1962; Hansen and Rattray, 1965). These solutions provide a firm theoretical basis for understanding the physical dynamics of estuarine systems in which an upper and lower layer are present.

Gravitational circulation also occurs in coastal waters that are well mixed vertically by winds, waves, or bottom-generated turbulence. In such systems, horizontal differences in salinity, and therefore density, still cause a seaward pressure gradient and associated net seaward flow.

The amount of water transported as part of gravitational circulation is always greater than the amount of freshwater discharge. For example, if river discharge into an estuarine system measures R units (in $m^3 s^{-1}$), the surface outflow at the mouth of the same estuary can be 25 R units (Schubel and Pritchard,

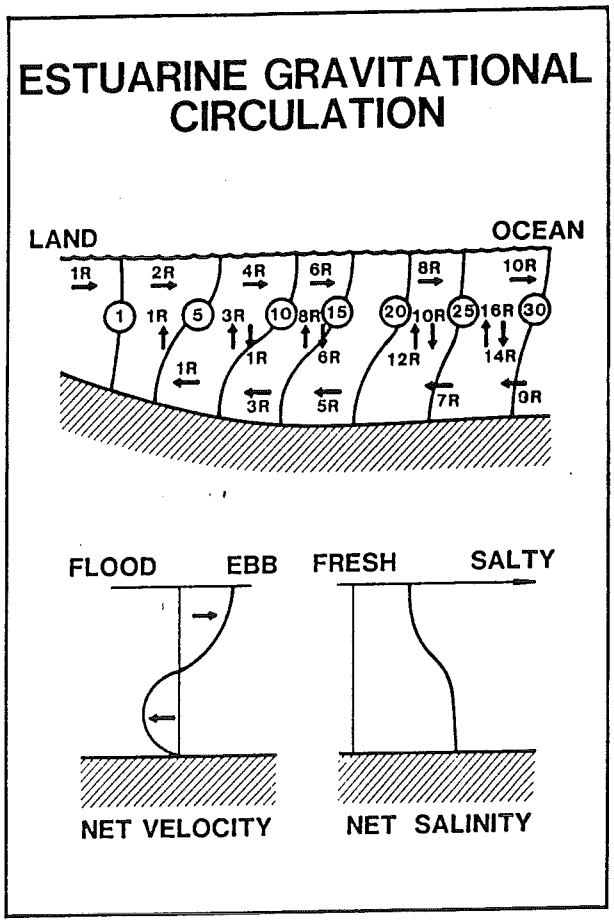

Fig. 8. Schematic estuarine gravitational circulation (after Kjerfve, 1989).

1972), implying that 24 R units enter the estuary in the bottom layer. This concept is diagrammed in Fig. 8 (cf. Dyer, 1973; Kjerfve, 1989). Obviously, the flushing time is significantly shorter for a system with a well developed gravitational circulation. A little bit of freshwater discharge into an estuarine system goes a long way in driving gravitational circulation.

The resulting salinity distribution (cf. Fig. 8) is primarily responsible for the density gradients. In embayments and estuaries, salinity differences have a much greater influence on circulation than either temperature or pressure changes (see Kjerfve, 1979). Temperature differences can, however, drive a gravitational circulation in lagoons that receive little or no freshwater runoff. Intense solar heating of shallow lagoons sometimes causes excessive evaporation, and, because of restricted passages to the ocean, super-elevated salinities in the interior of the lagoon (Collier and Hedgepeth, 1950). In many areas of the world, e.g. northern Australia, there are large fluctuations in the seasonal discharge. Wolanski and Ridd (1986) and Wolanski (1986, 1988) observed that during the dry season, there exists a salinity maximum zone in many tropical Australian estuaries. The salinity maximum is often a few ppt in excess of the coastal salinity and is located halfway between the head and the mouth of the estuary because the combined evaporation from the water surface and evapotranspiration from the adjacent mangrove forest exceeded the runoff. Apparently this situation occurs commonly in many tropical estuaries and mangrove systems and gives rise to a diffusive, ocean-directed transport of salt (Wolanski and Gardiner, 1981). This upstream salinity maxima could also give rise to an inverse gravitational circulation (Wolanski, 1988) and would certainly have implications for mangrove development.

Whereas ocean salinity is 35 ppt, lagoons may commonly exhibit salinities in excess of 90 ppt (Noye, 1973) or higher. This is especially true during the summer in arid or semi-arid regions. Collier and Hedgepeth (1950) suggested that this process sets up an inverse estuarine circulation, with oceanic inflow in a surface layer and outflow of dense saline lagoon water in a bottom layer. It is somewhat questionable whether this is a reasonable hypothesis. Lagoons are often very shallow and open and can thus easily become vertically mixed, particularly by wind. Complete vertical mixing inhibits development of two-layered flow, inverse or otherwise. Rather, salinity or density differences are manifested as differences between ebbing and flooding flow and across the channel rather than with depth. This points to a combination of tides and winds as being more important in driving circulation in lagoons.

Residual estuarine circulation is also caused by instantaneous tidal currents. Strong tidal currents are modified by the bathymetry and geometry of the embayment or estuary. Although the tidal flow is largely oscillatory, it produces a residual tidal circulation through non-linear interactions with bathymetry as a result of bottom friction, shoaling, and changes in width. This usually manifests itself in slight differences in the strength of maximum ebb and flood currents and in the duration of ebbing and flooding tides. When currents are averaged over one or more tidal cycles, the result becomes a net non-zero current induced by the oscillatory tidal flow, and is often stronger than the gravitational circulation.

Non-linear effects in tidal currents occur because of variable cross-sectional width, differences in water depth, existence of tidal flats, and channel curvature, all of which can create large spatial velocity gradients. The time-averaged (residual) tidal currents are often systematically ebb-directed on one side of an estuarine cross-section and flood-directed on the other (Kjerfve, 1978; Kjerfve and Proehl, 1979) (Fig. 9). This is frequently referred to as lateral circulation, and is the result of boundary interaction and channel curvature rather than Coriolis effect. Oppositely directed net currents in a cross section do not imply a net loss or gain of water in the long term. Still, residual tidal circulation is in many systems responsible for systematic export or import of water-borne constituents.

Tidal circulation is particularly pronounced in estuaries with shallow water depth and large tidal range. For example, Kjerfve and Proehl (1979) measured residual tidal flow of 0.5 m s^{-1} in North Inlet, South

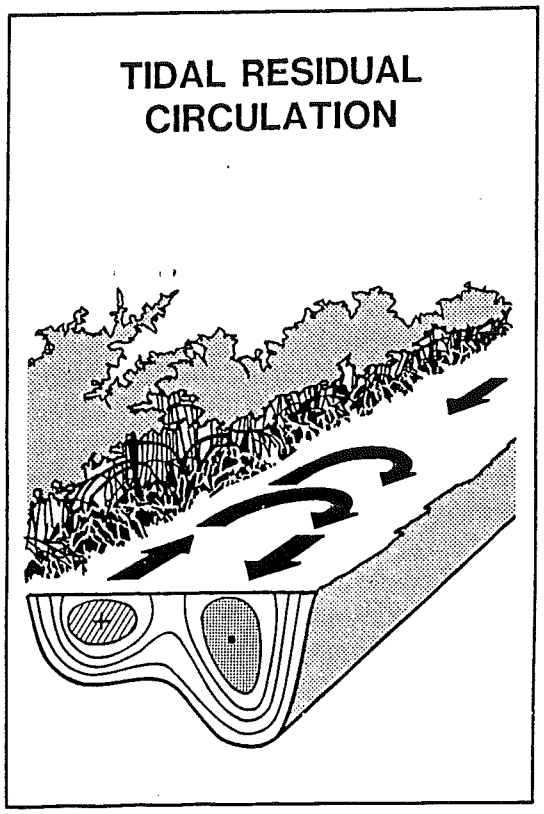

Fig. 9. Tidally driven circulation in estuaries (cf. Kjerfve and Proehl, 1979).

Carolina, USA, and Tee (1976) modeled residual tidal circulation in the Bay of Fundy up to 1 m s^{-1}. Tidal and gravitational circulations co-exist in many systems, although the interaction between these circulation types has received only scant attention. In shallow systems with a tidal range of 2 m or greater and a moderate to high river flow, neither tidal nor gravitational circulations can be ignored.

Wind-driven circulation is particularly important in coastal lagoons. Large expanses of open water, shallow water depth, small tidal range, and low freshwater inflow are conditions that favor dominance of wind-driven currents and water level variations. These currents have not been well-studied because they are highly variable and are often masked by gravitational and tidal flows. Because the wind is variable over a range of periods from minutes to weeks, it is seldom practical to calculate the circulation associated with winds. Rather, the wind-driven, instantaneous currents are of prime interest as mixing agents and in causing material dispersion.

An important energy input to coastal and inshore waters comes from meteorological frontal passages. These can recur every three to twenty days and are most energetic in higher latitudes, but can still be important within the distribution range of mangroves. The duration over which estuarine currents must be averaged to yield the wind-driven circulation is therefore very long, a multiple of the frontal passage cycle (Weisberg, 1976a; Weisberg and Sturges, 1976). This usually makes it impractical to measure the wind-driven circulation and difficult to assess the exact influence of winds on the circulation. However, variations in mean water levels are clearly related to meteorological forcing. If the semidiurnal and diurnal water level changes are filtered out, the mean sea level is still quite variable as a result of meteorological forcing (Fig. 10). Although this forcing can be due to local wind stress, it is probably more often a result of far-field forcing of shelf waters by storm systems.

Several empirical studies point to a major response of the time-averaged estuarine flow to wind-forcing. Weisberg (1976b) found that approximately 48% of the current variability in the Narragansett Bay was related to meteorological variability on time scales longer than two days. Similarly, Cannon (1978) and Holbrook et al. (1980) showed that even deep currents in inlets and fjords can be well-correlated with meteorological events. Water surface slopes as large as 4×10^{-5} radians were attributed to 10 m s^{-1} wind forcing in a Louisiana bar-built estuary (Kjerfve, 1973), and Smith (1977) found significant water exchange between Corpus Christi Bay, Texas and the Gulf of Mexico due to meteorological forcing. These wind tides in Texas lagoons have been well documented (Collier and Hedgepeth, 1950; Copeland et al., 1968). During northerly winter storms, water piles up in the south end of the lagoons. This sets up a seiche movement, with water oscillating back and forth over the length of the lagoon, at a period that depends on the length and depth of the system, but is usually a few hours. The ecological significance of these wind tides is dramatic-a water level change of only a few centimeters can expose hundreds of square kilometers of mudflats or inundate an equally large area of coastal salt marshes and grasslands.

Theoretical solutions of the hydrodynamic equations indicate that a steady, along-estuary wind stress will significantly augment the gravitational circulation (Rattray and Hansen, 1962; Hansen and Rattray, 1965). The effect of a down-estuary wind is to increase the net surface outflow but at the same time increase the net inflow at depth. On the other hand, in the case of a steady wind blowing into the estuary, the resulting net surface current may be flood-directed, a mid-layer would experience net ebb flow, and the net bottom-flow would be much reduced and flood-directed.

The circulation in many coastal plain estuaries exhibits modes which sometimes differ from theory. These modes were initially not reported in the literature because they were thought of as being just "unusual events" (Pritchard, 1978). Elliott (1976), however, identified six different circulation modes based on field data from a coastal plain estuary: (1) classical circulation, with surface outflow and bottom inflow; (2) reverse circulation, with surface inflow and bottom outflow; (3) three-layered circulation, with surface and bottom inflow and outflow at mid-depth; (4) reverse three-layered circulation, with surface and bottom outflow and inflow at mid-depth; (5) discharge circulation, with outflow at all depths, and (6) storage circulation, with inflow at all depths. The classical estuarine circulation was the most common mode in the estuary. It occurred 43% of the time and lasted, on the average, five tidal cycles. The other modes occurred a smaller percentage of the time and usually lasted for one to four tidal cycles. The most remarkable conclusion of this study is that 57% of the time, classical estuarine circulation was not the most common circulation mode. Estuarine circulation is seldom in steady state, but rather exhibits complex temporal and spatial variabilities. Several independent mechanisms are responsible for altering estuarine circulation modes. These include changing wind stress, variations in river discharge, varying tidal range due to fortnightly spring-neap tidal cycles, and far-field forcing from the coastal ocean.

4.3. Material Transport

Estuaries are regions where ocean water mixes with waters derived from land drainage. Mixing is a process whereby a water parcel or water mass becomes diluted or redistributed. The transport of water-borne materials in coastal water bodies is due to a combination of advection and molecular diffusion. But molecular diffusion, which is a measure of the degree of mixing, can always be ignored in natural systems because it is so small. Thus, the transport is really an advective process. Because of the need to average measurements over time, the total transport is parameterized into (1) a low- frequency advective transport component associated with the circulation and (2) a diffusive transport component associated with the turbulent mixing and net transport during the averaging time. Thus, the use of "advective" is rather arbitrary, and depends on the choice of averaging time, which is usually one tidal cycle. Thus, circulation is not a measure of the overall material transport, and it is not possible to deduce

mixing from circulation alone. The advective and diffusive transport components must both be considered to estimate the transport in coastal water bodies.

Water molecules from ocean and runoff sources cannot easily be differentiated. Thus, it is usually impractical to determine mixing by use of isotopic ratios of stable and radioactive hydrogen or oxygen atoms within water molecules. Rather, the distribution in time and space of dissolved materials in coastal waters is used to determine turbulent diffusion coefficients, which, multiplied by the gradient of the mean concentration, is a measure of the diffusive transport component. The dissolved substance is usually salinity, but could be any naturally occurring conservative and dissolved constituent or a dye or radioisotope introduced for the purpose of an investigation. Salinity distribution is most commonly used because (1) salinity is conservative, i.e., salt concentration cannot be altered by biogeochemical processes but only by conservative mixing processes (advection, diffusion, rainfall, evaporation, and freezing); (2) salinity in coastal waters is derived from the ocean source with a salinity of 35 ppt, whereas most land runoff has a salinity less than 0.6 ppt and a different ionic composition; and (3) salinity is measured quickly and easily in the field (cf. Kjerfve, 1979) and does not have to be determined with great precision on account of large temporal and spatial salt gradients within most coastal water bodies.

The overall transport of water-borne materials can be partitioned in a number of different ways and attributed to (1) river discharge, (2) tidal residual circulation, (3) gravitational circulation, (4) wind-driven circulation, (5) storage effects, (5) cross-correlation between velocity and concentration (tidal sloshing), (6) vertical and lateral velocity and salinity shear effects, (7) tidal trapping or chopping, and (8) short-term turbulent diffusion. All of these processes cannot necessarily be separated from each other. Mathematical decomposition of the transport into these different components and the use of field measurements to determine the relative contributions of the processes to the transport have been carried out by Bowden (1963), Pritchard (1969), Fischer (1972, 1976), Dyer (1974), and Murray and Siripong (1978), Kjerfve (1986b) and many others.

The process of tidal sloshing refers to the net transport of particles by oscillatory tidal currents over a tidal cycle. It is usually a major component of the overall transport in shallow tidal systems. When time-averaging the product of estuarine velocity and particle concentration, the integral seldom vanishes because of phase differences between current and concentration time-representations (Kjerfve, 1975; Kjerfve, 1986d). As a result, material transport due to this mechanism is usually transported into estuaries over a tidal cycle.

The shear effect is net transport due to systematic co-variations of velocity and particle concentration over (1) depth (vertical shear; Bowden, 1963); (2) width (lateral shear; Fischer, 1979); or (3) cross- section (cross-sectional shear; Hansen 1965). It is a major inward transport component in coastal systems with strong vertical gradients. Vertical shear and lateral shear are probably equally important (Dyer, 1974; Fischer, 1976; Murray et al., 1978; and Rattray and Dworski, 1980).

Transport due to tidal trapping occurs when water is temporarily caught in shoreline indentations and branching channels, because the tidal current oscillates past these shoreline features. The trapped water parcels and particles are released into the flow and replaced by new water and particles. The net effect is longitudinal material transport (Okubo, 1973; Fischer et al., 1979).

Mixing intensity and material transport in coastal systems is seldom in steady state over several tidal cycles. The same estuary may at times mix quickly and completely because of a frontal passage or strong winds and at times slowly and incompletely because of lack of winds. Similarly, variations in tidal range have been shown to have a profound effect on vertical mixing in the Chesapeake Bay (Haas, 1977). During neap tides with a small tidal range, tidal energy is limited, and the water column becomes

vertically stratified. This stable stratification inhibits vertical mixing. During spring tides, the tidal range and maximum currents are increased, and a sufficient level of tidal energy is available to break down the vertical density stratification. The result is enhanced vertical mixing, allowing nutrients and food particles in the bottom layer to mix up into the photic surface zone and enhance production. Many estuaries behave similarly and alternate between being stratified (limited vertical mixing) and well-mixed (complete vertical exchange) during the fortnightly spring-neap tidal cycle (Haas, 1977).

Many water-borne substances, including suspended sediment, settle out in estuaries and other coastal systems for a variety of reasons. Coastal systems are often sinks for particular constituents and the estuarine and coastal zone act as a filter. This is largely the case with fine-grained sediments from river sources as well as sand-sized sediments from the coastal ocean (Meade, 1969). Thus, one important question to ask is whether a dissolved or suspended constituent mixes conservatively within the estuary. It would do so if the material concentration changed in proportion to the change in salinity. Salinity is a conservative constituent and if a material concentration plotted linearly against salinity, it too would be conservative. Such a plot of salinity against a material concentration is referred to as a mixing diagram. Systematic deviation of a measured estuarine concentration from a straight line in a mixing diagram is interpreted to imply non-conservative behavior of the constituent, and this usually implies that the system is a sink for a particular constituent, or in some cases, a source.

Extreme care must be exercised in using mixing diagrams. The transformation from distance to salinity assumes that (1) measurements are averaged over one or more complete tidal cycles and (2) that concentrations in the ocean and river ends of the system do not fluctuate in time from one tidal cycle to the next (Officer, 1979; Officer and Lynch, 1981; Loder and Reichard, 1981). These assumptions are seldom met in the strict sense. Thus, deviations from a straight line in a mixing diagram may not necessarily mean non-conservative behavior, which in turn could lead to incorrect transport estimates.

4.4. Classification

Hansen and Rattray (1966) produced a useful dynamical classification scheme of estuarine systems based on two non-dimensional parameters. They classified estuaries or coastal systems in a diagram form (Fig. 11) by plotting stratification vs. gravitational circulation. The stratification parameter is the ratio between the net bottom to surface salinity difference to the net depth-averaged salinity. The gravitational circulation parameter is the ratio between the net surface flow to the freshwater flow. The net surface flow assumes steady state and is taken as a representative value across an estuarine section to smooth out lateral effects. The freshwater flow is simply the freshwater discharge divided by the cross-sectional area (Hansen and Rattray, 1966; Kjerfve, 1979; Kjerfve, 1989). The classification diagram can be used to display how particular systems change seasonally. Hansen and Rattray (1966) found that most estuaries could be grouped into four regions on their diagram.

Class 1 estuaries are either coastal lagoons or bar-built systems and are subdivided into two subgroups. Class 1a estuaries are well mixed vertically and include bar-built systems such as North Inlet, South Carolina, (NI) and Mississippi Sound. Class 1b estuaries exhibit vertical stratification and include the Vellar estuary, India (VE). Both subclasses lack gravitational circulation. Net upstream salt transport takes place due to turbulent diffusion processes alone, which in this case includes residual tidal flow and wind-driven currents.

Class 2 estuaries include partially mixed coastal plain estuaries and are divided into well mixed (2a) and weakly stratified (2b) sub-classes. Class 2 estuaries are characterized by a reasonably well- developed gravitational circulation and longitudinal transport by both advection and turbulent diffusion transports. Some examples are the South Santee River, South Carolina (SS), James River, Virginia (JR), and the Narrows of Mersey, UK, (NM).

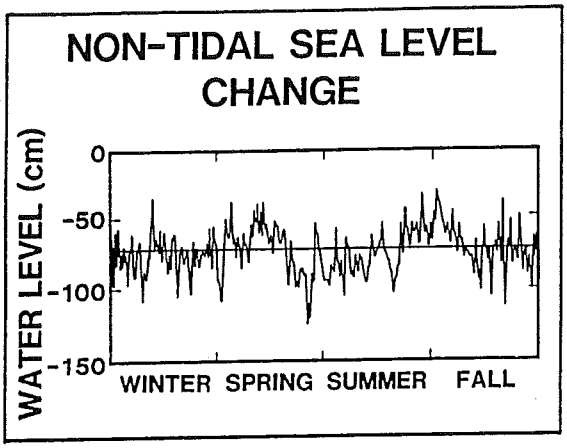

Fig. 10. Nontidal variations in sea level in a salt marsh system (after Kjerfve, 1989).

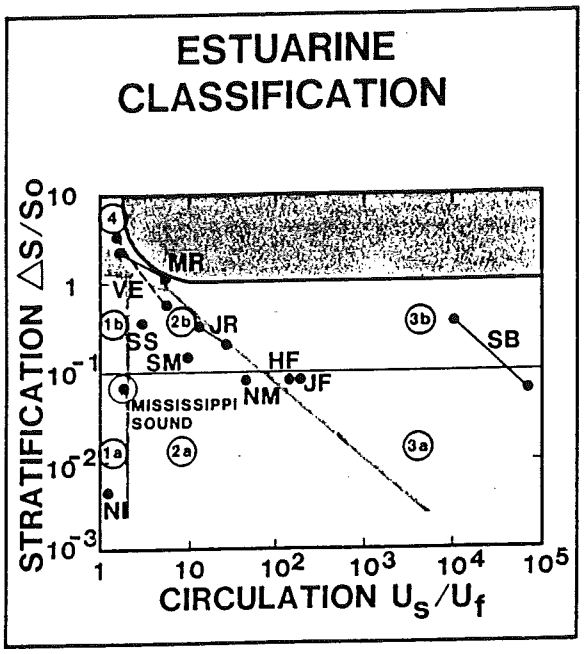

Fig. 11. Estuarine classification based on circulation and stratification (Hansen and Rattray, 1966).

Class 3 estuaries are characterized by strong gravitational circulation and medium to strong stratification. This class includes most fjords, e.g., Silver Bay, Alaska, (SB) and Himmerfjrd, Sweden (HF), and a number of estuarine straits, including the Strait of Juan de Fuca, Washington (JF).

Class 4 estuaries are strongly stratified systems without gravitational circulation. Vertical mixing is caused by entrainment due to breaking internal waves. The lower Mississippi River (MR) belongs in this category.

5. STUDY DESIGN

5.1. Philosophy

To accomplish a meaningful estuarine hydrographic study in mangrove environments requires a carefully planned sampling strategy. An optimum study design depends, however, on the hypotheses to be tested and the overall objectives. There is thus no simple cookbook recipe for such. This manual is designed on the assumption that the study objectives are to (1) describe the hydrological characteristics of a coastal system consisting of mangrove wetlands, adjacent estuarine water mass, and bordering turbid coastal marine waters separated from the shelf waters by a sharp water mass front, (2) estimate mass balances of a mangrove-estuarine system from direct and indirect measurements of water-borne material fluxes from the system, and (3) analyze field and map measurements to allow a synthesis of the dominant hydrological processes in support of hypothesis testing and subsequent modeling. Thus, a major component of the study consists of making hydrographic measurements in the water body bordering the mangrove system. This section is concerned with designing a strategy for carrying out such hydrographic measurements in an estuary or enclosed water body.

Estuaries and other semi-enclosed coastal systems typically experience large spatial and temporal variations in material concentrations, water elevation, and flow velocity as a result of tidal influence, freshwater discharge, meteorological forcing, and basin geometry and geomorphology. Both horizontal and vertical spatial variations are the norm. For example, the classical estuarine circulation (cf. Dyer, 1973) emphasizes processes operating in only two dimensions, along the length of the estuary or channel axis and over depth. It is now recognized, however, that lateral variability in the longitudinal flow and transport may be just as important as the longitudinal-vertical processes in contributing to a residual circulation and material flux over one or more tidal cycles (Dyer, 1977; Uncles and Kjerfve, 1986).

To facilitate analytical solutions to governing equations, estuaries have often been assumed to operate in a quasi-steady state fashion, implying that temporal changes primarily occur on tidal and shorter time scales, not exceeding a day. Long-term trends are assumed to be non-existent. This usually doesn't agree with measurements, however, and coastal water bodies are seldom in quasi-steady state. Even when averaging flows and transports over complete tidal cycles, comparison of successive residual flows and transports indicates that circulation and dispersion can experience dramatic low-frequency fluctuations due to changing meteorological conditions and river flow variations (Elliott, 1976).

Semi-enclosed coastal systems are therefore difficult to study analytically, which is why it is now common to implement numerical circulation and dispersion models on coastal systems to simulate tidal water elevations, currents, material distributions, and fluxes. Modeling does not remove the need for field work, however; high-quality field measurements are still necessary for model calibration and verification. Choosing an optimum sampling strategy is thus now more important than ever because the same data needed to describe a hydrological system are also needed as input rates to the model. The data must also be collected in such a manner that it can be used to verify the model. These data requirements place extra importance and constraint on the field strategy in terms of selecting (1) location of sampling stations, (2) number of sampling stations and depths, (3) sampling frequency, (4) sampling duration, and (5) types of measurements. These parameters will vary with each study, the geographic and physical characteristics of the system, and the available personnel effort.

5.2. Sampling Stations along an Estuary

For adequate horizontal characterization of estuarine processes, distance between stations along the main axis of an estuary should be great enough that differences in mean station values are larger than the sampling errors, yet small enough that gradients between stations are reasonably linear (Kjerfve, 1979).

In practice, this means at least one sampling station for every 5 ppt change in salinity along the axis of an estuary. Assuming, as is so often the case in many tropical countries, that little or no prior information about the estuarine dynamics exists, a preliminary survey should be conducted to identify the optimal station locations. Because far-field forcing from the adjacent ocean can have profound effects on physical processes in estuaries and enclosed waters, it is always desirable to establish reference stations in either the coastal boundary layer or offshore waters, whenever feasible.

5.3. Sampling Stations across an Estuary

If discharge or flux of materials is a purpose of the study, it is usually necessary to sample from several stations in an estuarine channel or cross section. Three stations in a cross section are usually the minimum necessary (Kjerfve, 1979; Kjerfve et al., 1981). Boon (1977) showed how the instantaneous discharge error for a cross section decreased with a greater number of stations. But if the instantaneous lateral and vertical velocity distribution are known beforehand, a single sampling location in a cross section may suffice in determining flow discharge and material transport (Kjerfve, 1976; Kjerfve et al., 1981).

Kjerfve et al. (1981) developed a formula for selecting the number of cross-sectional stations necessary to ensure that the root mean square deviation of measured instantaneous discharge from the actual discharge is less than 15%. For a constant estuarine tidal prism, a deep water depth would typically imply a relatively narrow estuarine cross section and a shallow depth would imply a relatively wide cross section. The wider the cross section, the more significant lateral bathymetric irregularity is likely to exist. Thus, for deep estuarine systems, fewer lateral hydrographic stations are required for flux computations as compared to shallower water systems.

It is convenient to define a lateral station density parameter, β (m^2/station),

$$\text{as} \quad \beta = P/h_o N$$

where P (m^3) is tidal prism, h_o (m) is the average mean tide cross-sectional depth, and N is the number of sampling stations required to keep the maximum possible discharge or material flux "error" below 15% (Kjerfve et al., 1981). The tidal prism is computed as either the average water discharge (m^3/s) or average mass transport (kg/s) of a given dissolved or suspended constituent passing through the cross section during half a tidal cycle. Even in the absence of detailed velocity measurements, both P and h_o can easily be estimated from a hydrographic chart and tide table.

The lateral station density parameter, β, is conveniently computed based on water flux measurements, which usually agree well with constituent fluxes. The equation for β is useful in determining N, the optimum number of cross-sectional stations in an estuarine flux study. To achieve a percentage error less than 15%, $\beta = 2 \times 10^6$ m^2/station could be used to select the minimum number of lateral stations, i.e., by solving for N in the above equation (Kjerfve et al., 1981).

When selecting station locations it is also necessary to consider the bathymetry, particularly if the goal is to calculate material flux. Shallow areas and channels in the estuarine system should be given adequate representation (Kjerfve, 1976; et al., 1981). For example, when sampling along a cross section where distinct channels and shallow areas exist, a station should be designated in each bathymetric region for accurate flux measurements (Kjerfve et al., 1981).

5.4. Number of Sampling Depths

For adequate definition of vertical profiles, velocity and concentration measurements should be made from several depths, provided the water depth at a sampling station is sufficiently great. For shallow estuarine systems, it is common practice to make vertical measurements every meter between surface and

bottom. All these measurements are not necessarily used in the analysis; rather, interpolated values at fixed relative depths are often chosen for the calculations of residual currents and fluxes (Kjerfve, 1975).

The United States Geological Survey (USGS) has established procedures for determination of depth-averaged velocity for discharge and flux calculations at a cross section (cf. Buchanan and Somers, 1969). They use six different methods based on velocity measurements made at various depths in the water column: (1) the vertical-velocity curve method, where measurements are taken at 0.1-depth increments between 0.1 and 0.9 of the total water depth; (2) the two-point method, where measurements are taken at 0.2 and 0.8 of the water depth from the surface; (3) the six-tenths-depth method, with one measurement taken at 0.6 of the depth from the surface; (4) the two-tenths-depth method, with one measurements made at 0.2 of the depth below the surface; (5) the three-point method, where measurements are made at 0.2, 0.6, and 0.8 of the depth; and (6) the subsurface method, where a measurement is made at some distance below the water surface, at least 0.5 m. This last method is used when depth soundings cannot be made. The USGS uses all six methods in different situations, depending on water depth and bathymetry. The two-point method is the one most often employed (Buchanan and Somers, 1969).

It is important to note that direct reading instruments record vertical profile measurements sequentially with depth. Thus, a reasonable estimate of the mean of the turbulent fluctuating value must be made at each depth. This takes at least a minute, and even then, if the instrument display is visual, operator bias is inevitable. Also, if direct measurements are made at several depths, the time lag between measurements must be taken into account in the analysis.

5.5. Sampling Frequency

Choosing the proper sampling frequency is essential to avoid aliasing the data sets. Aliasing is the introduction of variability into a data set because sampling was conducted too infrequently. If sequential data are sampled at a rate 1/dt, where dt is the elapsed time between samples, any significant variability at higher frequencies than the cut-off frequency, $f_c = 0.5dt$, will contaminate or alias the data set (Kjerfve, 1986). Hydrographic sampling should always be carried out in such a manner that major periodic variabilities are sampled at least 6-8 times during a single cycle. If the semidiurnal tide is the main source of velocity or salinity variability in an estuary, sampling should be conducted at least 6-8 equally spaced sampling times during a single tidal cycle. How aliasing can contaminate a time series record is illustrated in Fig. 12. If sampling is conducted at too low a frequency, it will cause variance that is actually at a higher frequency than the cut- off frequency to appear to be lower than the cutoff. Little can be done to correct data that have been measured at too low a sampling rate relative to the dominant periodicity that exists.

5.6. Sampling Duration

The selection of a suitable sampling duration for determining time-averaged estuarine conditions is critical. Elliott (1976) showed that time-averaged estuarine currents frequently reverse directions and can be highly variable from one tidal cycle to another. In most estuaries, the greatest portion of variability on time scales of 2 to 20 days occurs in response to meteorological forcing, e.g., wind stress and atmospheric pressure fluctuations. Weisberg (1976a) argued that averaging over only a few tidal cycles is not enough to obtain meaningful non-tidal current or flux estimates. To address long term net transport of a constituent, it is essential to make measurements for many consecutive tidal cycles. Thirty or more may be necessary (Weisberg, 1976a; Kjerfve et al., 1981). If the sampling duration is too short, the resulting time averages will not be representative of long-term conditions in an estuary. On the other hand, if the objective is, for example, to predict the maximum concentration of a pollutant in response to varying discharge along the axis of an estuary, a long-period mean would be of little help. Rather, a tidal simulation model study might be the best way to address such a problem.

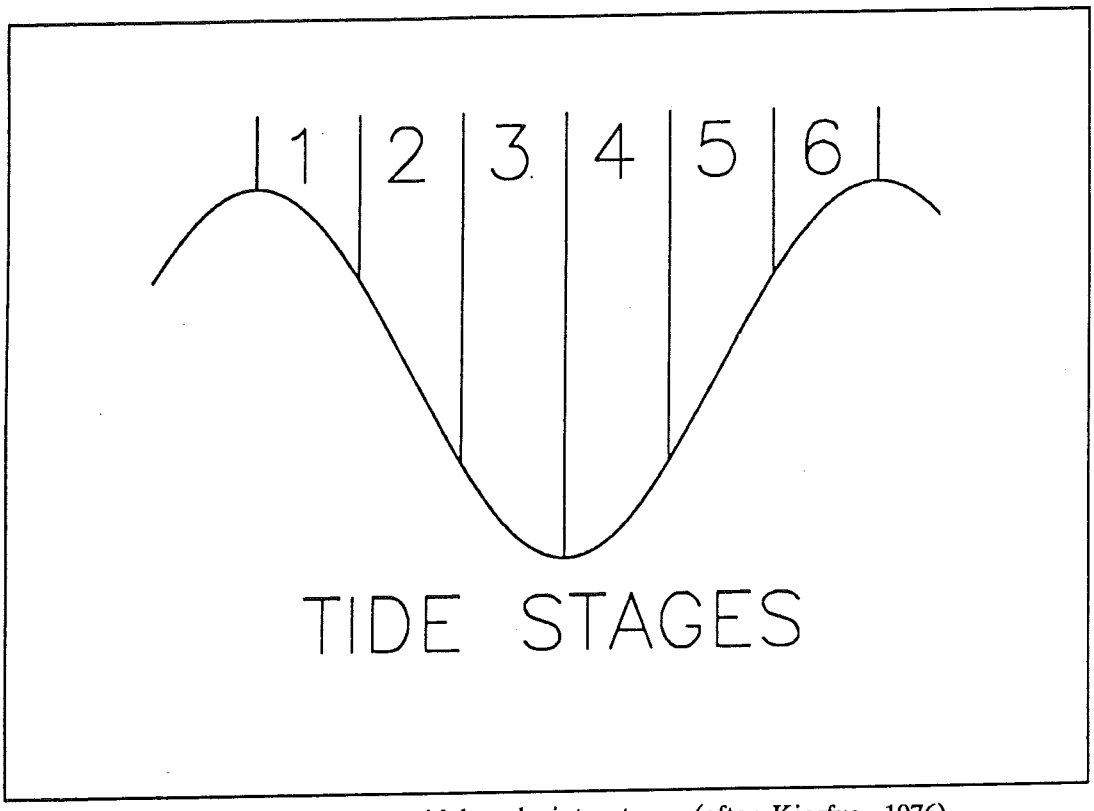

Fig. 12. Division of an arbitrary tidal cycle into stages (after Kjerfve, 1976).

5.7. Sampling Procedure

Because many hydrographic surveys in estuaries employ direct reading instruments, a sampling duration of 12.5 hrs or 25 hrs is common. Ideally, a boat should be anchored at each station. During the Project Outwelling study in the North Inlet salt marsh (Kjerfve and Proehl, 1979; Kjerfve et al., 1981), up to 11 boats were simultaneously anchored on four-point moorings using augers screwed into the bottom. This ensured that each boat maintained a constant position from ebb to flood tide so that the measurements of water depth could be used to measure tidal height. It became necessary to re-adjust the length of the four anchor lines repeatedly, keeping them pulled tight, so that the boats were not pulled under the water surface as the tide rose or allowed to drift with the current as the tide fell. Anchoring the boats in this fashion ensures that sampling can be done simultaneously from many platforms at fixed, equally spaced time intervals.

This is often impractical because of logistic constraints. Usually, a hydrographic sampling team only has access to one or two small boats. A series of stations along the axis of the estuary must therefore be sampled sequentially over complete tidal cycles using one or more roving boats. These boats should be employed to sample stations in a fixed order at preset, equally spaced time steps. One hour or 1.5 hours is usually the longest acceptable interval between measurements at a single station. If roving boats are used, a single boat must cover a number of stations repeatedly and return to the original station, let us say every 1.5 hours. The number of required boats thus depends on size of the estuary, number of stations, boat speed, and proficiency of the sampling crew. In analyzing the data, it is desirable to use data points for the same time from each station. This can be done by a cubic spline interpolation of data time series from each station, interpolating values at desired times and using these in the analysis (Kjerfve, 1979).

An alternative sampling strategy is to sample fixed stages of the tidal cycle on successive tides and then average all data from the same stage but from different cycles. This is analogous to stratified sampling in statistics, with tidal stage as the variable on which the blocking is done. Kjerfve (1976, 1978) successfully used this scheme in several estuarine studies, alternately using 6 and 8 stages (Fig. 12). Calculation of the exact duration of tidal stages should be done prior to sampling, and the times should be adjusted afterwards by allocating measurements to the correct stage. The idea is that most of the variability in hydrographic data occurs as a function of tidal stage. This sampling technique makes it possible to calculate means and standard deviations of measurements within each stage for an average tidal cycle during the sampling period. This sampling strategy is useful when a single investigator with access to only one boat wants to conduct a hydrographic study of estuarine waters.

6. GEOGRAPHIC CHARACTERISTICS

6.1. Drainage Basin

A first step in a hydrological investigation of a mangrove wetland system is the determination of a number of geographical parameters to provide the investigator with an overview of the system. This allows him to approach the study holistically, which ensures that specific details and measurements are considered as a component of the whole landscape, of which the mangrove ecosystem usually is only a small part. For environmental decision makers and managers, this is also a good approach for emphasizing how activities within the drainage basin might indeed impact the mangrove ecosystem. Diversion of rivers, damming of rivers, major construction, pollution discharge, and agricultural and other activities within the drainage basin will ultimately impact the mangrove wetlands. This, in turn, can have long-term consequences for the state of health of the renewable mangrove resource and the role that mangroves play in fueling coastal fisheries.

The first task should be determination of size and extent of the watershed or drainage basin, of which the mangrove system usually constitutes the marine fringe in tropical coastal environments. This is best accomplished by tracing from a topographic map in the scale range from 1:25,000 to 1:250,000. Although drainage basins are not usually marked on maps, it is easy to estimate the extent of a drainage basin by following rivers, streams, and tributaries upstream and using topographic information on the map to identify drainage divides. The drainage basin should be traced and the area determined using either (1) a planimeter or (2) counting the number of 1x1 mm squares covered by the drainage basin and converting this to km^2 depending on the scale of the map. The latter can be accomplished easily by taping the traced outline map against a backlit window, placing the 1x1 mm tracing or engineering sheet on top of the map, and retracing the desired area onto this sheet. For example, using either a planimeter or the square-counting technique, the drainage basin of the Lagoa Mundaú-Lagoa Manguabe system (Fig. 13) in northeastern Brazil was estimated to measure 7,300 km^2. In comparison, the lagoons cover only 90 km^2, and the fringing mangrove system occupies a smaller area still. These determinations were made using a map of scale 1:250,000. Had it been possible to use a larger scale map, for example, 1:50,000, the resulting area estimates would probably be both somewhat different and more accurate. On the other hand, the extra time and effort to improve on area and volume estimates is often unworthwhile; they can better be spent on other tasks. The initial consideration of the entire mangrove drainage system emphasizes the point that human activities 150-200 km away, in the case of the Mundaú-Manguabe system, can impact the mangrove ecosystem.

6.2. Mangrove Area

The second step is the determination of the extent and area of the mangrove wetland. This can usually be accomplished by tracing the mangrove ecosystem boundaries on a topographic map. When in doubt, use aerial photographs, satellite images, and personal observations and knowledge in estimating the boundaries. The area of the overall mangrove system can be determined by planimetry or by counting the number of 1 mm^2 squares and converting scales.

A useful next step is to get a more detailed determination of topography and bathymetry of the mangrove system for construction of a hypsometric area versus height diagram. This can be a time consuming chore, but a hypsometric curve is a very helpful tool in interpreting the extent of sediment infilling, the tidal prism, and the degree of inundation of a mangrove wetland. This information is also invaluable in hydrodynamic modeling of water flow and material transport. Application of continuity principles to estuaries with similar tidal range and period but with varying hypsometric characteristics gives rise to significant differences in peak currents, duration of flood and ebb tides, and mass transport rates and directions (Boon and Byrne, 1981; Seelig and Sorensen, 1978).

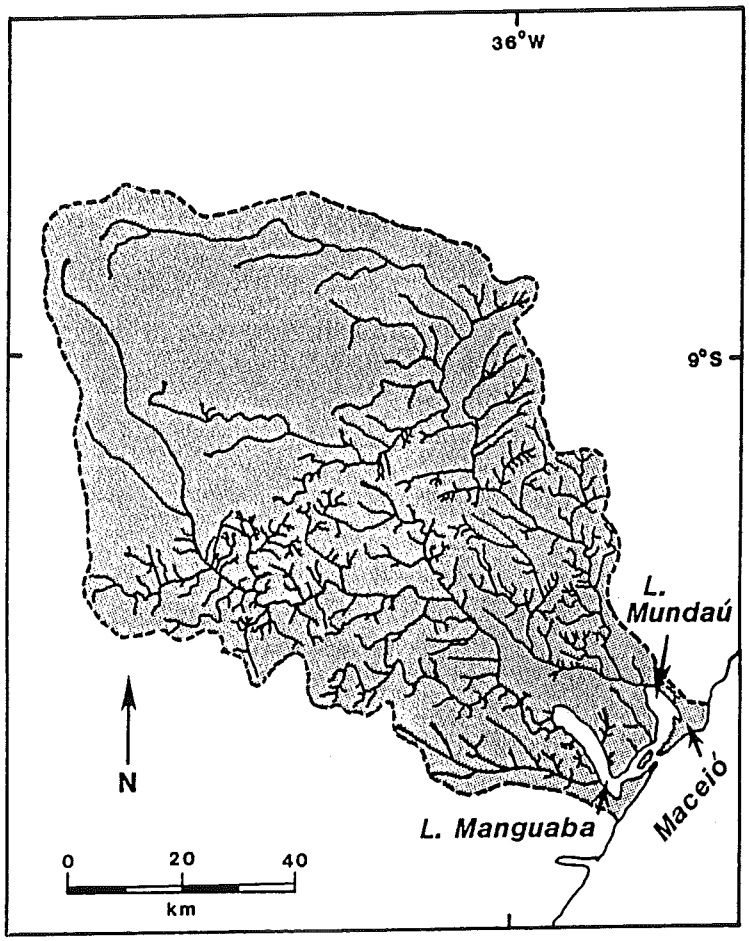

Fig. 13. Drainage basin for a tropical lagoon system in Alagoas, Brazil.

6.3. Topography and Bathymetry

The topography of a mangrove area can be determined using standard surveying techniques. Because the total relief within a vegetated mangrove wetland is usually less than the tidal amplitude, vertical elevations usually need to be measured with a precision of 1-2 cm to yield useful results. Topographic mapping involves measurements of vertical elevation changes of the ground every 10-30 m along transects through a mangrove wetland, using a levelling instrument (level) and a rod, and referencing the measurements to established bench marks. These are usually tied into national elevation networks. In the case where a bench mark does not exist or is located too far away from the mangrove area, it becomes necessary to establish a relative benchmark. This can be done by pounding a metal post securely into the ground and using the top of the post as the relative benchmark, or selecting a marker on a stable concrete building or bridge as the vertical elevation to which all other measurements are referenced. The benchmark serves not only as a reference mark for (1) topographic measurements but also as a reference for (2) bathymetric surveys and (3) tidal water level measurements.

Using a level and rod to measure the topography along transects through mangrove wetlands is not an easy task because of (1) soft and unstable substratum, (2) tangled mangrove roots, (3) tidal inundation, and (4) numerous tidal creek channels. The best time for establishing elevation transects is at low tide during the dry season. Even then, the topographic determination can be a formidable undertaking.

In addition, the bathymetry of tidal channels and adjacent waters must be determined separately. This is usually done from a small boat, using either (1) a fathometer, or (2) a weighted line marked off in

meters and decimeters. A number of cross sections should be selected from a map or chart. The bathymetry should be measured for each cross section every 1-100 m, depending on the size of the estuary or creek, using fixed bearings on each side of the channel to aid in location of measurement points. Because tidal creeks most often vary in depth from 2-10 m, it is usually satisfactory to make depth measurements to the nearest 10 cm. Greater precision is seldom feasible because of waves. Care must be taken to note the time of a bathymetric transect and to obtain the tidal water elevation for the same time from an adjacent tide gauge or from tidal prediction. The tide gauge reading should presumably have been referenced to the local bench mark; if not, this needs to be done.

Once the topography and bathymetry have been established for a sufficiently large number of points in the mangrove wetland and adjacent estuaries and creeks, it is time to draw elevation and depth contour lines for the system as a whole. The more measurement points, the more accurate the resulting map. The measurements are almost never spaced evenly across the system because of the way the measurements were made along transects. Thus, the contour mapping is not straightforward and is a mixture of art and science. In drawing contours, it is wise to remember that both depth and elevation for the most part vary normal to channel and estuary sides. Also, vegetation within mangrove wetlands is often a clue to distance to the nearest creek or elevation, which can be used as an aid in the construction of a contour map. The choice of contour intervals depends on number of measurement points, precision of measurements, and vertical relief within the mangrove wetland. As a rule of thumb, a hypsometric diagram should be based on at least 10 points, but preferably more. The contour interval should be chosen to have at least 3-5 data points within the vegetated wetlands area. This usually implies a contour interval of 20-30 cm. The plotting of contours can either be done manually or using a computer contouring routine such as the National Center for Atmospheric Research (NCAR) software package (McArthur, 1983). If a computerized contour routine is used, it is always necessary to verify that contours are plausible and to edit the contour plot accordingly. The areas between contour lines can be determined by the use of a planimeter or counting 1x1 mm squares, and will be used to construct a hypsometric diagram.

Eiser and Kjerfve (1986) used an alternative method to measure the topography of a salt marsh system, but it could also prove useful in mangrove studies as long as the mangrove canopy is not too dense. Their method involves taking a series of aerial photographs of the tidal wetland every half hour from slack low to slack high water. The overflights should ideally be made on a spring tide when the entire wetland floods at high water. Photographs should be taken on a rising rather than falling tide to ensure that no residual pools of water stranded on the swamp will appear in the images. False-color infrared film, for example, Kodak Aerochrome 2443 23x23 cm transparency film, is ideal because the wetted swamp surface absorbs a much larger percentage of incoming infrared radiation than the dry wetland area, thus providing clear delineation between wet and dry areas. Delineation is usually too faint on visible-wavelength film. The large film format is preferable for ease in digitizing.

The aerial photographs must be rectified before digitizing because small changes in the altitude and attitude of the plane between successive passes will change the scale of the image. A simple way to rectify an image (Eiser and Kjerfve, 1986) is to construct a base map from the first series of photographs, marking key reference points. Each successive image is projected onto the base map by repositioning an overhead projector until the image aligns with the base map. The water boundary is then drawn on the map. This process is repeated until land and water boundaries, in half-hour increments, have been drawn onto the base map for the entire flood tide. If instantaneous tidal water surface slopes are sufficiently small and the system is not too large, the land and water boundaries will coincide with topography contour lines. If these conditions are not met, it is necessary to correct for water surface slopes (Eiser and Kjerfve, 1986). The Eiser and Kjerfve (1986) contour map of a South Carolina salt marsh drainage basin is shown in Fig. 14. The change in flooded area between sequential overflights, i.e., between contours, can be measured using a planimeter or by counting 1x1 mm squares on the base map.

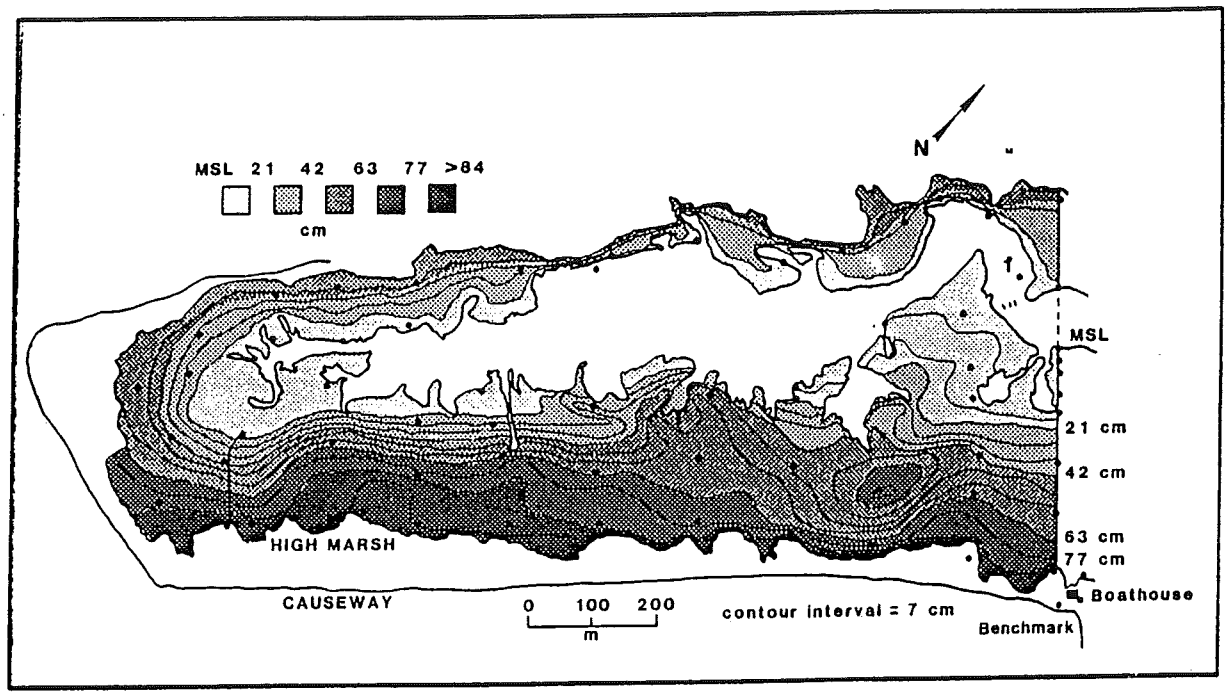

Fig. 14. Topography of the Bly Creek salt marsh basin in South Carolina (after Eiser and Kjerfve, 1986).

6.4. Hypsometric Characteristics

Strahler (1952) was the first to describe a wide class of erosional landforms using a hypsometric relationship, i.e., a diagram of elevation as a function of area. Boon (1975) and Boon and Byrne (1981) modified Strahler's relationship and applied it to tidal wetland systems. Their hypsometric relationship can be expressed

$$a/A_{max} = \{1-h/H\}^{\tau}/\{r+(1-r)(1-h/H)^{\tau}\}$$

where A_{max} is the total basin area flooded at the highest water elevation, the basin full stage; a is the portion of the total basin area above an elevation contour h; and H is the water elevation difference between basin full stage and the minimum water level h = 0 for which the water-covered area of the basin equals A_{min}. The constant $r = A_{min}/A_{max}$ can be calculated directly from the topographic and bathymetric map of the mangrove system. The parameter, τ, must be determined empirically for any basin. It is always positive and has been found to vary from 1.0 to 5.0 for a number of basins (Boon and Byrne, 1981). The values of the parameters r and τ control the shape of the theoretical hypsometric curve, shown in Fig. 15 for $r = 0.1$ and $\tau = 2.1$.

Constructing a hypsometric diagram for a mangrove basin consists of plotting the values of h/H vs. a/A_{max} for a range of elevation contours. The parameter r is calculated from the basin area data. The next step is to plot the theoretical curves for the hypsometric relationship for a series of different τ-values, probably in the range 1-5. The theoretical curve that best fits the field data allows the determination of τ.

A hypsometric diagram can be used to compare mangrove basins of different scales and indicates (1) relative proportion of sediment infilling and (2) tidal prism. The area under the hypsometric curve represents the proportion of solid matter within a basin. A mature basin consists of much more solid matter than water with values of g approaching 1. An immature basin consists of more equal parts solids and water with a value of τ in the vicinity of 5. The tidal prism for any tidal period is represented by the portion of the diagram to the right of the hypsometric curve (Fig. 15) between high water (HW) and low water (LW) marks. By using a planimeter or counting $1 \times$ mm squares corresponding to this diagram area and converting to dimensional scales, the actual tidal prism in m^3 can be calculated.

7. FRESH WATER BUDGETS

7.1. Importance of Fresh Water Input

The input of fresh water to estuaries, lagoons, and other coastal ecosystems has profound effects. For one, freshwater input mixes with denser saline coastal waters to create pressure gradients, which drive the gravitational circulation, thus significantly enhancing the flushing of the system. The amount of freshwater discharge largely determines the distribution of salinity within the receiving coastal water body, the extent of intrusion of saline waters, and the flora and fauna species that can survive in a particular area. Thus, fresh water input is ultimately responsible for creation of the brackish to saline coastal wetland environment in which mangrove species thrive.

Further, high rates of fresh water discharge into coastal systems usually correspond to a greater rate of input of terrestrial sediment, as well as increasing the rate of transport of marine sands from the adjacent coastal ocean into estuary, lagoon, and wetland areas as a consequence of the gravitational circulation (Meade, 1969). Because nutrients, bacteria, heavy metals, and other constituents are usually adsorbed onto terrestrial sediment particles, the rate of freshwater input is also often highly correlated with the input of these various constituents. Biological production is also greatly enhanced as a result of the availability of nutrients carried to the coast by the fresh water.

Rates of terrestrial input of water, sediment, nutrients, etc., via rivers and streams are not easy to determine, but it is essential to do so to develop hydrological budgets for mangrove systems. The input rates depend on (1) drainage basin water balance, (2) drainage area, (3) local climate, (4) drainage basin geology, (5) drainage basin topography, and (6) human impact on the drainage basin, such as population centers, agricultural practices, and irrigation, sewage disposal, and water withdrawal. The annual freshwater runoff is largely the difference between rainfall and evapotranspiration, and depends on climate, vegetation, percolation or infiltration, and relief. According to Milliman (1979), river systems

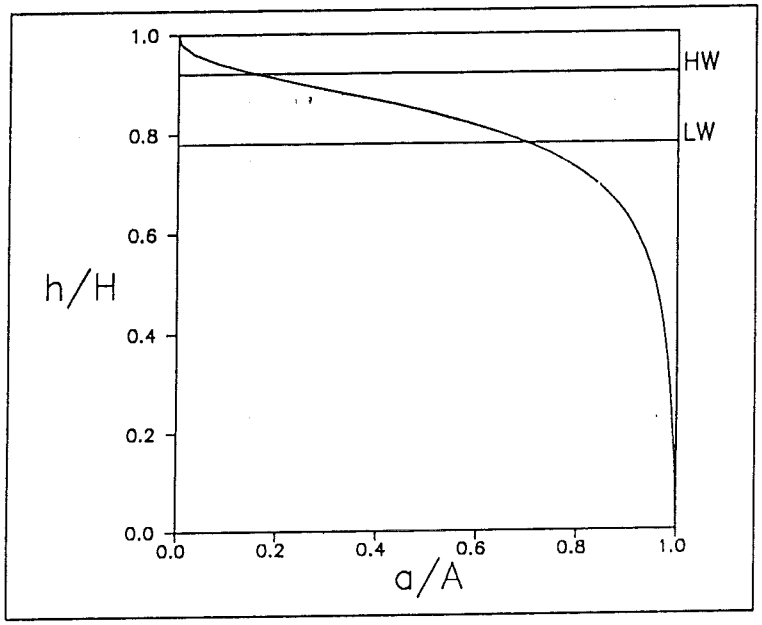

Fig. 15. Schematic hypsometric curve for a salt marsh basin (after Boon and Byrne, 1981).

draining humid mountains and desert areas are likely to yield the highest rates of sediment transport into coastal systems, whereas low-lying drainage basins, independent of latitude, yield low transport rates. A further complication arises in estimating transport rates, because average or typical rates of water and constituent inputs into coastal systems do not usually take into account catastrophic events. It has been demonstrated that single catastrophic river flooding events lasting no more than a few days can deliver the equivalent of the average sediment input for 25-725 years (Schubel and Hirschberg, 1978; Milliman, 1979). It is almost impossible to measure catastrophic inputs, and they are seldom included in annual budgets. Nevertheless, catastrophic inputs are certainly the most significant factor in delivering terrestrial sediment to the coastal area, and thus in providing the soils on which mangrove systems develop.

In carrying out a hydrological investigation of a mangrove system, it is desirable to (1) estimate input rates and (2) develop a material budget or balance. This must be done for the fresh water but is equally important to calculate for any other constituent to be studied, e.g., sediment, nutrients, organic matter.

7.2. Fresh Water and Material Input Rates

The most practical manner in which to measure directly the surface runoff from a river or a stream is the application of a rating curve. This is also the most commonly used method to measure runoff on a routine basis. For very small streams, the blocking of the stream and construction of a weir for use in discharge measurements can also be successful.

A rating curve is the plot of river stage (relative surface elevation in meters) vs. discharge (Q, usually expressed in m^3/s). As an example, the rating curve for the Santee River near St. Stephens, South Carolina, is shown in Fig. 16. A rating curve is specific to each river cross section. The site for a rating curve should be selected with care.

First, it must be upstream of most of the tidal rise and fall of water level, and certainly far upstream of any oscillating tidal currents, which render the rating curve useless. Second, the cross section should ideally be well defined by river banks or outcrops, exhibit a minimal adjacent floodplain, and be stable in the long term. Thus, cross sections from point bars or cut banks are usually unsuitable.

One or more permanent bench marks must be established for a cross section where a rating curve is to be developed. Relative benchmarks are most common. All river stage measurements must be referenced

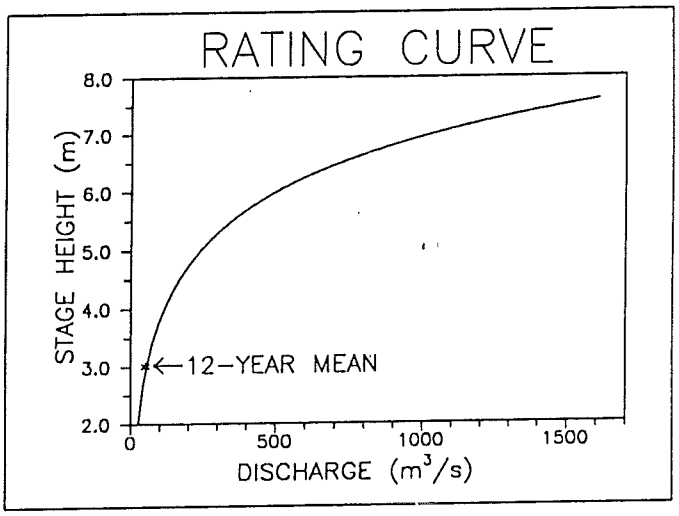

Fig. 16. Rating curve for the Santee River, SC, at St. Stephens.

to this benchmark. The construction of a reliable rating curve takes time. Stage measurements must be made over the extreme range of stages that occur, and the discharge must be measured for each stage. A method for computing the discharge in a river or estuarine cross section is described in the chapter on data analysis and synthesis. Log-linear curve fitting of stage and discharge measurements usually yields coefficients of determination better than 0.99. As more stage and discharge measurements are obtained, a rating curve should be updated.

To determine monthly or annual estimates of freshwater discharge, the river stage is measured once a day. Because river stage usually changes slowly relative to tidal rise and fall of water level, it is in most instances sufficient to sample river stage daily rather than more frequently. The stage is converted to discharge from the rating curve. By averaging the daily data for either a month or a year, the desired average estimates can be calculated. Although the stage to discharge conversion and the calculation of mean discharge usually are computerized, they can equally well be carried out manually.

Stage measurements can be made automatically using a recording water level gauge based on a float and a counterweight in a stilling well (pipe), a pressure sensor, a bubble gauge, a capacitance gauge, or a resistance gauge. The stage can just as well be measured manually by installing a tide staff marked in meters and centimeters. The staff can advantageously be attached to bridge pilings. It must be taller than the total range of the local river stage, easy to read, and referenced to the local benchmark. The staff probably needs to be cleaned occasionally, and the reference to the local benchmark should be verified regularly.

Because of the location of river stage gauges upstream of tidal influence, drainage from a substantial area of a basin is often ungauged. To correct the discharge, it is necessary to prorate the measured discharge, Q m^3/s, for the ungauged portion of a basin. The simplest method is to assume that the runoff from the basin area, a (km^2), below the rating curve site is proportional to the runoff from the area, A-a (km^2), above the gauge. The corrected total discharge, QT (m^3/s), from the entire drainage basin area, A (km^2), can then be expressed as

$$QT = QA/(A-a)$$

The rate of mass transport of river-borne materials can conveniently be estimated at the rating curve site by drawing daily water samples and analyzing these for constituents of particular interest. With estimates of mean cross-sectional sediment, nutrient, heavy metal concentrations (expressed as g/m^3), etc., the suspended and dissolved rate of downstream transport (kg/s) is obtained by multiplying the concentration by the river discharge. Of course, this usually requires a large effort.

Sometimes it may be possible to develop a statistical relationship between discharge and a constituent concentration so that estimates of mass transport can be obtained directly from the stage readings. Milliman (1979) warns, however, that applying this technique to suspended sediments is likely to yield errors of at least 50%, especially in small stream systems. Also, the relationship between sediment concentration and discharge usually exhibits seasonal patterns.

7.3. Climatic Water Balance

A mangrove ecosystem manager or scientist must often estimate the amount of freshwater input to a coastal system from a minimum of available data. Water resource engineers routinely simulate discharges from continuous rainfall and stream measurements and application of the unit hydrograph principle. But this method is often impractical in estuarine, lagoonal, and wetland studies, which require knowledge of monthly freshwater input rates and corresponding salinity distributions, rather than knowledge of the arrival time of a flood crest. For the coastal manager or scientist, it is advantageous to apply a climatological approach to the water balance. This can be accomplished for any system by obtaining a

minimal amount of additional measurements and by utilizing summaries of climatological data. Summaries are available for most locations. Thus, the approach to be followed here focuses on a climatological determination of the water balance for an entire drainage basin.

In general, the monthly or annual fresh water balance for a drainage basin can be expressed (Sellers, 1965)

$$r = \Delta f + g + s + E_a$$

where r is rainfall, Δf is surface runoff or discharge, g is infiltration to the groundwater, s is soil moisture storage, and E_a is actual evapotranspiration, which is the sum of evaporation from the surface and the transpiration by the vegetation cover. Each quantity is expressed in depth/time, usually mm/month or m/month.

Whereas E_a is the true water loss to the atmosphere by evaporation and transpiration, the potential evapotranspiration, E_p, represents the potential water loss under a set of ideal conditions, including (1) unlimited soil water supply as a result of frequent and sufficient rainfall or constant irrigation, and (2) complete, homogeneous vegetation cover. Actual and potential evapotranspiration rates will only be identical when the rainfall exceeds potential evapotranspiration, otherwise $E_p < E_a$.

When r exceeds E_p, there is water surplus, surface runoff is generated, and infiltration to the groundwater takes place. But when E_p exceeds r, there is a water deficit, and the vegetation must draw upon the soil moisture storage to sustain growth. Thus, after a period of water deficit, a period of soil moisture recharge will follow. When the recharge is complete, water surplus is attained, and surface and groundwater runoff are again generated.

The difference between potential and actual evapotranspiration

$$D = (E_p - E_a)$$

is used to calculate the soil moisture deficiency, which is the sum of daily or monthly values of D from the beginning of the soil moisture depletion period until such a time that r is greater than E_p. Thus, the soil moisture deficiency is the time integral of a rate and is measured in water depth, e.g. mm or m, rather than as depth/time. After a period of soil moisture deficiency, soil moisture recharge takes place during the beginning of the water surplus period before runoff commences.

Thornthwaite and Mather (1955) developed a technique for monthly water balance calculations based on the difference between precipitation and potential evapotranspiration. Because potential evapotranspiration is a measure of the maximum amount of water that can be evaporated by the available energy for an unlimited water supply, it is largely dependent on net radiation. It can be calculated based on monthly mean temperatures and latitude (Thornthwaite and Mather, 1957). The water balance can be calculated provided that the following data are available: (1) monthly or daily air temperatures, (2) monthly or daily precipitation rates, (3) latitude of the location, and (4) the water holding capacity of the soil. Tables for this computation are presented by Thornthwaite and Mather (1957).

Besides computation of the overall local water balance, the surface freshwater runoff is of particular interest to the investigator of hydrological processes in mangrove systems. In the case where a river or stream enters a mangrove system and an upstream rating curve has been established, the surface runoff is already known. More commonly, however, a rating curve does not exist and the fresh water discharge needs to be determined without establishing a rating curve.

The rainfall over the entire drainage basin represents the upper limit of water available for surface

runoff. This limit can be calculated by multiplying monthly or yearly rainfall data (in m) with the portion of the drainage basin (m^2) representative of each rainfall gauge, and summing these products over the entire basin area. By dividing the resulting volume by the appropriate time (month or year converted to seconds), the upper limit of the monthly or annual discharge (usually expressed in m^3/s) is established.

The runoff ratio, $\Delta f/r$, defines the fraction of the rainfall that becomes surface runoff. This ratio approaches 1 for very heavy rainfall environments and zero for sparse rainfall areas. Although it varies widely for small drainage basins, it averages 0.20 for major river basins (Holland, 1978). For example, the runoff ratio measures 0.03 for the Darling River in Australia, a temperate arid basin; 0.16 for the Niger River, a subtropical semi-arid basin; and 0.46 for the Amazon River, a wet tropical basin (Holland, 1978). It is often used as a climatic index (Sellers, 1965). The runoff ratio depends primarily on basin evapotranspiration rates.

Empirically, the runoff ratio can often be expressed as

$$\Delta f/r = e^{-\alpha/r}$$

(Holland, 1978), where the exponential function can be expanded into a power series and approximated by

$$\Delta f/r = 1 - \alpha/r$$

as long as α/r is substantially smaller than 1. By rearranging the terms, it follows that

$$\alpha = r - \Delta f$$

which approximately holds true when there is substantial runoff, and the averaging time is sufficiently long.

The most common model to relate the runoff to precipitation from field data is

$$\ln(\Delta/r) = -E_p/r$$

(Schreiber, 1904), where the potential evapotranspiration is taken to vary with the mean temperature (and thus latitude and elevation) according to

$$E_p = 1.2 \times 10^{3} \exp\{-4.62 \times 10_3/T\}$$

(Holland, 1978), where the air temperature, T, is expressed in Kelvin (K). Although not reflected in this model, E_p also varies with vegetation type, canopy coverage, surface slope, and soil type.

An alternative model proposed by Sellers (1965) defines the runoff ratio as a linear function of rainfall,

$$\Delta f/r = ar$$

where a is a regional constant, which seemingly varies from 0.04 to 1.0 m^{-1} (Sellers, 1965). A warning is in place. Both of the above runoff-precipitation models, like most runoff-precipitation models, work only for long-term climatic data, but are even then subject to a lot of variability.

Open water bodies lose water to the atmosphere via evaporation. Depending on the particular situation, it may be desirable to calculate this water loss as a component of the water balance. The water loss to the atmosphere by evaporation (E cm/day) can be calculated from a mass transfer equation

$$E = NW(e_o - e_a)$$

(Harbeck, 1962), where W is the wind speed in m/s, e_o is the saturation vapor pressure in millibars (mb) at the temperature of the water surface (List, 1951), e_a is the vapor pressure of the air in mb at the same

elevation as the windspeed is measured, and N is a dimensional mass transfer coefficient. It is convenient to make the wind speed and vapor pressure measurements at a 2 m elevation. Standard meteorological measurements at 10 m may require a 10-25% correction of the resulting evaporation rate. Harbeck (1962) applied this mass transfer approach to reservoirs and found the transfer coefficient varies with surface area of a reservoir according to

$$N = 0.0146/A^{0.05}$$

for reservoirs with surface area (A in km^2) up to 121 km^2. For example, with a vapor pressure difference of 10 mb and a 4.47 m/s wind speed over a reservoir with a 4.05 km^2 surface area, the mass transfer coefficient measures 0.0136, and the evaporation rate measures 0.61 cm/day. This corresponds to a water evaporation loss of 24,705 m^3/day or 0.29 m^3/s. Although this bulk formula was developed for reservoirs, it is also applicable to many estuarine and lagoon environments. Extrapolation of the formula to very large water bodies, however, may not necessarily yield realistic evaporation rate.

8. HYDROGRAPHIC MEASUREMENTS

8.1. Initial Considerations

Hydrographic studies should be conducted during both neap and spring tides. To avoid serious navigation problems due to shallow water, it is best to start sampling at high tide to get initial boat access to all stations. Sampling should always start during daylight hours, but if necessary, can be extended into the dark hours when personnel are familiar with the local navigation obstructions and can find the stations. It is difficult to start sampling in the dark before sampling stations are well known and agreed upon.

Hydrographic studies of an estuary, lagoon, or mangrove wetland should always include (1) basic meteorological measurements from one site collected at least every 3 hours, (2) tidal time series measurements of water elevation at one or more fixed locations at least once an hour, and (3) estimates of freshwater discharge from stream gauging or water budget calculations. Hydrographic measurements from predetermined stations within the navigable waters should minimally include (1) local water depth, (2) compensation depth, (3) current velocity, (4) water temperature, (5) conductivity or salinity, and (6) collection of at least one liter of water for verification of salinity measurements and laboratory analysis for total suspended sediment (TSS) concentration and other constituents. If the hydrologic measurements are one component in an ecological study to estimate chlorophyll-a, nutrients, and other material fluxes to and from a mangrove system, it is essential that chlorophyll-a, nutrients, etc., are determined from the water samples drawn at the same time that the physical measurements are made. The time of each measurement or sample should be noted carefully. Measurements and collection of water samples should ideally be made at one meter intervals over the water column, beginning near the surface and ending near the bottom. Measurements should ideally be made more closely spaced where the vertical profiles exhibit strong gradients, i.e., at the halocline (or thermocline). When dissolved oxygen concentration or transmissivity profile measurements are made, the data can be used to calculate compensation depth and the depth of the photic zone, respectively, as long as a sufficient number of vertical measurements have been collected. As an alternative, hydrographic measurements in estuaries are often limited to three sampling depths: near surface, at mid-depth, and near bottom. When the water depth is sufficiently shallow, or the mixing is strong, this is usually satisfactory. In addition, it is often desirable to (1) make regular estimates of mass transport by floating litter fall, and (2) determine bottom sediments.

8.2. Water Elevation

Tidal water level measurements can be made with a variety of measurement devices. A government agency in each country is usually in charge of installing and maintaining self-recording water level gauges at coastal locations to analyze water level variability and to provide tidal predictions. The most commonly used instruments for water elevation measurements are (1) a float and a counterweight in a stilling well and (2) a pressure gauge. Measurements are most often made automatically, using either (1) a pen-device that produces an analog trace on paper, or (2) a digital recorder which is programmed to sample the water elevation at a fixed sampling frequency, usually either every 6 minutes or once an hour. Most important, the gauge must be referenced to a local bench mark and verified against the benchmark, ideally as often as once a month. This is particularly important if determination of the long term, relative change in sea level is a study objective.

In most mangrove wetlands and in many estuarine locations in tropical countries, tidal gauges do not exist. Mangrove scientists or managers must therefore arrange to measure the tide themselves during a hydrographic study. This can either be accomplished by installation of a self-recording water level gauge, if the budget permits, or by manual recording of tidal water elevation changes using a tide staff. A tide staff is marked with large numerals in meters and centimeters and should be installed with increasing

numbers corresponding to increasing water level. A tide staff can readily be attached to dock or bridge pilings or driven into the bottom substratum, sufficiently near the bank, so that the scale can be read by eye or with the aid of binoculars. It is essential that the staff is referenced to the local benchmark. A tide staff must be installed securely enough so that it shifts neither up nor down during a field study. By ensuring the vertical datum of tidal measurements, it is possible to compare the extent of flooding of a mangrove wetland between seasons and years.

Tidal water elevation measurements should minimally be made at one location in waters adjacent to the mangrove wetland being studied. However, measurement of tidal water elevation time series at more than one location within an estuarine system is usually very helpful and allows for calculation of water level slopes, tidal progression, frictional dissipation of tidal energy, and tidal amplification because of converging channel banks and shoaling water depth. One reasonable approach is to select a downstream and an upstream location for measurements of tidal elevation time series.

Tidal water elevations should be measured at least hourly (ideally on the hour), but on the half-hour if possible. Measurements should be continued for the duration of a hydrographic study in increments of complete semidiurnal tidal cycles, i.e., 12.42 hours.

Better yet is to measure tidal water elevation time series for a minimum period of 29 consecutive days and nights or 696 consecutive hourly measurements. Such data make it possible to use standard computerized programs for tidal harmonic analysis and subsequent tidal predictions. It is strongly recommended that one or more 29-day tidal time series be measured for each study location. The procedures for harmonic analysis at tidal frequencies are covered in detail by Pugh (1987) and Franco (1988).

8.3. Current Velocity

Of all hydrographic measurements, current velocity is the most difficult to determine. It is a vector quantity and usually varies greatly in magnitude and direction relative to its resultant value over the tidal period. Also, most velocity sensors will disturb the flow and cause deviation from the true value.

Velocity measurements can be divided into two types: (1) Eulerian, where the current velocity is determined at one location as a function of time, and (2) Lagrangian, where the path of a water parcel is determined over time by use of tracers such as dyes or drogues. Eulerian measurements are most common in coastal water bodies. They can be made with a current meter, which is either suspended from a boat or moored a fixed distance above the bottom using surface floats or sub-surface lifts. The measured velocity represents a spatial average for the surface area of the sensor normal to the flow.

Numerous different types of current velocity sensors exist for Eulerian measurements. For low-budget studies in mangrove wetland systems, the most practical and useful current measuring device is the current vane (Kjerfve and Medeiros, 1989) (Fig. 17), an improvement on the current cross (Kjerfve, 1982). Current vanes can be used for current measurements at different depths in enclosed water bodies, tidal channels, mangrove creeks etc. as long as surface gravity waves are minimal. Current vanes function as submerged drags which are suspended by a line from an anchored boat. They are cheap to build, simple to operate, require no power source, and are inexpensive and reliable.

By knowing the area (A) of the vane normal to the flow and the mass (M) of the vane while suspended in water, the current speed (v) can be determined by using an inclinometer to measure the angle (φ) between the line and the vertical, such that

$$v = [2Mg/\sigma AC_D]^{0.5} \; [\tan \alpha]^{0.5}$$

where g is gravity (9.81 m/s^2), σ is water density (1020 kg/m^3), and C_D is a non- dimensional drag coefficient which was found to vary from 1.39 to 1.48 (Kjerfve and Medeiros, 1989). By attaching different lead weights to the current vane, the angle, φ, can be maintained within the limits of 10°-30°, for which the dynamic range of the measuring technique is optimum. Each angle determination should be a 10-30 s average by eye to filter out small scale turbulent fluctuations in the flow field. The horizontal flow direction can be determined with a compass, and the measurement depth is given by the amount of line paid out multiplied by cos α.

The velocity range in which the vane can be used is a function of its size and mass. Kjerfve and Medeiros (1989) constructed current vanes out of 30x30 cm Lexan sheets, bent along the middle to form a V-shaped vane with a 60° angle. The useful velocity range is 0.1-1.6 m/s when the submerged mass of the vane plus attached weight was alternately 1.6 and 6.2 kg. Kjerfve and Medeiros (1989) found that for these specifications, the standard error of the mean was less than 6 cm/s. The calibration curves for their heavy (6.2 kg) and light (1.2 kg) vanes are shown in Fig. 18. It is feasible to construct current vanes with a good dynamic response in other velocity ranges by varying construction material, size and mass of the vane.

Besides not functioning well in the presence of moderate wind waves, current vanes are unsuitable for turbulence measurements. They must also be operated completely manually, which is another shortcoming. But for use in low-budget studies without available sophisticated instrumentation, they are excellent and yield reliable data.

Other options for making Eulerian current velocity measurements in estuaries and coastal waters are much more expensive as compared to the use of current vanes. For example, Byrne and Boon (1973) used a propellor current meter. The rotation rate of the propellor increases with current speed, and direction is

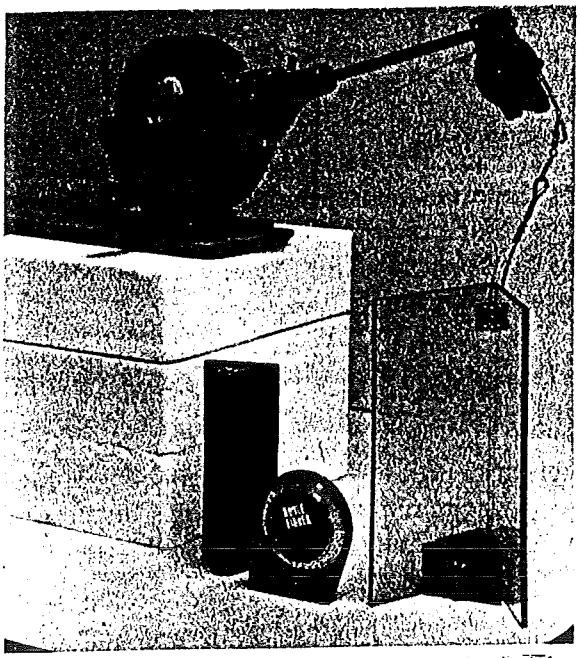

Fig. 17. Current vane with an attached 1-kg weight, an alternate 7-kg weight, an inclinometer, and a reel with stainless steel wire with which to suspend the vane into the water.

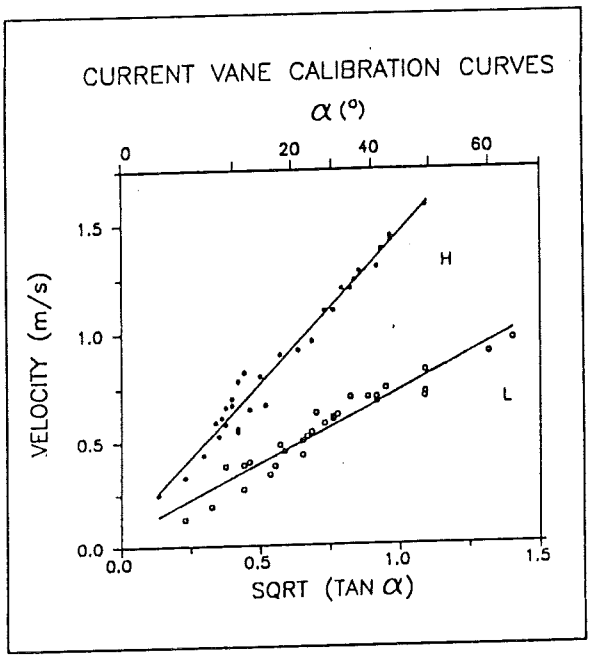

Fig. 18. Calibration curve for current vanes (after Kjerfve and Medeiros, 1989).

sensed through a vane. The propellor current meter has good response characteristics for measuring horizontal currents in estuaries and include different means of recording the measured data. Other far more expensive options are the use of (1) electromagnetic current meters with internal RAM (Random Accessible Memory), or (2) acoustic doppler current profilers (ADCP's). Both are normally moored on or from the bottom rather than used from a surface vessel. The ADCP is the most complex and costly, but represents the state of the art. It yields complete vertical profiles of horizontal vector currents several times per second. It is based on the principle of doppler shift between transmitted and received signals, which are scattered by particulates within depth-specific vertical bins. An ADCP for shallow water applications may have approximately 20 bins, each measuring somewhat less than 1 m.

Lagrangian measurements are less common in estimating circulation and water exchange in mangrove wetlands, because a water tracer quickly encounters *Rhizophora* prop roots along the boundaries. This gives rise to a boundary-induced dispersion. Radio-isotopes or dye tracers, such as rhodamine and fluorescein, can be used to tag a particular water parcel. The movements of local water parcels may be determined from the spatial distribution of the tracer concentration with time. The spreading of a dye patch can be used to measure turbulence characteristics of the flow. Dyes are better suited for estimating eddy diffusivity than for circulation features (Talbot and Talbot, 1974). Other methods of making Lagrangian current measurements include sea-bed drifters, drift bottles, and various drogues.

8.4. Temperature, Conductivity, Salinity, Density

Water temperature can be measured by several means. Mercury thermometers, based on the thermal expansion of mercury, have long been used in oceanographic applications. They are capable of measuring temperature with a precision of ± 0.01 °C. The preferred sensor, however, is the thermistor, a semi-conductor whose electrical resistance varies inversely with temperature. Small temperature changes cause the resistance to vary by an order of magnitude. Thermistors can be made very small, they respond almost instantaneously to temperature variation, and they are capable of measuring temperature with a precision of ± 0.001 °C.

Salinity can be measured directly by several means. The classical technique is to perform silver nitrate titration on a water sample (Strickland and Parsons, 1968). This method has a precision of ± 0.01 ppt. For quick estimates of salinity to a precision of ± 1 ppt, a refractometer can be used. The refractometer is relatively inexpensive and is ideal for pre−study surveys of the estuarine salinity distribution, but is less suitable for hydrographic studies because of the low precision.

For accuracy and reliability, however, electrical conductivity measurements are preferred. Salinity can be computed from conductivity and water temperature measurements, provided the latter two are made simultaneously (e.g. Kjerfve, 1979). For a constant conductivity, salinity varies with water temperature. Electrical conductivity measurements are quick and easy to make and yield about the same precision as the most accurate silver nitrate titration method. The salinometer is the most frequently used instrument for measuring conductivity and water temperature. The relationships from which to compute salinity from conductivity and temperature are given in UNESCO (1981a, 1981b, 1986c, 1987b).

Water density, in turn, is calculated from temperature and salinity values (Kjerfve, 1979). In shallow water situations, it is not necessary to consider the effect of pressure on density. Although salinity has the most effect on density in estuaries because of the range in salinity from fresh to oceanic waters, and salinity itself is usually of the most interest to biological scientists, it is still necessary to convert the salinity and temperature data to density values for use in calculating gravitational circulation and other dynamic characteristics of estuarine behavior.

8.5.Total Suspended Solids (TSS)

The collected water samples can, of course, be used for a variety of different analyses, but this discussion will be limited to determination of total suspended solids concentration. Besides temperature and conductivity measurements, TSS is another parameter that should be measured routinely as a component of any hydrographic study. Differences in surface TSS in inshore waters are easily observed in satellite images (cf. Collins and Pattiaratchi, 1984; Lindell et al., 1985; Curran et al., 1987; Jensen et al., in press) or observed from aerial photographs. These provide clues useful in the interpretation of hydrodynamic characteristics.

To obtain water samples for laboratory measurement of TSS, a least a 1-liter sample bottle, e.g., a Niskin bottle should be used. The bottle should be filled with water, but leave some air at the top so that mixing can take place when the bottle is shaken. Note, however, that when collecting water samples for dissolved oxygen measurements, absolutely no air bubbles should exist in the sample bottle.

Of several different techniques to measure TSS concentrations, filtration is the most common, easiest, and least expensive method, and is the only one to be covered here (Dr. D. Nelson, personal communication). Centrifuging will produce more accurate results, but it is far more time consuming and requires expensive equipment.

For filtration, use pre-dried and pre-weighed filter papers, either Millipore, Nucleopore, or glass fiber filters, depending on availability and preference. Most commonly, filter papers have a diameter of 47 mm. A mesh size of 1.2 micra is preferable to a 0.45 micron mesh, which rapidly clogs during the filtration process. Millipore filters are the most readily available, but (1) they tend to lose weight as water is filtered through them, and (2) particles that should pass through the filter do not always because of build-up of static charge. Nucleopore filters are more permeable than Millipore filters, but (1) flocculated particles tend to fall apart as they pass through the filter openings, and (2) mesh holes tend to overlap. Glass fiber filters are most often preferable because (1) they have high permeability, (2) they develop negligible static charge between particles and paper, and (3) organic filtrate can readily be burned off (500 °C for 30 minutes) without leaving much residue. Unfortunately, they are also the most expensive.

Filter papers should be pre–dried in a 50–60° oven for one hour or longer. All filter papers are more or less hygroscopic and, as a result, can change their weight by more than 10%. Thus, it is important to transfer the filter paper from an oven or desiccator to a balance and weigh the paper immediately because air moisture rapidly accumulates on the filter paper. This is particularly a problem with Millipore filters. After weighing each filter paper, it is good practice to verify that the balance is zeroed; if not, make necessary adjustments.

When filtering a sample, stir the water in the bottle in a rotary manner for at least one minute to prevent flocculation and ensure that particles are evenly distributed in suspension. Simply shaking the bottle up and down will not prevent flocculation from occurring within a water sample. Immediately thereafter, pour the sample into the filter container and pump the sample through the filter by creating vacuum pressure behind the filter. This can be done using either a hand-held or electric vacuum pump. As much water as possible should be filtered to ensure good results; 500 ml is usually a reasonable choice in estuaries. After filtering, flush the filter paper with distilled water several times to remove salts. Next, dry the filter paper in a 50–60 °C oven, place filter into desiccator or transfer to balance, weigh the filter with the filtered sample, and record the difference between the filter paper with the sample and the filter by itself.

It is important to routinely verify the level of error in the analysis. As a general rule, TSS determination should include (1) blank determination of changes in five filter paper weights in every batch

of samples to ensure minimum hygroscopic weight change, and (2) three to five replications on every water sample to obtain a statistical measure of analysis errors. Extreme care must be taken in the weighing process because of the amount of moisture that can accumulate on the paper after removal from the oven or desiccator. The filtration procedure will at best yield an accuracy of 10%, taking into account all the variables that can affect the analysis process.

As a typical example, assume that 500 ml of water is filtered. If the weight of the filter paper and sample is 87.3 mg and the weight of the filter paper by itself is 75.6 mg, the sample weight is 11.7 mg. This yields a TSS concentration of 23.4 mg/l or ppm. An error of only 2.0 mg in weighing the filter paper by itself produces a calculated concentration anywhere from 19.4 to 27.4 mg/l. Extreme care should be exercised in (1) handling wet filter papers containing a sample to avoid tearing off the edges of the filter paper, (2) carefully washing out all salts, and (3) weighing each filter paper or sample accurately to the nearest 10^{-5} g.

9. DATA ANALYSIS

9.1. General Comments

The data analysis and synthesis are almost always the most time consuming portions of a hydrologic field study in coastal environments, mangrove systems included. All too often, field measurements are reported as numerical values in tables or figures without a serious attempt at (1) explaining where, when, and how the data were collected, (2) subjecting the data to a more in-depth analysis, or (3) synthesizing the results and drawing logical conclusions. This is unfortunate.

To attempt a generalized discussion of data analysis and synthesis is not possible, however, because the analyses and statistical treatments depend on the questions that were asked when the study was designed. This manual is therefore not an attempt to present a generalized data analysis and synthesis procedure, but rather to suggest a few ways in which to handle (1) time series data from water level gauges, and (2) repeated hydrographic measurements collected at stations within the water body adjacent to a mangrove wetland during one or more tidal cycles. These types of data might be collected during ecological studies to determine budgets of water, salt, nutrients, TSS, organic matter, etc., for mangrove systems, or to estimate advective fluxes between the system and the adjacent ocean. Once preliminary data analysis and synthesis chores are completed, it is possible to proceed with more interesting endeavors, such as analysis of the intensity of gravitational circulation, tidal and wind mixing, exchange rates, flushing times, water and material turn-over times, residence and transit times, frequency and extent of tidal inundation, dispersion characteristics, assimilative capacity of estuarine and coastal boundary layer waters, numerical modeling, and the application of remote sensing to the mangrove wetland and surrounding waters.

9.2. Tidal Analysis

To describe the salient tidal characteristics of a water body minimally includes harmonic analysis of a time series of at least hourly data from a water level gauge. The longer the time series, the better the tidal characterization. Government agencies usually have the resources to collect tidal water level data for many years. These data can be used to (1) describe tidal characteristics, (2) produce tidal predictions, (3) analyze storm surges in response to typhoons or hurricanes, (4) determine seasonal changes in water level due to water temperature changes and fresh water runoff events, and (5) measure the long-term local trend of relative sea level change.

Tidal analysis is usually performed on either 365 or 29-day long time series records of hourly data. If missing data points exist, these must be interpolated prior to carrying out the analysis. The interpolation is not a straightforward process and should never be attempted for more than 5% of the total length of a time series. The harmonic analysis of a water level time series, h(t), is the fitting of a series of sine and cosine curves in a least squares fashion to the original water level record. The water elevation

$$h(t) = H_0 + \Sigma\ f\ H\ \cos\ [at + (V_0 + u) - \kappa]$$

(Schureman, 1941), where H is the amplitude of the i-th constituent; H_0 is mean water elevation; t is local time; a is speed of the constituent tide (Table 1); f is a slowly varying tidal node factor, and $(V_0 + u)$ is Greenwich equilibrium argument, both determined from look-up tables (Schureman, 1941); and κ is the epoch of the i-th constituent tide from which the Greenwich epoch, °G, is computed (Schureman, 1941; Dietrich et al., 1980). The mathematics and programs for carrying out the harmonic tidal analysis are given by Dennis and Long (1971 and 1972) and Pugh (1987), and require a digital computer for the calculation.

The input to the analysis is a sequence of continuous, digitized water elevations, e.g., 696 hourly data points for a 29-day analysis. In addition, it is necessary to specify the exact latitude of the tide gauge and

Table 1. Principal harmonic constituents.

Name	Symbol	Angular Velocity (°/hr)	$M_2 = 100$
	Long-period constituents		
Solar annual	Sa	0.0411	1.3
Solar semiannual	Ssa	0.08214	8.0/4.0
Lunar monthly	Mm	0.54437	9.1/4.6
Lunar fortnightly	Mf	1.09803	17.2/8.6
	Diurnal constituents		
Luni-solar diurnal	K_1	15.04107	58.4
Principal lunar diurnal	O_1	13.94304	41.5
Principal solar diurnal	P_1	14.95893	19.4
Larger lunar elliptic	Q_1	13.39866	7.9
Smaller lunar elliptic	M_1	14.49205	3.3
Small lunar elliptic	J_1	15.58544	3.3
	Semidiurnal constituents		
Principal lunar	M_2	28.98410	100.0
Principal solar	S_2	30.00000	46.6
Larger lunar elliptic	N_2	28.43973	19.2
Luni-solar semidiurnal	K_2	30.08214	12.7
Larger solar elliptic	T_2	29.95893	2.7
Smaller lunar elliptic	L_2	29.52848	2.8
	Shallow water tides		
	M_4	57.96820	—
	S_4	60.00000	—
	M_6	86.9523127	—

note whether local time is local standard time or local summer time. It is usually preferable to consistently reference the measurement time to either local standard time or GMT (the standard time at the 0° longitude at Greenwich, UK).

The output from the analysis consists of amplitudes and phases for sinusoidal curves at precise, determined frequencies. The phase is called epoch if its reference time is GMT. Each sine-curve is referred to as partial or constituent tide. The frequencies correspond to the frequencies of the tide-producing force (Defant, 1960; Bowden, 1983). Diurnal tides carry a 1-subscript, implying approximately one tide period per day, whereas semidiurnal constituents carry a 2-subscript, because they occur twice daily or have a period of approximately 12 hours. Tidal constituents with periods of either semimonthly, monthly, semiannual, annual, or longer periods carry letter subscripts. A number of tidal constituents are generated by shallow water nonlinear effects. These have no correspondence to tide-producing forces and are either a (1) compound tide of semidiurnal frequency, or (2) an overtide with a period equal to a fraction of the semidiurnal period. In the latter case, they are subscripted, e.g., 4, 6, or 8, indicating approximately 4, 6, or 8 tides per day, respectively.

A listing of some of the major constituent tides, their designations, periods, and theoretical comparison to $M_2 = 100$ are listed in Table 1. A number of tidal characteristics can be calculated directly from the harmonic amplitude and phase values (Schureman, 1941; Palmer et al., 1980). A summary of the more useful such tidal characteristics are listed in Table 2.

9.3. Interpolating Vertical Data Profiles

At a station, the hydrographic data are collected only at finite points, more or less irregularly spaced vertically between the surface and the bottom. For analysis, however, the data need to be standardized by interpolating the shape of each profile and resampling data points at regularly spaced vertical intervals for analysis. Thus, the analyzed data are often not the measured values, but rather the interpolated ones.

Interpolating data profiles can either be done graphically or numerically. Numerical interpolation is preferable because the data can be analyzed quickly on a computer without introducing operator error. The interpolation can also be accomplished manually by first drawing the entire profile as a smooth curve through each of the measured data points, and then using a proportional divider to read off the interpolated data at the desired amount of depths.

Table 2. Tidal statistics based on harmonic constants (after Palmer et al., 1980). Whenever phases are used, the °-sign is indicated.

Parameter	Formula	Interpretation
Form Number	$(K_1 + O_1)/(M_2 + S_2)$	Semidiurnal tide
Inequality Phase Relationship	$M_o° - (K_1° + O_1°)$	Diurnal inequality predominantly in high waters
Phase Age	$0.98(S_2° - M_2°)$	Time that spring tide occurs after new or full moon
Mean Range	$2.2(M_2)$	Average tidal range (semidiurnal and diurnal)
Spring Range	$2.0(M_2 + S_2)$	Average range during spring tide (semidiurnal)
Neap Range	$2.0(M_2 - S_2)$	Average range during neap tide (semidiurnal)
Tropic Range	$2.0(K_1 + O_1)$	Average range during tropic tide (diurnal)
Equatorial Range	$2.0(K_1 - O_1)$	Average range during equatorial tide
Diurnal Age	$0.91(K_1° - O_1°)$	Time that tropic tide occurs after the maximum semimonthly declination of the moon

Numerically, a series of cubic splines can be fitted (Pennington, 1970; Carnahan and Wilkes, 1973) to the measured depth-values of velocity, temperature, salinity, and other parameters (Kjerfve, 1979). The shape of each vertical profile is thus interpolated between the top and the bottom data points and extrapolated to the boundaries, in a similar manner in which a draftsman would draw a line with a flexible French curve through a sequence of points. With n depth measurements, the spline interpolation technique requires that n-1 piecewise continuous third order polynomials be determined, assuming that the curvature (or second derivative) is continuous as the curve passes through each data point. Provided that suitable boundary conditions exist at the first and nth data points, a unique solution will result. It is usually assumed that either there is no curvature (second derivative with respect to depth equals zero) or

the curvature is constant (third derivative with respect to depth equals zero) at the end points. By knowing either the slope or curvature at the end points, the profiles can be extrapolated to the surface and bottom. To minimize errors introduced by the extrapolation, the topmost measurement should be made as close to the surface as possible and the deepest measurement should be made less than 1 m above the bottom.

Fitting the velocity profile in the bottom boundary layer requires special considerations. Under conditions of neutral stability and steady flow, the velocity profile close to a hydraulically rough boundary is given by the logarithmic profile (Dyer, 1970; Sternberg, 1972)

$$U(z) = U_*/k \ \ln \ (z/z_o)$$

where U is horizontal velocity (m/s) and varies with distance abover the bottom, z (m); z_o is the dynamic roughness length (m), which represents the distance above the bottom where the velocity is zero; k is von Karman's universal non-dimensional constant equal to 0.4; and U_* is the friction velocity (m/s), which is constant in the boundary layer and is given by

$$U_* = (\tau/\sigma)^{1/2}$$

where τ is the bed shear stress (N/m^2); and σ is water density, assumed to be constant and equal to 1,020 kg/m^3.

The depth-varying horizontal flow speed, U(z), is a 2 .60-minute time-average, usually of data averaged every 10 minutes. The parameters, U_* and z_o, can be determined from an experiment of simultaneous current speed measurements at several heights above the bottom by regression of ln(z) on U(z). This, however, requires several simultaneous measurements within the bottom 1–2 m of the water column, a task that usually cannot be accomplished during routine hydrographic studies.

Proceeding in a different manner, it is convenient to define a non-dimensionalized drag coefficient,

$$C_1 = (U_*/U_1)^2$$

where U_1 is the current speed 1 m above the bottom. For any bottom boundary surface, C_1 approaches a constant value whenever the appropriate Reynolds number exeeds 10^5–1.5×10^5, which corresponds to a U_1 value in the range 10–15 cm/s (Sternberg, 1972). For many estuaries with relatively level silty sand beds, the drag coefficient can be assumed equal to 0.003 (Sternberg, 1972; Kjerfve, 1979). This fixes the value of z_o, but is not too much of a problem because the calculations are relatively insensitive to different values for z_o.

Assuming $C_1 = 0.003$ and measuring U_1, the velocity one meter above the bottom, it is possible to solve for the friction velocity, U_*. Using the computed value of U_*, the boundary shear stress may be calculated.

As an example, if $U_1 = 0.5$ m/s, it follows that $U_* = 0.0274$ m/s, and $\tau = 0.765$ N/m^2. A value of C_1 of 0.003 implies a fixed value of z_o of 0.00068 m. Measurements of detailed profiles have shown that z_o is variable, depends greatly on the surface shape and grain size, and may range through several orders of magnitude; however, these variations do not have as large an effect on the drag coefficient.

Cubic spline fitting is a convenient technique for constructing complete vertical profiles of current speed, temperature, salinity, and density from surface to bottom, based on discrete vertical measurements of current speed, water temperature, and conductivity. The fitting of the velocity profiles does warrant extra consideration near the boundary. The assumption of neutral stability in the lowest meter is usually acceptable in view of friction-induced boundary turbulence. The steady assumption necessary to assume the existence of the logarithmic current speed profile is not restrictive, because the current speed varies primarily on a time-scale of the tidal period, whereas U_1 is a 10-minute mean.

Kjerfve (1979) developed a standardized computer analysis program, PROFILE, which fits vertical profiles through each set of data points and yields as output the values of the two orthogonal horizontal velocity components, temperature, salinity, and density at any number of equally spaced depth intervals. The choice of 11 data points to define ten equally spaced depth intervals from surface to bottom is often convenient. In addition, PROFILE computes friction velocity, bottom sheer stress, and salinity and density from conductivity and temperature data (Kjerfve, 1979).

9.4. Net Discharge Computations

The net discharge per unit width through an estuarine cross section is expressed as $\langle Q \rangle$ (m^2/s), and is estimated from velocity profile measurements at each hydrographic station. With m stations in a cross section, it is possible to integrate the m estimates of $\langle Q \rangle$ numerically and arrive at a net cross–sectional discharge $\langle Q_T \rangle$, expressed in m^3/s. In general, the net discharge per unit width, $\langle Q \rangle$, is given by

$$\langle Q \rangle = 1/T \Sigma [\Sigma v(z,t)\ dz]\ dt$$

where z is depth, t is time, T is the period of time-averaging, and v(t) is the time-varying velocity normal to a cross section. The depth-averaged velocity is calculated from

$$\overline{v(t)} = 1/10\{\tfrac{1}{2}v(n_o,t) + \sum_{j=1}^{9} v(n_j,t) + \tfrac{1}{2}v(n_{10},t)\}$$

using 11 interpolation points in construction of the velocity profiles from a surface value at n_o to the bottom value at n_{10}. The surface and bottom velocities are weighted by ½ because they are representative of only half the depth as compared to the velocity values at n_1 through n_9. Actually, it is not necessary to include $V(n_{10},t)$, because the velocity at the water-sediment interface is always zero; nevertheless, it has been included to emphasize that for salinity, temperature, and other parameters, this term is non-zero. $\langle Q \rangle$ is a cross-correlation of the depth-averaged velocity and the water depth and is computed from

$$\langle Q \rangle = 1/n\{\tfrac{1}{2}v(t_o)d(t_o)d(t_o) + \sum_{k=1}^{n-1} v(t_k)d(t_k) + \tfrac{1}{2}v(t_n)d(t_n)\}$$

With m stations in a cross section, the total net cross-sectional discharge $\langle Q_T \rangle$ (m^3/s) is given by

$$\langle Q_T \rangle = \sum_{i=1}^{m} w_i \langle Q \rangle_i$$

where w_i is the width over which velocity measurements at one hydrographic station are assumed representative. It is usually convenient to choose the w-width such that a station is located in the middle of each sub-cross section of the estuary. The w's are also usually selected to be of equal widths.

This approach assumes that the estuarine cross section is rectangular. For stations in shallow water near the sides of a channel, the width will vary with time, particularly where there are extensive intertidal areas. A closer approximation to the net cross-sectional discharge can be made assuming w to be a function of time. In this case, the total net discharge (m^3/s) per sub-section becomes

$$\langle Q_T \rangle = 1/T\{\tfrac{1}{2}v(t_t)d(t_o)w(t_o) = \sum_{k=1}^{n-1} v(t_k)w(t_k) + \tfrac{1}{2}v(t_n)d(t_n)w(t_n)\}$$

The total net cross-sectional discharge would again be given by a summation over the m stations.

9.5. Net Flux Computations

The goal of many biological, chemical, and geological investigations of tidal channels in salt marsh and mangrove environments is to determine the time-averaged fluxes of various dissolved or suspended constituents. The net flux per unit width, $\langle F \rangle$ (kg/ms), of any constituent may be written

$$\langle F \rangle = 1/T \int \overline{\sigma(t)c(t)v(t)d(t)}\, dt$$

(Kjerfve 1975, 1979), where c(t) is the concentration of a dissolved or suspended constituent expressed as mass constituent per mass of constituent in solution; and $\sigma(t)$ is water density. In flux computations, $\sigma(t)$ can often be considered constant and equal to 1,020 kg/m^3, because $\sigma(t)$ varies only slightly compared to c(t) and v(t). The overbar represents a depth-average of the product of three instantaneous quantities and is computed as

$$\overline{\sigma(t)c(t)v(t)} = 1/10\{\tfrac{1}{2}\sigma(n_o,t)c(n_o,t)v(n_o,t) + \sum_{j=1}^{9} \sigma(nj,t)c(n_j,t)v(n_j,t)\}$$

It should be noted that because $v(n_{10},t) = 0$ at all times, the term representing the triple-product at the bottom vanishes and has been omitted from the above equation. If $x(t) = \sigma(t)c(t)v(t)$, then the net flux per unit width, $\langle F \rangle$, is computed from

$$\langle F \rangle 1/n\{\tfrac{1}{2}x(t_o)d(t_o) = \sum_{k=1}^{n-1} x(t_k) + \tfrac{1}{2}x(t_n)d(t_n)$$

It is, of course, necessary to measure the concentration of all constituents of interest, for example, TSS, particulate organic carbon, nitrate, nitrite, phosphate, etc., at several depths between the surface and bottom at the same time that velocity and other hydrographic measurements are measured. Depth profiles of the concentrations must be constructed, and values interpolated for each depth, station, and sampling time. This can be a very time consuming process.

9.6. Cross–sectional Area Weighting

In estuarine flux studies, it is desirable to evaluate water discharge, material fluxes, and concentration distributions in channel cross sections. As a step towards this goal, it is common to illustrate how parameters vary spatially in the cross section by constructing graphs showing lines of equal values (isopleths) of time–averaged or net quantities. Velocity, material concentration, and material flux measurements are often plotted onto a graph representing the cross-sectional area at mean tide. This requires special care when the tidal range is an appreciable fraction of the water depth at mean tide.

Kjerfve and Seim (1984) showed how this averaging procedure can be carried out so that net cross-sectional distribution plots properly conserve net discharge, net cross-sectional concentration, and net material flux. A planimeter used on these plots to evaluate, for example, net material flux would yield correct and consistent results.

To measure the net flux from a cross-sectional graph at mean tide should be done with discrimination, because the measures could either underestimate or overestimate the time–averaged quantity itself, depending on the phase angles between currents, water depth, and concentration (Kjerfve, 1975). The variability of the cross-sectional area during different stages of the tide is the culprit, giving rise to a Stokes' drift as a component of the overall net flux. This component is overlooked if the averaging is not done properly (Kjerfve and Seim, 1984).

Consider a quantity, f(y,z,t), tidally induced to oscillate with time, t, which, because of physical or biological processes, varies laterally (y) or vertically (z) in a cross section. The quantity f(y,z,t) could be velocity, material concentration, or material flux. Because of tidal action, the cross–sectional area, defined as

$$A(t) = \Sigma\Sigma \; dydz$$

Oscillates more or less sinusoidally around the net cross-sectional area, A_o. The degree to which A(t) oscillates can be quantified as a percentage of the variation, $\Sigma = 100$ x standard deviation of $A(t)/A_o$.

In constructing graphs of net distribution of f(y,z,t) in a channel cross section, it is first necessary to calculate time–averages of f(y,z,t) everywhere in the cross section, i.e.,

$$f_o(y,z) = \Sigma f(y,z,t)dt/T$$

where T is one or more complete tidal cycles. This is not exactly straightforward, because the integration of $f_o(y,z)$ over the mean cross-sectional area,

$$F_\bullet = \Sigma\Sigma f_o(y,z)dA$$

must equal the time-average of the instantaneous discharge, concentration, or material flux, respectively, such that $F_\bullet = F_o$, where

$$F_o = \Sigma \; [\Sigma\Sigma \; f \; (y,z,t)dA] \; dt/T.$$

and represents the time average of the cross-sectionally averaged quantity.

The problem is in the numerical evaluation of f_o in tidal estuaries where ϵ exceeds a few percent. For each cross-sectional measurement position, Kjerfve (1975, 1979) proposed time-averaging of f at non-dimensionalized depths between surface and bottom. As the tide varies, the depth is telescoped up or down accordingly. An f_o-value is the average of n sequential f-values. Each of these f-values is estimated for the same position relative to the total depth. At the same time, they are estimates at varying absolute depths below the surface, depending on tidal stage. $F_\bullet$ is then estimated numerically by multiplying each f_o-value by a percentage of A_o and summing the products over the cross section. The resulting $F_\bullet$-value will in general not equal F_o except in the absence of tides. From experience, the disagreement between $F_\bullet$ and F_o increases with increasing ϵ.

The objective is to develop an alternative averaging scheme for water bodies, with substantial ϵ values such that $F_\bullet = F_o$. With a sufficiently dense set of f-measurements in a cross section, repeated an adequate number of times, F_o can by evaluated numerically by first computing instantaneous area-integrations of f, and then averaging these over time (Kjerfve, 1979; Kjerfve and Seim, 1984). $F_\bullet$ can also be calculated numerically by area-integrating of f_o. For consistency in analysis and interpretation of field data, it seems reasonable to make sure that cross-sectional parameter graphs of $F_\bullet$ do indeed equal to F_o. The difficulty lies in the construction of an appropriate isopleth plot of f_o (y,z) or the computation of the time-average of f (y,z,t) for which ϵ differs from zero.

The term f (y,z,t) can represent either velocity [L/T], material concentration [M/L^3], or material flux [$M/L^2/T$]. In an estuarine-mangrove flux study, velocity measurements should be made simultaneously with nutrient, salinity, and other concentration determinations at each cross-sectional sampling point. The material flux is simply the product of velocity and concentration (Kjerfve, 1979). Velocity and

concentrations are usually measured at several depths for each location in an estuarine cross section. Vertical profiles are interpolated from surface to bottom, usually p = 3, 5 or 11 equidistant points. The number of lateral sampling locations, m, usually varies from 1 to 11, depending on cross-sectional width, tidal prism, and logistic capability (Kjerfve et al., 1981, 1982). The constant sampling rate. dt, has varied between studies from 20 minutes to 1.5 lunar hours with the constraint that the minimum sampling duration, ndt, equals the period of a complete tidal cycle. Most often the sampling duration is taken to be an even number of consecutive tidal cycles (usually two or four) to minimize effects of tidal diurnal inequality.

Let f (i,j,k) represent the f-value at lateral position i = 1,2,...m; at interpolated depth j = 1,2,... p; and at sampling time k = 1,2,...n. This f-values is representative for a sub-area, a (i,j,k), of the total instantaneous cross-sectional area (Fig. 19). The time-average of a (i,j,k,) is given by

$$a_o(i,j) = \sum_{k=1}^{n} a(i,j,k)/n$$

which sums to the net cross-sectional area, i.e.,

$$A_o = \sum_{i=1}^{m} \sum_{j=1}^{p} a_o(i,j)$$

it is now possible to rewrite

$$F_\bullet = \sum_{i=1}^{m} \sum_{j=1}^{p} f_o(i,j)\ a_o(i,j)$$

and

$$F_o = \sum_{k=1}^{n} [\sum_{i=1}^{m} \sum_{j=1}^{p} f(i,j,k)\ a(i,j,k)]/n$$

respectively. It is then easy to show that if the time-average of f(i,j,k) is written

$$f_o(i,j) = [\sum_{k=1}^{n} f\ (i,j,k)\ a(i,j,k)]/[na_o(i,j)$$

the condition that $F_\bullet$ equals F_o is satisfied. Similarly, the root-mean square (rms) deviation of f(i,j,k) may be expressed as

$$f_{rms}(i,j) = \{\sum_{k=1}^{n} [f\ (i,j,k)\ a(i,j,k) - a_o(i,j)\ f_o(i,j)]^2/[(n-1)\ a_o^2(i,j)]\}\ ½$$

The summation of $f_{rms}(i,j)$ over the entire cross section is similarly identical to the temporal rms deviation of the instantaneous cross-sectional flux from the F_o-value.

Distribution of time-averaged and rms quantities in a tidal estuarine cross section is most consistently displayed by plotting $f_o(i,j)$ and $f_{rms}(i,j)$, respectively, for the m lateral stations and p interpolated depths on the net cross-sectional area, A_o. The advantage of proceeding in this manner is that flow, concentration, or flux measurements are properly weighted by the appropriate, instantaneous

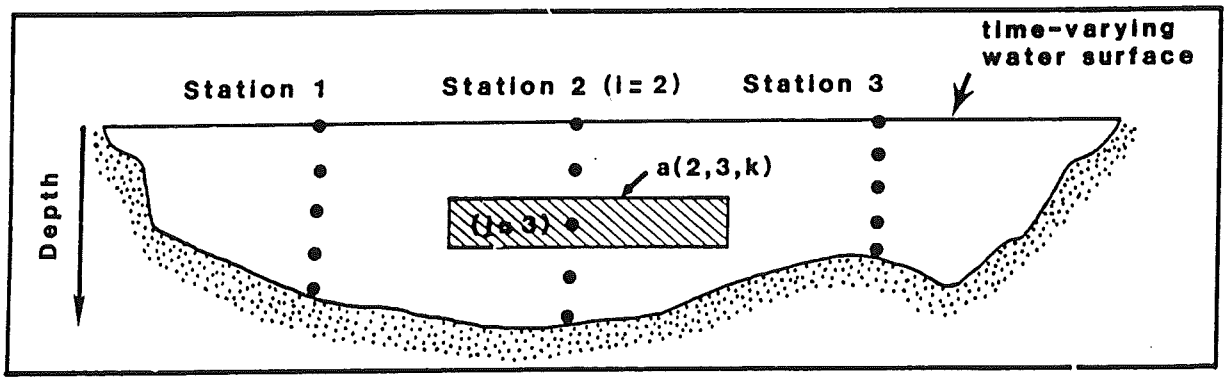

Fig. 19. Subarea a(2,3,k) in an estuarine cross–section (after Kjerfve and Seim, 1984).

cross-sectional sub-area (Fig. 19), such that consistency is maintained whether time-averaging is performed before area-averaging or vice-versa.

Similarly, the rms computations yield consistency. The f_{rms}-values are most readily interpreted as the intensity of the water or material tidal transport, or in the case of concentration, the time-variability of the tidal concentration variation.

10. A CASE STUDY: KLONG NGAO, RANONG, THAILAND*

10.1. Project Description

During 1988 – 1989, a multidisciplinary UNDP/UNESCO-NRCT field project was carried out in the Klong Ngao mangrove wetlands (Fig. 20) near Ranong, Thailand. The Klong Ngao (Lat N 9° 5′ and Long E 98° 3′) is a shallow tidal creek, draining 11.5 km^2 of mangrove wetlands and an additional 18.9 km^2 of adjacent hilly terrain (Chunkao et al., 1985). It is part of a larger mangrove system lying on the extensive deltaic plain of the Kra Buri, which forms the border between Thailand and Burma. The Kra Buri debauches into the Andaman Sea on the western side of the Kra peninsula (Fig. 20). Its deltaic plain is largely colonized by mangrove vegetation, which is in part undisturbed and represents one of the most well-developed mangrove systems in Thailand. *Sonneratia* and *Avicennia* spp. grow along creek banks and near the shoreline. *Rhizophora* spp. and *Bruguiera gymnorhiza* occupy nearly two-thirds of the basin area, and both *Acrostichum* and *Xylocarpus* spp. are common along tidal creeks near the inland margin of the basin. *Excoecaria* and *Lumnitzera* spp., although common to the region, do not grow in great numbers in the Klong Ngao basin.

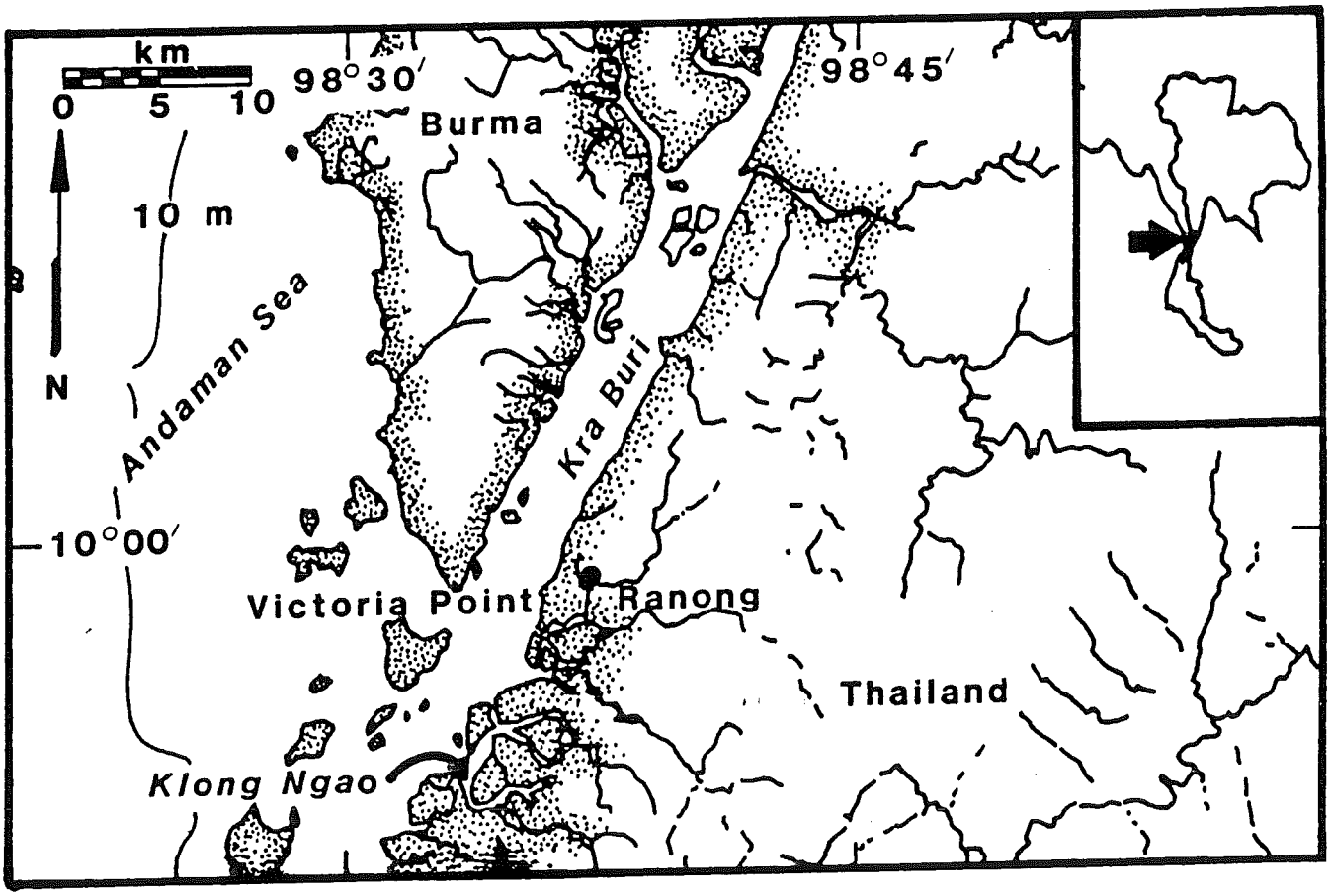

Fig. 20. Area map showing relationship of Klong Ngao and Kra Buri.

* This chapter was co-authored by Dr. Gullaya Wattayakorn, Department of Marine Science, Chulalongkorn University, Bangkok 10330, Thailand; and with assistance from Supaporn Rakkhiew, Ladawan Itthipatachai, Nittaratana Paphavasit and Pramot Sojisuporn.

Table 3. Hydrographic sampling dates on Klong Ngao with tidal and rainfall statistics.

Date	Tidal Range (m)	24-Hour Rainfall (r_d, mm)	Rainfall for Prior 7 Days (r_w, mm)
Dry Season			
10 Apr 1988	1.4	0	33
18 Apr 1988	3.4	0	2
Wet Season			
4 May 1988	3.3	24	165
23 May 1988	1.4	1	68
6 Jul 1988	2.3	3	61
26 Aug 1988	3.5	3	30
4 Sep 1988	0.6	0	107
26 Sep 1988	4.4	75	460

Sampling consisted of (1) determination of water depth, (2) measurements of current velocity, (3) appraisal of conductivity and temperature from which salinity was calculated (Foffonoff and Millard, 1983), and (4) collection of water samples for laboratory analysis of carbon, nutrients, and sediment concentrations. Vertical profiles of current velocity and water quality parameters were made at three depths: 1.0 m below the surface, at mid depth, and 1.0 m above the bottom. Current vanes (Kjerfve and Medeiros, 1989) were used to measure creek-parallel current speeds in the range $0.2-1.9$ m^{s-1} with a mean error less than 0.06 m_s^{-1} at each depth. A weighted line was used to measure depth. Conductivity and temperature were alternately measured using a YSI salinometer, a refractometer, and collection of water samples for titration. A 1 liter Hydro-Bios water sampler was used to collect water samples.

All water samples were filtered immediately in the laboratory using 0.7 fm Whatman GF/C filters. Total dissolved nitrogen (TN), nitrite (NO_2), nitrate (NO_3), total phosphorus (TP), phosphate (PO_4), and silicate (SiO_2) concentrations were determined by the methods of Strickland and Parsons (1972). Total suspended sediment (TSS) concentration was also determined by filtering water samples through pre-weighed 0.7 fm Whatman GF/C filters. After drying at 100°C, the filters were reweighed. Chlorophyll—a analysis was accomplished spectro-photometrically (Strickland and Parsons, 1972). As quality control, at least two samples per tidal cycle were replicated five times for each of the above parameters, with standard deviations less than 6% of the means for NO_2, NO_3, SiO_2, Chl-a, and TSS; less than 10% for PO_4; less than 30% for TP, and less than 50% for TN.

Additional time series measurements were made in support of the outwelling study. A Seba Hydrometrie GMBH recording tide gauge was installed at the mouth of Klong Ngao (near station #1) in June 1988 and maintained until December 1988. Tide staffs were installed at stations #1 and #5 and relied on for tidal data for the first four sampling dates (Table 3). Meteorological measurements (wind speed and direction, atmospheric pressure, temperature, humidity, rainfall, irradiance, and evaporation) were made routinely at the Meteorological Department weather station in Ranong and some measurements daily (irradiance and relative humidity) at the Mangrove Forest Research Center of the Royal Thai Forestry Department near the head of Klong Ngao. Cross—sectional creek bathymetry was determined with a fathometer. The topography of the mangrove-covered area was estimated from water depth measurements along creek—normal boardwalks at four locations.

In addition, we collected surface-floating mangrove litter by installing a 25 m surface-skimming net across Klong Ngao near station #4, where the creek is 47 m wide. The net was stretched from one bank towards the middle of the creek, using a second boat, for 30 min every 2 lunar hours. The litter consisted

All components of the UNDP/UNESCO–NRCT field project were conducted in the Klong Ngao mangrove wetlands (Fig. 21), including an outwelling experiment. The field work was complicated by semidiurnal macrotidal conditions, which both inundated the entire system at high tides and made it difficult to navigate a small boat in the creek during low tides. Intense and frequent rainfall during sampling also complicated matters. The annual rainfall at Ranong, Thailand, measures 4.02 m, and it rains an average of 190 days per year. The local weather is dominated by the relatively dry northeast monsoon, December–March, and the wet southwest monsoon, May – October. According to Köppen (1900), the climate is classified as tropical monsoon, A_m.

The Klong Ngao wetland is strongly influenced by tides, resulting in periodic inundation of the entire wetland, oscillating tidal currents, and semidiurnal variations in the concentration of water quality parameters. To calculate resultant material fluxes out of or into the mangrove system, it was necessary to make measurements over a complete tidal cycle and then calculate residual material fluxes as the average of the instantaneous flux estimates.

10.2. Design and Measurements

The mangrove outwelling experiment consisted of repeated hydrographic sampling from five stations along Klong Ngao (Fig. 21) over eight different tidal cycles during 1988 (Table 3). The design was based on similar studies in temperate salt marsh systems (Kjerfve et al., 1981; Dame et al., 1986), although a simpler design because of logistics and financial constraints. Sampling was conducted sequentially at each station from a small boat with measurements made 8–12 times per tidal cycle at each station. Sampling began near daybreak and continued for 12.4 hours. All measurements were made in the center of Klong Ngao based on the assumption that cross–sectional variability remained small relative to longitudinal changes. Also, Kjerfve and Wolaver (1988) showed that data from a single cross-sectional station can be used to estimate longitudinal fluxes in tidal creeks. Selection of a single station in each cross section was dictated by logistic constraints.

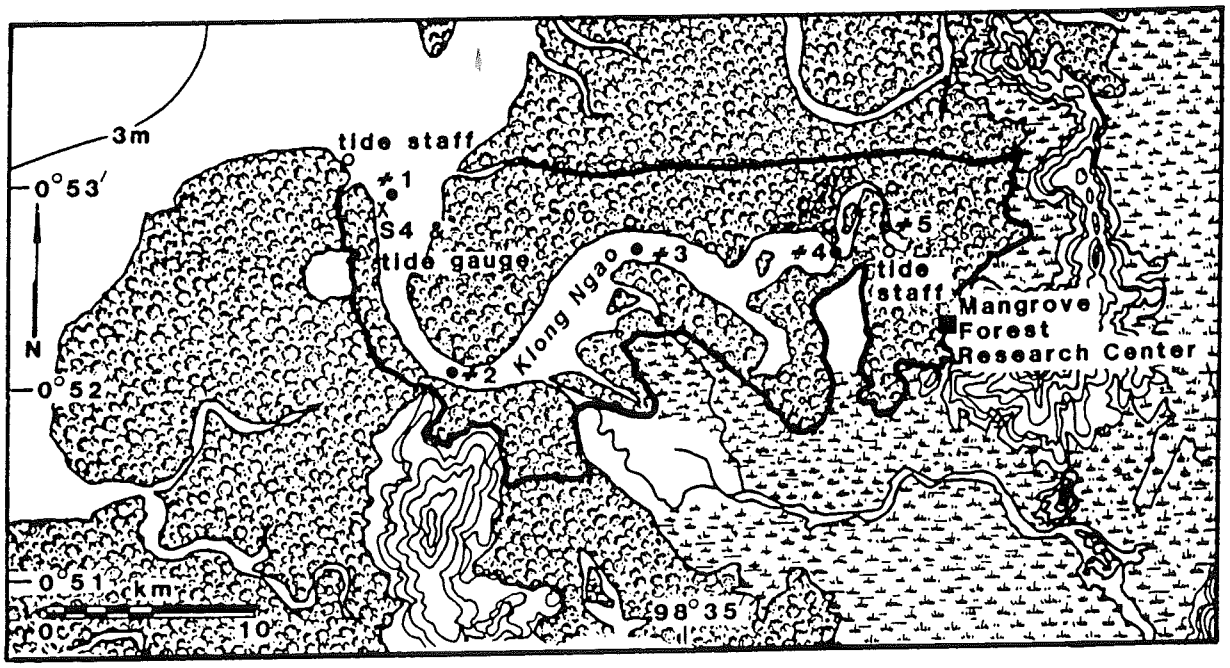

Fig. 21. Map of the Klong Ngao and adjacent mangrove wetlands. The solid black outline defines the Klong Ngao tidal watershed.

mostly of mangrove leaves. The litter samples were dried for 48 hrs at 75°C and weighed. A portion of the sample was ashed to facilitate the calculation of carbon as the difference between dry weight and ash residual.

10.3. Sea Level Variations

The Andaman sea experiences a seasonal variation in mean sea level as a result of the change in monsoons and the steric effect (Pattullo et al., 1955). Low mean sea level typically occurs in January and February, and the high mean sea level in July and August. Interpolating from multi-year measurements in Rangoon, Burma, and Ko Ta – Phao Noi, Thailand, mean sea level varies 0.37 m seasonally at Ranong.

The composite tide along the Andaman Sea coast is predominantly semidiurnal and propagates from north to south with high water at Ranong lagging high tide at Mergui, Burma, 275 km to the north, by 1.5 hours. Most constituent tides also propagate from north to south (McCammon and Wunsch, 1977; Hydrographic Department, 1979). The tidal range at the mouth of Klong Ngao measures 2.5 m on the average but is 30% lower than the tide at Mergui (Hydrographic Department, 1979). Comparison of tide staff readings at stations #1 and #5 half–hourly during several complete tidal cycles during our study indicated that (1) the tidal amplitude remains constant along Klong Ngao, and (2) high water at the mouth leads high water at the head of the creek by 1 hour.

The analog data records from the tide gauge near station #1 in Klong Ngao were digitized hourly and subjected to harmonic analysis (Schureman, 1941; Dennis and Long, 1972; Franco, 1988). The water elevation can be expressed as

$$h(t) = H_0 + fH \cos [at + (V_0 + u) - k]$$

where H is constituent tide amplitude; H_0 is mean water elevation; a is speed of the constituent tide in rad/hour, calculated as 2π; f is tidal node factor and $(V_0 + u)$ is Greenwich equilibrium argument from look-up tables; and k is the epoch of the constituent tide from which the Greenwich epoch, °G, is computed (Schureman, 1941).

Several 29-day records were analyzed separately, and the major harmonic constants (Table 4) were found to be in good agreement with McCammon and Wunsch (1977). The tidal amplitudes agree well from month to month and exhibit a pronounced fortnightly spring–neap tide modulation. Spring tides have an average range of 3.3 m and neap tides an average range of 1.0 m. All local shallow water compound tides and overtides, including M4, are small with amplitudes less than 0.07 m.

Table 4. Statistics for the seven largest constituent tides at the mouth of Klong Ngao during three 29-day periods in 1988. Data for the K_2 constituent are inferred (cf. Franco, 1987).

Constituent	Symbol	Period (T, hr)	Amplitude 1–29 Jun	(H, m)/Epoch 1–29 Jul	(°G) 2–28 Sep
Principal lunar diurnal	(O_1)	25.82	0.05/198	0.06/191	0.03/194
Luni-solar diurnal	(K_1)	23.93	0.12/221	0.12/220	0.14/214
Larger lunar elliptic	(N_2)	12.66	0.32/095	0.02/169	0.33/081
Principal lunar	(M_2)	12.42	1.11/082	1.16/079	1.06/085
Principal solar	(S_2)	12.00	0.57/123	0.59/109	0.50/123
Luni-solar semidiurnal	(K_2)	11.97	0.16/126	0.16/112	0.14/126
Principal lunar overtide	(M_4)	6.21	0.03/069	0.04/072	0.07/099
Mean level relative to MSL	(H_o)		+0.22 m	+ .15 m	−0.03 m

10.4. Hypsometric Characteristics

A combination of (1) tidal characteristics, (2) water depth measurements made at high tide from the four boardwalks, and (3) planimetry of creek and mangrove areas using a 1:50,000 topographic map, allowed calculation of a crude hypsometric curve for the Klong Ngao creek-mangrove basin area and the computation of various area and volume characteristics for the system (Table 5).

Table 5. Distance, area, and volume characteristics for Klong Ngao and adjacent mangrove wetlands.

Station	Distance (km)	Cross–sectional Area (MSL, m^2)		
5	0.0	15.0		
4	0.9	77.0		
3	2.6	430.0		
2	4.8	1,370.0		
1	6.5	1,200.0		
Surface area of entire drainage system			30.4 km^2	
Surface area of creek/mangrove system			11.5 km^2	
Water covered area at bankful tide stage			2.7 km^2	
Water covered area at mean tide			2.5 km^2	
Creek Volume ($\times 10^6$ m^3):		Spring low tide		2.3
		Mean sea level (MSL)		5.1
		Spring high tide		10.5
Tidal Prism ($\times 10^6$ m^3):		Neap tide		2.2
		Mean tide		3.5
		Spring tide		8.3

We used the hypsometric information and the tidal data from Klong Ngao to calculate the percent of the time that the tides inundate the different area of the mangrove system. We found that the mangrove wetland area above bankfull stage is only inundated 9% of the time. Specific locations within the wetland at higher elevations are flooded less frequently, and the system as a whole is only inundated 1% of the time.

10.5 Freshwater Balance

Klong Ngao is not gauged, and it was not feasible to make direct measurements of freshwater runoff into the Klong Ngao during the eight tidal cycles in 1988. Rather, we estimated the freshwater runoff from a simple water balance model (Schreiber, 1904). Such simple models should be used with extreme care. However, since direct measurements were lacking, the modeling approach represents the best solution to estimate the freshwater runoff.

The runoff ratio, q/r is the ratio of freshwater runoff and rainfall, and was approximated as

$$\triangle f/r = \exp\{-E_o/r\}$$

(Schreiber, 1904; Sellers, 1965; Holland, 1978) where $\triangle$ f is runoff [$L\,T^{-1}$], r is rainfall [$L\,T^{-1}$], and E_o is potential evapotranspiration. In an earlier study, Apakupakul (1985) estimated mean monthly rainfall and potential evapotranspiration rates for Ranong based on daily measurements 1964–1980. We used these data to calculate the runoff ratio (Table 6). We assumed that (1) the rainfall for each of the eight tidal

cycles was uniform over the drainage basin, (2) the calculated monthly runoff ratio was representative of the 1988 sampling dates, and (3) the rainfall, r_w, for 7 days prior to each sampling date (Table 3) can be used to calculate an average freshwater runoff for each of the eight tidal cycles (Table 6). Comparing freshwater runoff to the tidal prism, i.e. the tidal water volume exchange per tidal cycle (Table 6), indicates that tidal water exchange is an order of magnitude greater than the freshwater exchange. This technique for calculating freshwater runoff is rather crude, provides a reasonable estimate, but should be used with caution.

Table 6. Freshwater characteristics of the Klong Ngao system.

Tidal cycle	△f/r	Runoff (Q, m^3 s^{-1})	River inflow (m^3) per tidal cycle
10 Apr 1988	0.40	0.7	0.03×10^6
18 Apr 1988	0.40	0.0	0.00×10^6
4 May 1988	0.80	6.6	0.30×10^6
23 May 1988	0.80	2.7	0.12×10^6
6 Jul 1988	0.87	2.7	0.12×10^6
26 Aug 1988	0.89	1.3	0.06×10^6
4 Sep 1988	0.88	4.7	0.21×10^6
26 Sep 1988	0.88	20.3	0.91×10^6

10.6. Constituent Concentrations

The study generated an enormous amount of data, more than 1,000 concentration determinations per constituent. Here, it is only feasible to present the time-averaged, cross-sectionally weighted concentration data at the mouth of Klong Ngao as an indicator of constituent concentration levels (Table 7) during four tidal cycles in the 1988 for which flux computations were carried out.

Table 7. Cross–sectionally weighted net concentrations at station #1 for four tidal cycles during the wet season.

Constituent	4 May	23 May	4 Sep	26 Sep
Salinity (ppt)	0.20	0.14	0.41	0.36
NO_2 (ug–at N/l)	0.71	0.31	1.18	1.03
NO_3 (ug–at/l)	2.25	2.64	4.31	4.11
TN (ug–at/l)	0.29	0.37	0.12	0.12
PO_4 (ug–at/l)	2.63	2.54	3.77	3.69
TP (ug–at/l)	20.3	22.7	34.3	31.9
S_iO_2 (ug–at/l)	8.7	6.4	5.7	5.3
Chl-a (ug/l)	121	82	140	132
TSS (mg/l)	14.6	13.9	17.0	14.7
TOC (ppm)				

10.7. Material Flux Computations

Several current vanes were lost during the field sampling and could not be replaced in a timely fashion.

This resulted in lack of current velocity measurements during four of the eight tidal cycles: 10 and 18 April, 6 July, and 26 August (cf. Table 6). Thus, water discharge and material fluxes were only calculated for those four tidal cycles during the wet season for which velocity measurements were available.

Water and material exchanges between the creek-mangrove system and the adjacent coastal ocean were calculated for the cross–section at station #1 (Fig. 6). Computation of material fluxes for complete tidal cycles was achieved by cross–multiplying velocity, area, and concentration at fixed intervals (Kjerfve et al., 1981). The objective was to calculate net or time-averaged material fluxes over a complete tidal cycle.

Recognizing that (1) the tidal period varies between cycles and (2) water and material fluxes may vary as a result of changes in the storage within the system, the duration of a tidal cycle needed careful definition. To calculate net material fluxes without regard to differences in storage, a tidal cycle was defined to last from the time of the first measurement until the water level again reached the same elevation for the second time, approximately 12.4 hours later. Proceeding in this manner, the net water flux can be expected approximately to equal the freshwater runoff, and the cumulative tidal ebb discharge to equal the cumulative tidal flood discharge.

A number of preliminary data processing steps were necessary. A cubic spline (Kjerfve et al., 1981) was fitted to each vertical velocity profile, and bank-parallel velocities were interpolated for the top, middle, and bottom thirds of the water depth. To allow unbiased time-averaging, we spline-fit curves through each of the velocity and concentration time series. New velocity and concentration values were interpolated every lunar hour from the beginning to the end of the tidal cycle, and these interpolated values were subjected to further analysis.

Each depth and time interpolated velocity, vi, was assumed representative of the cross–sectional area, ai, corresponding to a depth interval (top, mid, or bottom) at one particular lunar hour. The instantaneous discharge for each portion of the cross section was written

$$q_i = a_i v_i$$

and the total instantaneous cross-sectional water flux, q(t) [$m^3\ s^{-1}$], was calculated as

$$q(t) = \Sigma q_i$$

for i = 1,2,3. Similarly, water samples were collected at three depths, which more or less corresponded to the same depths as those for which the velocities were interpolated. The corresponding time–interpolated concentrations were denoted c_i and expressed in [M L^3].

Instantaneous cross–sectional fluxes, f(t) [kg s^{-1}] of nutrients (nitrate, nitrite, phosphate, silicate), organic carbon, and suspended sediment were calculated as

$$f(t) = \Sigma\ a_i\ v_i\ c_i$$

for i = 1,2,3 for the four tidal cycles. Based on the assumption that the depth variations in the horizontal velocity is small, as indicated by the velocity profiles, it was possible to estimate the instantaneous cross–sectional flux as

$$f(t) = q_a\ [\Sigma\ a_i\ c_i / \Sigma\ a_i]$$

Net and root-mean-square variations of water and material fluxes, respectively, were calculated according to Kjerfve et al. (1981) as

$$q_N = \Sigma\ q_k/12$$

$$q_{RMS} = [\Sigma\ (q - q_N)^2/11]^{1/2}$$

$$f_N = \Sigma\ f_k/12$$

$$f_{RMS} = [\Sigma\ (f_k - f_N)^2/11]^{1/2}$$

The computed net and rms water and material flux results for a number of constituents are summarized in Table 8.

Table 8. Net and rms constituent fluxes as calculated for four tidal cycles in 1988. Positive values are exports and negative fluxes imports.

Constituent		4/5	23/5	4/9	26/9
Water	net	+163	−10	+28	+43
$m^{3/s}$	rms	706	283	107	344
Salt	net	+4.9	−0.0	+0.7	+1.0
1000 kg/s	rms	21.2	8.7	2.8	7.4
NO_2	net	+44	−10	+1	+8
0.01 g/s	rms	193	54	18	351
NO_3	net	+176	−10	+6	−7
0.01 g/s	rms	678	178	26	849
TN	net	+142	−157	+110	+433
0.01 g/s	rms	1860	1058	494	2266
PO_4	net	+135	−10	+3	+4
0.01 g/s	rms	668	420	21	114
TP	net	+177	−39	+1	+85
0.1 g/s	rms	567	229	20	578
S_i	net	+70	+38	+28	+4
g/s	rms	373	197	108	343
Chl-a	net	+142	−8	+9	+52
0.01 g/s	rms	633	176	43	270
TSS	net	+15	−0	+2	+9
kg/s	rms	72	23	6	77
TOC	net	+1.0	−0.0	+0.4	0.6
kg/s	rms	4	4	2	4

10.8. Estimation of Litter Flux

Organic matter is typically exported from mangrove wetlands (Boto and Bunt, 1981), a conclusion based on the large amount of litter produced within a mangrove system. The residual flux of mangrove litter (fL), in our case leaves, as measured with a surface-skimming net near station #4 during the hydrographic measurements during the eight tidal cycles was calculated from

$$fL = \Sigma(wC/wN)\ mk\ (124/30)$$

where the width of the creek wN = 47 m; the width of the net wN = 25 m; mk represents the mass of litter, positive for export and negative for import; the subscript k indicates sampling times k = 1,2...6; and the weighting factor indicating that the net was deployed 30 min every 2 lunar hours. The results, as reported in Table 9, have been adjusted to indicate the export of mangrove litter per day, rather than per tidal cycle, and expressed as the flux from that section of the Klong Ngao mangrove system upstream of the sampled section, approximately 2 km^2.

The results indicate that mangrove leaf litter was exported from the Klong Ngao system during every tidal cycle. This result is fairly robust because it is based on data from eight tidal cycles. The maximum litter transport occurred during the spring tidal cycles on 18 April and 4 May, just at the onset of the wet season. The rates of transport were quite low, however. Leaves make up 85% of the total litterfall in the Ranong forest, measuring 2.0 kg/ha/day on the average during the 1988 sampling.

Our outwelling estimates suggest that only 0.3% to 12.5% of the mangrove leaf litter fall is exported from the system with the currents. Poovachiranon and Chansang (1982) reported litter export from a Phuket mangrove system during spring tides of 900 kg/ha/day, three times as great as our maximum rate. This is possibly explained by the larger tidal range in the Phang-nga Bay area.

Table 9. Export of mangrove litter (mostly in the form of leaves) as determined from the sampling with the surface-skimming net (expressed both as dry weight and as carbon).

Litter Flux	TC1	TC2	TC3	TC4	TC5	TC6	TC7	TC8
Dry Weight g/ha/day	6	250	152	12	9	27	6	40
Carbon g/ha/day	5	208	124	10	8	23	5	31

10.9. Final Comments

The above data are given as examples of the results of the Ranong outwelling study. Listing of the results in a table, however, is obviously not the end of the analysis. Next should follow an evaluation of the statistical significance of the means. The resultant fluxes are usually 1–3 orders of magnitude smaller than peak instantaneous fluxes. Thus, an assessment of the extent to which resultant material fluxes are statistically significant is a crucial analysis step (Spurrier and Kjerfve, 1988). Hydrodynamic modeling is usually another step in the analysis of flow and flux data in an estuarine system. Here, no attempt has been made to cover modeling although it was a component of the Ranong study. Application of numerical modeling to mangrove systems has successfully been concluded by Wolanski et al. (1980) and Wolanski (1985). An ecological interpretation of the results, synthesis, and discussion of the observations are important and necessary remaining steps to conclude the study. However, these topics are beyond the scope of this manual. Rather, the presentation of some results from the Klong Ngao study serves to demonstrate how calculations that can be made with data which are collected systematically without the benefit of sophisticated instrumentation and big budgets.

9. REFERENCES

Aksornkoae, S. 1986. Mining impacts of mangrove ecosystem in Thailand. pp. 107–114. In: Proceedings of the Workshop on Human Induced Stresses on Mangrove Ecosystems, Bogor, Indonesia. UNDP/UNESCO Regional Project RAS/79/002.

Anderson, J.A.R. and J. Muller. 1973. Palynological study of a Holocene peat and a Miocene coal deposit from NW Borneo. Pollen et Spores 15:291–351.

Apakupal, R. 1985. The rainy season in southern Thailand. pp. 51–61. In: Proceedings of the International Seminar on Environmental Factors in Agricultural production, Thailand.

Barnes, R.S.K. 1980. Coastal lagoons, the natural history of a neglected habitat. Cambridge University Press, Cambridge. 106 pp.

Bird, E.C.F. 1972. Mangroves and coastal geomorphology in Cairns Bay, north Queensland. Journal of Tropical Geography 35:11–16.

Bird, E.C.F. and N.J. Rosengren. 1986. Mangrove and coastal morphology. pp. 17–28. In: Report of the Workshop on mangrove ecosystems dynamics. Motupore Island Research Station, Port Moresby, New Guinea. UNDP/UNESCO Regional Project RAS/79/002.

Blasco, F. 1984. Climatic factors and the biology of mangrove plants, pp. 18–35. In: The mangrove ecosystem: research methods. UNESCO Paris.

Boon, J.D., III. 1975. Tidal discharge asymmetry in a salt marsh drainage system. Limnology and Oceanography 20:71–80.

Boon, J.D., III. 1977. Suspended solids transport in a salt marsh creek – an analysis of errors. In: B. Kjerfve (ed.), Estuarine Transport Processes. University of South Carolina Press.

Boon, J.D., III and R.J. Byrne. 1981. On basin hypsometry and the morphodynamic response of coastal inlet systems. Marine Geology 40:27–48.

Boto, K.G. and J.S. Bunt. 1981. Tidal export of particulate matter from a northern Australian mangrove system. Estuarine, Coastal and Shelf Science 13:247–255.

Boto, K.G. 1982. Nutrient and organic fluxes in mangroves, pp. 239–258. In: B.F. Clough (ed.), Mangrove ecosystems in Australia: Structure, function and management. Australian National University Press, Canberra.

Bowden, K.F. 1963. The mixing processes in a tidal estuary. International Journal of Air and Water Pollution 7:343–356.

Bowden, K.F. 1983. Physical oceanography of coastal waters. Halsted Press, New York. 302 pp.

Brooks, D.A. and C.N.K. Mooers. 1977. Wind–forced continental shelf waves in the Florida current. Journal of Geophysical Research 82:2569–2576.

Buchanan, T.J. and W.P. Somers. 1969. Discharge measurements at gaging stations. Techniques of water-resources investigations of the United States Geological Survey, Chapter A8, Book 3. United States Government Printing, 65 pp.

Byrne, R.J. and J.D. Boon, III. 1973. An inexpensive, fast response current speed indicator. Chesapeake Science 14:217–219.

Cannon, G.A. (ed.). 1978. Circulation in the Strait of Juan de Fuca: some recent oceanographic observations. NOAA Technical Report ERL 399–PMEL 29. 49 pp.

Carlton, J.M. 1974. Land building and stabilization by mangroves. Environmental conservation 1: 285–294.

Carnahan, B. and J.O. Wilkes. 1973. Digital computing and numerical methods. John Wiley & Sons.

Chapman, V.J. and J.W. Ronaldson. 1958. The mangrove and salt-marsh flats of the Auckland Isthmus. New Zealand Department of Scientific and Industrial Research Bulletin 125:1–79.

Chapman, V.J. 1975. Mangrove vegetation. Leuterhausen, Strauss & Cramer, Lehre. 425 pp.

Chapman, V.J. 1977. Wet coastal ecosystems. Elsevier Scientific Publishing Company. Amsterdam. 428 pp.

Chapman, V.J. 1976. Mangrove vegetation. J. Kramer, Vaduz. 447 pp.
Chunkao, K., W. Niyom, and S. Tantanawarit. 1985. Sediment and water flow affected to estuarine zone and its productivity. pp. 209–216. In: Proceedings of the International Seminar on Environmental Factors in Agricultural Production, Thailand.
Clough, B.F, T.J. Andrews, and I.R. Cowan. 1982. Physiological processes in mangroves, pp. 193–210. In: B.F. Clough (ed.), Mangrove ecosystems in Australia: Structure, function and management. Australian National University Press, Canberra.
Clough, B.F. 1987. Measurement of mangrove productivity. pp. 256–264. In: C.D. Field and A.J. Dartnall (eds.), Mangrove ecosystems of Asia and the Pacific, status, exploitation, and management. Proceedings of the Research for Development Seminar held at the Australian Institute of Marine Science, Townsville, Australia.
Clough, B.F. amd R.G. Sim. 1989. Changes in gas exchange characteristics and water use efficiency of mangroves in response to salinity and vapour pressure deficit. Oecologia 79:38–44.
Coleman, J.M., S.M. Gagliano, and W.G. Smith. 1970. Sedimentation in a Malaysian high tide tropical delta, pp. 185–197. In: J.P. Morgan (ed.), Deltaic sedimentation, modern and ancient. Special publication no. 15. Society of Economic Paleontologists and Mineralogist.
Coleman, J.M. and L.D. Wright. 1975. Modern river deltas: variability of processes and sand bodies, pp. 99–150. In: M.L. Broussard (ed.), Deltas, models for exploration. Houston Geological Society, Houston.
Coleman, J.M. 1976. Deltas: processes and models for deposition and for exploration. Continuing Education Publication Company, Inc., Champaign, IL. 61820.
Collier, A. and J.W. Hedgepeth. 1950. An introduction to the hydrography of tidal waters of Texas. Publication of the Institute of Marine Science 1:125–194.
Collins, M. and C. Pattiaratchi. 1984. Identification of suspended sediment in coastal waters using airborne thematic mapper data. International Journal of Remote Sensing 5:635–657.
Copeland, B.J., J.H. Thompson, Jr., and W.B. Ogletree. 1968. Effects of wind on water levels in the Texas Laguna Madre. Texas Journal of Science 20:196–199.
Curran, P.J., J.D. Hansom, S.E. Plummer, and M.I. Pedley. 1987. Multispectral remote sensing of nearshore suspended sediments: a pilot study. International Journal of Remote Sensing 8:103–112.
Dame, R., T. Chrzanowski, K. Bildstein, B. Kjerfve, H. McKellar, D. Nelson, J. Spurrier, S. Stancyk, H. Stevenson, J. Vernberg, and R. Zingmark. 1986. The outwelling hypothesis and North Inlet, South Carolina. Marine Ecology–Progress Series 33:217–229.
Davies, G.R. 1970. Carbonate sedimentation, eastern Shark Bay, Western Australia. American Association of Petroleum Geologists Memoirs 13:85–168.
Davies, J.L. 1973. Geographical variation in coastal development. Hafner Publishing Co., New York.
Defant, A. 1960. Physical oceanography, Vol. 2. Pergamon Press, New York. 598 pp.
Dennis, R.E., and E.E. Long. 1971. A user's guide to a computer program for harmonic analysis at tidal frequencies. NOAA Technical Report NOS 41. National Oceanic and Atmospheric Administration. Rockville, MD. 11 pp.
Diemont, W.H. and W. van Wijngarrden. 1975. Sedimentation patterns, soils, mangrove vegetation and land use in the tidal areas of west Malaysia, pp. 513–528. In: G. Walsh, S. Snedaker, and H. Teas (eds.), Proceedings of the International Symposium on Biology and Management of Mangroves, Vol. II.
Dietrich, G., K. Kalle, W. Krauss, and G. Siedler. 1980. General oceanography, an introduction. 2nd edition. John Wiley & Sons, New York. 626 pp.
Dyer, K.R. 1970. Current velocity profiles in a tidal channel. Geophysical Journal of the Royal Astronomical Society 22:153–161.
Dyer, K.R. 1973. Estuaries: A physical introduction. John Wiley and Sons, New York.
Dyer, K.R. 1974. The salt balance in stratified estuaries. Estuarine and Coastal Marine Science 2:273–281.

Dyer, K.R. 1977. Lateral circulation effects in estuaries. In: Estuaries, geophysics and the environment. National Academy of Sciences. Washington, DC.
Eiser, W.C. and B. Kjerfve. 1986. Marsh topography and hypsometric characteristics of a South Carolina salt marsh basin. Estuarine, Coastal and Shelf Science 23:595–605.
Elliott, A.J. 1976. A study of the effect of meteorological forcing on the circulation in the Potomac estuary. Special Report 56. Chesapeake Bay Institute. The Johns Hopkins University, Baltimore, MD.
Emery, K.O. and E. Uchupi. 1972. Western North Atlantic Ocean: Topography, rocks, structure, water, life, and sediments. American Association of Petroleum Geologists Mem. 17. Tulsa, OK.
Fairbridge, R.W. 1980. The estuary: its definition and geodynamic cycle, pp. 1–35. In: E. Olausson and I. Cato (eds.), Chemistry and biogeochemistry of estuaries. John Wiley and Sons, New York.
Fischer, H.B. 1972. Mass transport mechanisms in partially stratified estuaries. Journal of Fluid Mechanics 53:671–687.
Fischer, H.B. 1976. Mixing and dispersion in estuaries, pp. 107–133. In: M. van Dyke, W. Vincinti, and J.V. Wehausen (eds.), Annual review of fluid mechanics, Vol. B.
Fischer, H.B., E.J. List, R.C.Y. Koh, J. Imberger, and N.H. Brooks. 1979. Mixing in Inland and Coastal Waters. Academic Press. 483 pp.
Foffonoff, N.P., and R.C. Millard, Jr. 1983. Algorithms for computation of fundamental properties of seawater. UNESCO Technical Papers in Marine Science 44. 53 pp. Unesco, Paris, France.
Franco, A.S. 1988. Tides: Fundamentals, analysis and prediction. Second edition. Fundaçao Centro–Tecnológico de Hidráulica (FCTH), São Paulo, Brazil. 249 pp.
Galloway, R.W. 1982. Distribution and physiographic patterns of Australian mangroves, pp. 31–54. In: B.F. Clough (ed.), Mangrove ecosystems in Australia: structure, function and management. Australian National University Press, Canberra.
Gibbs, R.J. 1970. Circulation in the Amazon River estuary and adjacent Atlantic Ocean. Journal of Marine Research 28:113–123.
Guralnik, D.B.(ed.). 1980. Webster's new world dictionary of the American language. Second college edition. Simon and Schuster. New York. 1,692 pp.
Haas, L.W. 1977. The effect of the spring-neap tidal cycle on the vertical salinity structure of the James, York, and Rappahanock Rivers, Virginia, USA. Estuarine, Coastal and Shelf Science 5:485–496.
Hansen, D.V. 1965. Currents and mixing in the Columbia River estuary. Ocean Science and Ocean Engineering, pp. 943–955. Transactions of the Joint Conference of the Mar. Tech. Soc. and Am. Soc. Limn. Ocean.
Hansen, D.V. and M. Rattray, Jr. 1965. Gravitational circulation in straits and estuaries. Journal of Marine Research 23:104–122.
Hansen, D.V. and M. Rattray, Jr. 1966. New dimensions in estuary classification. Limnology and Oceanography 11:319–326.
Harbeck, Jr., G.E. 1962. A practical field technique for measuring reservoir evaporation utilizing mass-transfer theory. pp. 101–105. In: U.S. Geological Survey Professional Paper 272E. U.S. Government Printing Office. Washington, D.C.
Hayes, M.O. 1978. Impact of hurricanes on sedimentation in estuaries, bays, and lagoons. pp. 332–347. in: Estuarine Interactions. M.L. Wiley (éd.). Academic Press, N.Y. 603 pp.
Hicks, S.D. and J.E. Crosby. 1974. Trends and variability of yearly mean sea levels, 1983–1972. NOAA Technical Memorandum No. 13, COM-74–11012. Rockville, MD. 16 pp.
Hoffman, J.S., D. Keyes, and J.G. Titus. 1983. Projecting future sea level rise: Methodology, estimates to the year 2100, and research needs. EPA 230–09– 007. Environmental Protection Agency, Washington, DC.
Holbrook, J.R., R.D. Muench, D.G. Kachel, and C. Wright. 1980. Circulation in the Straight of Juan de Fuca: recent oceanographic observations in the eastern basin. NOAA Technical Report ERL 412-PMEL 33. 42 pp.

Holland, H.D. 1978. The chemistry of the atmosphere and oceans. John Wiley & Sons, New York. 351 pp.
Hydrographic Department (UK). 1979. Co-tidal atlas South-East Asia. NP 215. Edition 1–1979. Taunton. 27 pp.
Jennings, J.N. and B.J. Coventry. 1973. Structure and texture of a gravelly barrier island in the Fitzroy Estuary, WA and the role of mangroves in shore dynamics. Marine Geology 15:145–167.
Jensen, J.R., B. Kjerfve, E.W. Ramsey, K.E. Magill, C. Medeiros, and J.E. Sneed. In Press. Remote sensing and numerical modeling of suspended sediment in Laguna de Términos, Campeche, Mexico. Remote Sensing of Environment.
Jimenez, J.A., A.E. Lugo, and G. Cintrón. 1985. Tree mortality in mangrove forests. Biotropica 17:177–185.
Johns, R.J. 1981. Dead patches in New Guinea mangrove communities. Abstracts. 13th International Bot. Congress. Sydney, Australia.
Johns, R.J. 1986. Natural disturbances in mangrove ecosystems. pp. 37–40. In: Report of the workshop of mangrove ecosystem dynamics. Motupore Island Research Station, Port Moresby. UNDP/ UNESCO Regional Project RAS/79/002, New Delhi, India.
Kjerfve, B. 1973. Dynamics of the water surface in a bar-built estuary. Ph.D. Dissertation. Louisiana State University. 91 pp.
Kjerfve, B. 1975. Velocity averaging in estuaries characterized by a large tidal range to depth ratio. Estuarine and Coastal Marine Science 3:311–323.
Kjerfve, B. 1976. Circulation and salinity distribution in coastal Louisiana bayous. Contributions in Marine Science 20:1–10.
Kjerfve, B. 1978. Bathymetry as an indicator of net circulation in well-mixed estuaries. Limnology and Oceanography 23:311–323.
Kjerfve, B. 1979. Measurements and analysis of water current, temperature, salinity, and density, pp. 186–216. In: K.R. Dyer (ed.), Hydrography and sedimentation in estuaries. Cambridge University Press, Cambridge.
Kjerfve, B. and J.A. Proehl. 1979. Velocity variability in a cross-section of a well-mixed estuary. Journal of Marine Research 37:409–418.
Kjerfve, B. and H.N. McKellar, Jr. 1980. Time series measurements of estuarine material fluxes. pp. 341–357. In: V.S. Kennedy (ed.), Estuarine Perspectives. Academic Press, NY. 533 pp.
Kjerfve, B., L.H. Stevenson, J.A. Proehl, T.H. Chrzanowski, and W.M. Kitchens. 1981. Estimation of material fluxes in an estuarine cross-section: a critical analysis of spatial measurement density and errors. Limnology and Oceanography 26:325–335.
Kjerfve, B. 1982. Calibration of estuarine current crosses. Estuarine, Coastal and Shelf Science 15:553–559.
Kjerfve, B., J.A. Proehl, F.B. Schwing, H.E. Seim, and M. Marozas. 1982. Temporal and spatial considerations in measuring estuarine water fluxes. In: V.S. Kennedy (ed.), Estuarine comparisons. Academic Press, New York.
Kjerfve, B. and H.E. Seim. 1984. Construction of net isopleth plots in cross-sections of tidal estuaries. Journal of Marine Research 42:503–508.
Kjerfve, B. 1986a. Comparative oceanography of coastal lagoons, pp. 63–81. In: D.A. Wolfe (ed.), Estuarine variability. Academic Press, New York.
Kjerfve, B. 1986b. The role of water currents in fluxes of carbon and nutrients through mangrove ecosystems. pp. 159–165. In: Report on the workshop on mangrove ecosystem dynamics. Motupore Island, Port Moresby, Papua New Guinea. UNESCO/UNDP Regional Project RAS/79/002, New Delhi, India.
Kjerfve, B. 1986c. Physical flow processes in Caribbean waters over a range of scales. pp. 38–47. In: Caribbean coastal marine productivity. Results of a planning workshop at Discovery Bay Marine Laboratory, University of the West Indies, Jamaica. Unesco Reports in Marine Science 41, Unesco. 59 pp.

Kjerfve, B. 1986d. Circulation and salt flux in a well mixed estuary. pp. 22–29. In: J. van de Kreeke (ed.), Physics of Shallow Estuaries and Bays. Springer–Verlag, Berlin. 280 pp.
Kjerfve, B., and T.G. Wolaver. 1988. Sampling optimization for studies of tidal transport in estuaries. American Fisheries Society Symposium 3:26–33.
Kjerfve, B. 1989. Estuarine geomorphology and physical oceanography. pp. 47– 78. In: J.W. Day, Jr., C.A.S. Hall, W.M. Kemp, and A. Yañez-Arancibia (eds.), Estuarine ecology. John Wiley and Sons, New York.
Kjerfve, B. and C. Medeiros. 1989. Current vanes for measuring tidal currents in estuaries. Estuarine, Coastal and Shelf Science 28:87–93.
Kjerfve, B. and K.E. Magill. 1989. Geographic and hydrodynamic characteristics of shallow coastal lagoons. Marine Geology 88:187–199.
Kjerfve, B., and P. Sojisuporn. 1989. Simulation of tidal discharge based on a hypsometric modeling approach. Unpublished manuscript.
Köppen, W. 1900. Versuch einer Klassifikation der Klimate, Vorzungsweise nach Ihren Beziehungen zur Planzwelt. Geographische Zeitschrift 6:593–611 and 657–677.
Lankford, R.R. 1976. Coastal lagoons of Mexico: their origin and classification, pp. 182–215. In: M.L. Wiley (ed.), Estuarine processes, Vol. II. Academic Press, New York.
LeBlond, P.H. and L.A. Mysak. 1978. Waves in the ocean. Elsevier Scientific Publishing Co., New York. 602 pp.
Lewis, R.R., III, R.G. Gilmore, Jr., D.W. Crewz, and W.E. Odum. 1985. Mangrove habitat and fishery resources of Florida. pp. 281–336. In: W. Seaman, Jr. (ed.), Florida aquatic habitat and fishery resources. Florida Chapter of the American Fisheries Society, Kissimmee, Florida. 543 pp.
Lindell, L.T., O. Steinvall, M. Jonsson, and Th. Claesson. 1985. Mapping of coastal water turbidity using Landsat imagery. International Journal of Remote Sensing 6:629–642.
List, R.J. 1951. Smithsonian Meteorological Tables. Publication No. 4014, Smithsonian Institution, City of Washington. 527 pp.
Loder, T.C. and R.P. Reichard. 1981. The dynamics of conservative mixing in estuaries. Estuaries 4:64–69.
Lot-Hergueras, A., C. Vazques-Yañes, and F. Menendez L. 1975. Physiognomic and floristic changes near the northern limit of mangroves in the Gulf Coast of Mexico. pp. 52–61. In: G. Walsh, S. Snedaker, and H. Teas (eds.), Proceedings of the International Symposium on the Biology and Management of Mangroves. Institute of Food and Agricultural Sciences, University of Florida, Gainesville.
Lugo, A.E. and S.C. Snedaker. 1973. The role of mangrove ecosystems: Properties of a mangrove forest in South Florida. Resource Management Systems Program, University of Florida, Gainesville. Report No. DI-SFEP-74–34. 62 pp.
Lugo, A.E. and S.C. Snedaker. 1974. The ecology of mangroves. pp. 39–64. In: Annual review of ecological systems, vol. 5.
Lugo, A.E. and C.P. Zucca. 1977. The impact of low temperature stress on mangrove structure and growth. Tropical ecology 18:149–161.
Macnae, W. 1966. Mangroves of eastern and southern Australia. Australian Journal of Botany 14:67–104.
Macnae, W. 1968. A general account of the fauna and flora of mangrove swamps and forests in the Indo-West-Pacific Region. Advances in Marine Biology 6:73– 270.
Macnae, W. 1974. Mangrove forests and fisheries. FAO/UNDP Indian Ocean Fishery Programme. Indian Ocean Fishery Commission. Publication IOFC/Dev/74/34. 35 pp.
Mann, K.H. 1982. Ecology of coastal waters: A systems approach. University of California Press. Berkeley, CA. 322 pp.
Martusubroto, P. and N. Naamin. 1977. Relationship between tidal forests (mangroves) and commercial shrimp production in Indonesia. Marine Research in Indonesia 18:81–86.

McArthur, G.R. (ed.). 1983. The SCD graphics utilities. NCAR Technical Note NCAR-TN/166+IA. National Center for Atmospheric Research, Boulder, CO.
McCammon, C., and C. Wunsch. 1977. Tidal charts of the Indian Ocean north of 15xS. Journal of Geophysical Research 82:5993–5998.
McMillan, C. 1971. Environmental factors affecting seedling establishment of the black mangrove on the central Texas coast. Ecology 52:927–930.
McMillan, C. 1975. Adaptive differentiation to chilling in mangrove populations. pp. 62–70. In: G.E. Walsh, S.C.Snedaker, and H.J. Teas (eds.), Proceedings of the International Symposium of Biology and Management of Mangroves. Institute of Food and Agricultural Sciences. University of Florida, Gainsville.
Meade, R.H. 1969. Landward transport of bottom sediments in estuaries of the Atlantic Coastal Plain. Journal of Sedimentary Petrology 39:222–234.
Milliman, J.D. 1979. Transfer of river-borne particulate matter to the oceans, pp. 5–12. In: River input to the ocean systems. J.-M. Martin, J.D. Burton, and D. Eisma (eds.). UNEP, UNESCO, SCOR, IOC Proceedings of workshop on river inputs to ocean systems (RIOS), Rome.
Milliman, J.D. 1988. Rising sea level and changing sediment influxes: Real and future problems for Indian Ocean coastal nations. IOC/UNESCO Workshop on Regional Cooperation in Marine Science in the Central Indian Ocean and Adjacent Seas and Gulfs. Workshop Report No. 37, Supplement, pp. 195–202.
Murray, S.P., D. Conlon, A. Siripong, and J. Santoro. 1975. Circulation and salinity distribution in the Rio Guayas estuary, Ecuador, pp. 345–363. In: L.E. Cronin (ed.), Estuarine research, Vol. 2. Academic Press, New York.
Murray, S.P. and A. Siripong. 1978. Role of alteral gradients and longitudinal dispersion in the salt balance of a shallow well-mixed estuary. pp. 113–124. In: B. Kjerfve (ed.), Estuarine Transport Processes. University of South Carolina Press, Columbia, SC.
Mysak, L.A. and B.V. Hamon. 1969. Low-frequency sea level behavior and continental shelf waves off North Carolina. Journal of Geophysical Research 74:1397–1405.
Nichols, M.M. and R.B. Biggs. 1985. Estuaries, pp. 77–187. In: R.A. Davis, Jr. (ed.), Coastal sedimentary environments. Springer-Verlag.
Nixon, S.W. 1980. Between coastal marshes and coastal waters—a review of twenty years of speculation and research in the role of salt marshes in estuarine productivity and water chemistry. pp. 437–525. In: Estuarine and wetland processes. P. Hamilton and K.B. McDonald. Plenum Press. New York.
Nixon, S.W., B.N. Furnas, V. Lee, N. Marshall, J.-E. Ong, C.-H. Wong, and W.-K. Gong. 1984. The role of mangroves in the carbon and nutrient dynamics of Malaysia estuaries. pp. 534–544. In: E. Seopadmo, A.N. Rao, and D.J. Macintosh (eds.), Proceedings of the Asian Symposium on Mangrove Environments: Research and Management. University of Malaya and UNESCO. Kuala Lumpur, Malaysia.
Noye, B.J. 1973. The Coorong—past, present, future. Publication 38, Department of Adult Education. The University of Adelaide, South Australia.
Officer, C.B. 1979. Discussion of the behaviour of nonconservative dissolved constituents in estuaries. Estuarine and Coastal Marine Science 9:91–94.
Officer, C.B. and D.R. Lynch. 1981. Dynamics of mixing in estuaries. Estuarine, Coastal and Shelf Science 12:525–533.
Okubo, A. 1973. Effect of shoreline irregularities on stream wise disperion in estuaries and other embayments. Netherlands Journal of Sea Research 6:213– 224.
Oliver, J. 1982. The geographic and environmental aspects of mangrove communities: climate. pp. 2–30. In: B.F. Clough (ed.), Mangrove ecosystems in Australia: structure, function and management. Australian National University Press, Canberra. 302 pp.
Ong, J.E., W.K. Gong, and C.H. Wong. 1981. Ecological monitoring of the Sungai Merbok estuarine mangrove eco-system. Technical Report. School of Biological Sciences, Universiti Sains Malaysia,

Penang, Malaysia. 49 pp.
Ong, J.E. 1982. Mangroves and aquaculture in Malaysia. Ambio 11:252–257.
Palmer, M.A., B. Kjerfve, and F.B. Schwing. 1980. Tidal analysis and prediction in a South Carolina estuary. Contributions in Marine Science 23:17–23.
Papadakis, J. (ed.). 1965. Potential evaporation. Buenos Aires. 54 pp.
Pattullo, J., W. Munk, R. Revelle, and E. Strong. 1955. The seasonal oscillation in sea level. Journal of Marine Research 14(1):88–156.
Penman, H.L. 1956. Evaporation: an introductory survey. Netherlands Journal of Agricultural Science 4:9–29.
Pennington, R.H. 1970. Computer methods and numerical analysis. 2nd ed. The McMillan Company.
Percival, M. and J.S. Womersley. 1975. Floristics and ecology of the mangrove vegetation of Papua New Guinea. Department of Forests, Division of Botany, P.O. Box 314, Lae, Papua New Guinea. 96 pp.
Poovachinaranon, S. and H. Chansang. 1982. Structure of Ao Yon mangrove forest (Thailand) and its contribution to the coastal ecosystem. Proceedings of the Biotrop Symposium on Mangrove Forests Ecosystem Productivity in South East Asia. A.Y. Kostermans and S.S. Sastroumoto (eds.), Biotrop Special Publication No. 17, pp. 101–111.
Pritchard, D.W. 1952. Salinity distribution and circulation in the Chesapeake Bay estuarine system. Journal of Marine Research 11:106–123.
Pritchard, D.W. 1955. Estuarine circulation patterns. Proceedings of the American Society of Civil Engineers 81(717):1–11.
Pritchard, D.W. 1956. The dynamic structure of a coastal plain estuary. Journal of Marine Research 15:33–42.
Pritchard, D.W. and R.E. Kent. 1956. A method for determining mean longitudinal velocities in a coastal plain estuary. Journal of Marine Research 15:81–91.
Pritchard, D.W. 1958. The equations of mass continuity and salt continuity in estuaries. Journal of Marine Research 17:412–423.
Pritchard, D.W. 1969. Dispersion and flushing of pollutants in estuaries. Proceedings of the American Society of Civil Engineering, Journal of the Hydraulics Division 95:115–124.
Pritchard, D.W. 1978. What have recent observations obtained for adjustment and verification of numerical models revealed about the dynamics and kinematics of estuaries, pp. 1–9. In: B. Kjerfve (ed.), Estuarine transport processes. University of South Carolina, Columbia, SC.
Pugh, D.T. 1987. Tides, surges, and mean sea level, a handbook for engineers and scientists. John Wiley and Sons, New York. 472 pp.
Rattray, M., Jr. and D.V. Hansen. 1962. A similarity solution for circulation in an estuary. Journal of Marine Research 20:121–133.
Rattray, M., Jr. and J.G. Dworski. 1980. Comparison of methods for analysis of the transverse and vertical circulation contributions to the longitudinal advective salt fluxes in estuaries. Estuarine and Coastal Marine Science 11:515–536.
Saenger, P. 1982. Morphological, anatomical and reproductive adaptations of Australian mangorves. pp. 153–192. In: B.F. Clough (ed.), Mangrove ecosystems in Australia: structure, function and management. Australian National University Press, Canberra. 302 pp.
Schaeffer-Novelli, Y., R.R. Adaime, T.M. Camargo, and G. Cintrón. 1985. Variability of the mangrove ecosystem along the Brazilian coast. Unpublished manuscript presented at the Eighth International Biennial Estuarine Research Federation Conference, Durham, NH. 36 pp.
Scholl, D.W. 1968. Mangrove swamps: geology and sedimentology. pp. 683–688. In: The encyclopedia of geomorphology. R.W. Fairbridge (ed.). Reinhold Book Corporation. New York. 1,295 pp.
Schreiber, P. 1904. Über die Beziehungen zwischen dem Niederschlag und der Wasserfhrung der Flüsse in Mittleeuropa. Meteorologische Zeitschrift. 21:441– 452.
Schubel, J.R. and D.W. Pritchard. 1972. The estuarine environment. Journal of Geological Education 20:60–68.

Schubel, J.R. and D. J. Hirschberg. 1978. Estuarine graveyards, climatic change, and the importance of the estuarine environment, pp. 285–303. In: M.L. Wiley (ed.), Estuarine interactions. Academic Press, New York.
Schureman, P. 1941. Manual of harmonic analysis and prediction of tides. Coast and Geodetic Survey Special Publication 98. United States Government Printing Office. Washington, DC. 313 pp.
Seelig, W.N. and R.M. Sorensen. 1978. Numerical model investigation of selected tidal inlet-bay system characteristics. American Society of Civil Engineers, Proceedings of the 16th Coastal Engineering Conference, Hamburg, West Germany, pp. 1302–1319.
Sellers, W.D. 1965. Physical Climatology. The University of Chicago Press, Chicago. 272 pp.
Smith, N.P. 1977. Meteorological and tidal exchanges between Corpus Christi Bay, Texas, and the northwestern Gulf of Mexico. Estuarine and Coastal Marine Science 5:511–520.
Snedaker, S.C. 1984. Mangroves: a summary of knowledge with emphasis on Pakistan. pp. 255–262. In: B.U. Haq and J.D. Milliman (eds.), Marine geology and oceanography of Arabian Sea & coastal Pakistan. Van Nostrand Reinhold Co., N.Y.
Spenceley, A.P. 1976. Unvegetated saline tidal flats in North Queensland. Journal of Tropical Geography 42:78–85.
Spurrier, J.D., and B. Kjerfve. 1988. Estimating the net flux of nutrients between a salt marsh and a tidal creek. Estuaries 11:10–14.
Sternberg, R.W. 1972. Predicting initial motion and bedload transport of sediment particles in the shallow marine environment. pp. 61–82. In: D.J.P Swift, D.B. Duane, and O.H. Pilkey (eds.), Shelf Sediment Transport. Dowden, Hutchinson, & Ross.
Stewart, R.W. 1957. A note on the dynamic balance for estuarine circulation. Journal of Marine Research 16:34–39.
Stocker, G.C. 1976. Report on cyclone damage to natural vegetation in the Darwin area after cyclone Tracey 25 December 1974. Forestry and Timber Bureau, Leaflet No. 127. 40 pp.
Stoddart, D.R. 1962. Catastrophic storm effects in the British Honduras reefs and cays. Nature (Lond.) 196:512–515.
Stoddart, D.R. 1965. Re-survey of hurricane effects on the British Honduras reefs and cays. Nature 207:589–592.
Stoddart, D.R. 1971. Coral reefs and islands and catastrophic storms. pp. 155–197. In: J.A. Steers (ed.), Applied coastal geomorphology. M.I.T. Press, Cambridge, MA.
Strahler, A.N. 1952. Hypsometric (area-altitude) analysis of erosional topography. Bulletin of the Geological Society of America 63:1117–1142.
Strickland, J.D.H. and T.R. Parsons. 1968. A practical handbook of seawater analysis. Fisheries Research Board of Canada, Bulletin 167.
Strickland, J.D.H., and T.R. Parsons. 1972. A practical handbook of seawater analysis. Fisheries Research Board of Canada Bulletin 167. Ottawa. 311 pp.
Sturges, A.A. 1865. Letter from Micronesia. The Friend 22:52–53.
Talbot, J.W. and G.A. Talbot. 1974. Diffusion in shallow seas and in English coastal and estuarine waters. Rapports et Procés-Verbaux des Réunions, Conseil International pour l'Exploration de la Mer 167:73–110.
Tee, K.-T. 1976. Tide-induced residual current, a 2–d non-linear numerical tidal model. Journal of Marine Research 34:603–628.
Thanikaimoni, G. 1987. Mangrove Palynology. UNDP/UNESCO Regional Project on Training and Research on Mangrove Ecosystems, RAS/79/002, and the French Institute, Pondicherry. Institut Français de Pondichery. 99 pp.
Thom, B.G. 1967. Mangrove ecology and deltaic geomorphology: Tabasco, Mexico. Journal of Ecology 55: 301–343.
Thom, B.G. 1982. Mangrove ecology—a geomorphological perspective. pp. 3–17. In: Mangrove ecosystems in Australia: structure, function and management. B.F. Clough (ed.). Australian National